CENTER FOR DRUG EVALUATION AND RESEARCH

APPLICATION NUMBER:

216718Orig1s000

CLINICAL PHARMACOLOGY REVIEW(S)

Office of Clinical Pharmacology Review

NDA Number	216718
Link to EDR	\\CDSESUB1\evsprod\NDA216718\0001
Submission Date(s)	January 28, 2022 (Modules 1,2,4,5) March 30, 2022 (Module 3) July 21, 25 and August 3, 2022 (Major amendment)
Submission Type	505(b)(1) Priority Review (major amendment led to 3 month extension)
Brand Name	SKYCLARYS™
Generic Name	Omaveloxolone (RTA-408)
Dosage Form and Strength	50 mg immediate release capsule
Route of Administration	Oral
Dosing regimen	150 mg (3x50 mg) once daily (QD) 1h before food
Proposed Indication	Treatment of Friedreich's Ataxia (FA) in patients ≥16y
Applicant	Reata Pharmaceuticals, Inc.
Associated IND	122349
OCP Review Team	&Adarsh Gandhi, Ph.D., &Michael Bewernitz, Ph.D., &Manuela Grimstein, Ph.D., &Hobart Rogers, Ph.D., #Yuching Yang, Ph.D., #Atul Bhattaram, Ph.D., #Bilal AbuAsal, Ph.D.
OCP Clearing Officials	*Mehul Mehta, Ph.D., *Ramana Uppoor, Ph.D., *Sreedharan Sabarinath, Ph.D.

&Primary Reviewer; #Team Leader; *Division Director, Deputy Director or Associate Director

Table of Contents

1. EXECUTIVE SUMMARY

The Applicant, Reata Pharmaceuticals, Inc., is seeking approval for omaveloxolone (SKYCLARYS™, RTA-408) (abbreviated as Omav in rest of the review) via the 505(b)(1) pathway for treatment of Friedreich's Ataxia (FA) in patients 16 years and older. Omav is a small molecule drug formulated as an immediate release oral capsule (50 mg strength). The proposed dosing regimen for Omav is 150 mg (3x50mg capsule) orally 1h before food. Omav is proposed to activate nuclear factor erythroid 2-related factor 2 (Nrf2), a transcription factor known to be decreased in FA patients.

To support the registration of (SKYCLARYS™), the Applicant is relying on Part 2 of a pivotal double-blind, placebo-controlled Phase 2 Study (Study 408-C-1402 a.k.a. MOXIe trial) and a long term extension study. Study 1402 enrolled 172 patients in part 1 and part 2. Part 1 was a short dose finding study (n=69). Part 2 was designed with no more than 20% patients with pes cavus (a foot deformity) (total n=103). The Applicant reported that Omav treatment improved mFARS (primary efficacy endpoint) by -1.93 points in patients with and without pes cavus, whereas mFARS score improved by -2.41 points in patients without pes cavus relative to placebo at Week 48. Analysis of the long-term OLE study included (1) delayed-start analysis (all patients from study 1402 received Omav starting at week-52), and (2) propensity matched natural history comparison with FA patients. The Applicant's OLE study with post-hoc analyses were used as supportive evidence of efficacy where FA patients who received Omav earlier had greater reduction in mFARS score (delayed start analysis) and propensity score matched FA patients on Omav had greater reduction in mFARS score at year 3 .

The Applicant also submitted biomarker data (from part 1 of study 1402) to provide mechanistic support for the activity of Omav in patients with FA. Frataxin deficiency in patients with FA causes suppression of Nrf2 and mitochondrial energy production. Since Nrf2 is downregulated in FA patients, activation of Nrf2 could be a potential therapeutic target for treatment of FA. Initially, the applicant claimed that the observed increase in liver enzymes (ALT, AST, and GGT), creatine kinase (CK) and ferritin (iron storage protein) in plasma of FA patients is a pharmacodynamic response resulting from Nrf2 activation. Towards the end of the review cycle, the Applicant endorsed only ferritin and GGT as biomarkers of Nrf2 activation. The Applicant claimed that the ferritin and GGT elevation can support mechanistic activity of Omav in FA patients. Although there was no conclusive support for GGT, ferritin was partly established as a clinical biomarker of Nrf2 activation in patients. Ferritin mRNA levels were dose dependently increased in PBMCs of cancer patients treated with Omav. However, the reliability of ferritin as a direct target of Nrf2 should be interpreted with caution as ferritin is also considered a marker of cellular damage.

The clinical pharmacology development program included a single ascending dose/food effect study, a 4-part clinical DDI study, a hepatic-impairment study, and a mass balance study. The primary focus of this review was to evaluate dose selection in the general population and dose-adjustment recommendations in special population (hepatic impairment), and with concomitant strong and

moderate CYP3A4 inhibitors. Acceptability of submitted biomarker data as supportive evidence for registration of SKYCLARYS™ were also reviewed.

1.1 Recommendations

The Office of Clinical Pharmacology has reviewed the information submitted in this NDA and is recommending approval. Key review issues with specific recommendations and comments are summarized below:

Review Issue	Recommendations and Comments
Pivotal or supportive evidence of effectiveness	The efficacy of Omav for the treatment of FA was established based on results from Part 2 of a randomized, double-blind, placebo-controlled study (RTA-408-1402, MOXIe). Supportive evidence of efficacy was based on additional analysis of results from the open label extension (OLE) of the same study in FA patients. Results from Part 2 and Extension study were compared using a propensity matched analysis which included the FA-COMS natural history data. Biomarker data were also used to provide potential mechanistic support of Omav through Nrf2 activation.
General dosing instructions	The recommended dosage of SKYCLARYS is 150 mg (3 capsules) taken orally once daily. Administer SKYCLARYS on an empty stomach at least one hour before eating. Swallow SKYCLARYS capsules whole. Do not open, crush or chew.
Dosing in patient subgroups (intrinsic and extrinsic factors)	<u>Intrinsic factors:</u> Dosing in patients with severe hepatic impairment (Child-Pugh Class C): • Omav should be avoided in patients with severe hepatic impairment Dosing in patients with moderate hepatic impairment (Child-Pugh Class B): • It is recommended to reduce the dose to 100 mg QD. If adverse events emerge, the dose should be further reduced to 50 mg QD. No dose adjustment is needed for Omav for the following intrinsic factors: • Mild, moderate, or severe renal impairment • Mild hepatic impairment ((Child-Pugh Class A) <u>Extrinsic factors:</u> Concomitant use with moderate CYP3A4 inhibitors: • It is recommended to avoid use. If concomitant use with moderate CYP3A4 inhibitors cannot be avoided, then reduce Omav dose to 100 mg QD. If adverse events emerge, further reduce Omav dose to 50 mg QD. Concomitant use with strong CYP3A4 inhibitors: • If concomitant use with strong CYP3A4 inhibitors cannot be avoided, Omav dose should be reduced to 50 mg QD. If adverse events emerge, co administration should be suspended. Concomitant use with weak CYP3A4 inhibitors:

	• No dose adjustment is required with concomitant use with weak CYP3A4 inhibitors. Concomitant use with moderate or strong inducers of CYP3A4: • Use with moderate and strong CYP3A4 inducers should be avoided.
Labeling	The review team recommends changes to the USPI – dose adjustment in FA patients receiving concomitant moderate or strong CYP3A4 inhibitors (sections 2.4 and 7.1), coadministration with combined hormonal contraceptives (sections 7.2 and 8.3), patients with moderate hepatic impairment (sections 2.5 and 8.6), pharmacodynamics (section 12.2) and pharmacokinetics (section 12.3).
Bridge between to-be-marketed and clinical trial formulations	The to-be-marketed (TBM) formulation was used in the pivotal efficacy study (408-C-1402, parts 1 and 2).

`

1.2 Post-Marketing Requirements and Commitments

1. Conduct a clinical drug interaction study to determine the effect of concomitant administration of a moderate CYP3A4 inducer on pharmacokinetics of omaveloxolone in healthy volunteers. Design and conduct the trial in accordance with the 2020 FDA Guidance for Industry entitled "Clinical Drug Interaction Studies - Cytochrome P450 Enzyme- and Transporter-Mediated Drug Interactions" (https://www.fda.gov/media/134581/download).

2. A clinical trial to assess the risk of QT prolongation with omaveloxolone to exclude mean QTc effects greater than 10ms.

2. SUMMARY OF CLINICAL PHARMACOLOGY ASSESSMENT

2.1 Pharmacology and Clinical Pharmacokinetics

Mechanism of Action

Omav selectively and reversibly binds to Keap1, resulting in the activation of Nrf2, a transcription factor that modulates the expression of genes involved in regulating mitochondrial function, oxidative stress, and inflammation.

Omav activity is dependent on the Keap1-Nrf2 pathway. By activating this pathway, Omav modulates the transcription of genes that protect the cell by three complementary and overlapping mechanisms:

- Modulates pathways involved in cellular metabolism and mitochondrial function.
- Increases the expression of antioxidative enzymes, elevates the levels of endogenous antioxidants, and reduces oxidative stress.
- Inhibits proinflammatory signaling pathways, including the nuclear factor-kappa B (NF-κB) pathway, and reduces the production of pro-inflammatory mediators.

In cells isolated from patients with Friedreich's ataxia and in neurons from mouse models of Friedreich's ataxia, Omav has demonstrated the ability to prevent cellular death, while restoring Nrf2 and promoting mitochondrial bioenergetic, antioxidative, and anti-inflammatory activities.

Absorption

The median (range) time to achieve peak plasma concentration was 7 to 14 (1 to 24) hours. The total plasma Omav exposure based on area under the concentration-time curve (AUC) increased in a dose-dependent and dose proportional manner over a dose range of 50 mg (0.33 times the recommended dosage) to 150 mg, but maximum Omav plasma concentration (C_{max}) increased in a less than dose proportional manner over the dose range in healthy fasted subjects

Administration of 150 mg Omav with a high-fat meal (800-1000 calories, approximately 150, 250, and 500 to 600 calories from protein, carbohydrate, and fat, respectively) caused a slight increase in the total exposure (AUC increased by ~15%) and an increase of ~350% in C_{max} as compared to administration under fasted condition (study 408-C-1703).

Distribution

Omav is ~97% bound to human plasma proteins. Blood/plasma ratio is ~0.7. Volume of distribution is 7361 L (105 L/kg for a 70 kg person).

Metabolism

Omav is majorly metabolized by CYP3A4 followed by CYP2C8 and CYP2J2. Following a single dose of [^{14}C]-Omav administered orally to healthy males (study 408-C-1805), Omav was found to be eliminated by metabolism to a series of 30 metabolites, of which 7 metabolites were quantified and identified. Metabolites M22 and M17 were major plasma metabolites that accounted for 18.6% and 10.9% of total plasma radioactivity, respectively. The other metabolites were minor, each accounting for less than 10% of total plasma radioactivity exposure. None of the metabolites has meaningful pharmacological activity.

Excretion

The mean(range) elimination half-life of Omav is 57h (32-90h) in healthy subjects. The primary route of elimination is through the feces, with 92.4% recovered in feces and less than 0.1% was recovered in urine (study 408-C-1805).

Special Populations

Hepatic Impairment

The effect of hepatic impairment on PK of Omav was assessed in a hepatic impairment study (study 408-C-1804). Compared to subjects with normal hepatic function, patients with mild hepatic impairment had ~29% higher C_{max}, while total exposure was comparable. In patients with moderate hepatic impairment AUC_{inf}, AUC_{0-t}, and C_{max} values were 64%, 56%, and 83% higher, respectively, compared to subjects with normal hepatic function. Patients with severe hepatic impairment had a 117% increase in AUC_{inf} compared to the normal hepatic group. The AUC_{0-t} values were 27% higher, while C_{max} was 32% lower, for the severe hepatic impairment group compared to the normal group.

Renal Impairment

From the mass balance study (study 408-C-1805), the contribution of renal elimination pathway for Omav in healthy subjects was shown to be very low (0.1% of total radioactivity recovered in urine). Therefore, a dedicated renal impairment study evaluating the impact of renal impairment on PK of Omav, and its metabolites is not needed.

Age, Sex, Race, and Body Weight

The effect of various intrinsic factors, like age, race, sex, and body weight was evaluated in the population PK analysis. Based on the popPK covariate analysis, only baseline age (median age in popPK dataset was 34 years; range 16-71 years) was found to have a significant influence on CL, suggesting a lower CL in older subjects. Simulations of popPK parameters showed that median steady state C_{max} and AUC in the group of subjects ≥ 65 years are 27% and 23% higher than the median steady state C_{max} and AUC of reference subject (34 years). The Applicant concluded that these differences between age groups are not clinically meaningful and are included in the range of inter-subject variability.

2.2 Dosing and Therapeutic Individualization

2.2.1 General dosing

The proposed dose for the treatment of FA is 150 mg (3 capsules of 50 mg each) once daily 1h before eating. This dosing regimen is same as used in part 2 of the pivotal Phase 2 clinical study (408-C-1402, MOXIe trial).

2.2.2 Therapeutic individualization

Hepatic Impairment

A dedicated hepatic impairment study was conducted with a single dose of 150 mg of Omav (study 408-C-1804). Based on the insignificant change in C_{max} and AUC_{inf} of Omav in mild hepatic impairment, no dose adjustment is needed for patients with mild hepatic impairment. The AUC_{inf} of Omav were 1.65-fold higher in moderate hepatic impairment and 2.17-fold higher in severe hepatic impairment patients. The review team recommended a reduced dose of 100 mg QD in moderate hepatic impairment patients is allowed. If adverse events emerge, the dose should be further reduced to 50 mg QD. Dosing in severe hepatic impairment should be avoided due to concerns related to adverse hepatic events and based on clinical benefit risk assessment in this population. Omav administration can only be resumed after hepatic impairment improves to normal (150 mg), mild (150 mg), or moderate (100 mg) status.

Renal Impairment

No dedicated renal impairment studies were conducted with Omav. From the mass balance study, Omav and its metabolites accounted for less than 0.1% of total radioactivity in urine. There were 14 patients with eGFR between 60-89 mL/min/1.73m^2 and 89 patients above 89 mL/min/1.73m^2 (total 103 patients

studied in part 2 of the pivotal study 1402). Also, based on safety coverage with up to 300 mg QD dosing for 12 weeks (from part 1 of study 1402), no dose adjustment is proposed for patients with mild, moderate, or severe renal impairment.

Age, Body Weight, Sex, and Race:

No dose adjustment is required for patients based on sex, race, age, or body weight. The effects of sex, body weight or race on Omav exposure were not significant. Age had a significant effect on CL of Omav, suggesting a lower CL in older subjects. Compared to a reference group of 34-year-old subjects, subjects ≥ 65 years of age receiving 150 mg once daily will have 25% higher $AUC_{tau,ss}$ and 18% higher $C_{max,ss}$, respectively. Overall, the change in Omav CL with age is not expected to be clinically significant. Omav can be administered without regards to the covariates of age, sex, race, or body weight (as dosed in the MOXIe trial, Study 408-C-1402).

Concomitant administration with CYP450 enzyme modulators:

In a clinical drug interaction study (408-C-1806), AUC_{inf} of Omav was increased by ~4-fold with concomitant administration of strong CYP3A4 inhibitor (itraconazole) and increased by ~1.25-fold with concomitant administration of moderate CYP3A4 inhibitor/P-gp inhibitor (verapamil). Due to increase in AUC_{inf} of Omav, it is recommended to avoid concomitant administration of Omav with strong or moderate CYP3A4 inhibitors. However, if avoiding is not possible, a reduced dose of 50 mg QD (with concomitant strong CYP3A4 inhibitor) or 100 mg QD (with concomitant moderate CYP3A4 inhibitor) dose for Omav is recommended. If adverse events emerge, administration of Omav should be discontinued with concomitant administration of strong CYP3A4 inhibitors while Omav dose should be reduced to 50 mg QD with concomitant administration of moderate CYP3A4 inhibitor.

No clinically significant differences in PK of Omav are expected following concomitant with use with weak CYP3A4 inhibitors, thus no dose adjustment is needed with concomitant administration of weak CYP3A4 inhibitor.

As there may be loss of efficacy, concomitant administration of Omav with moderate or strong CYP3A4 inducers should be avoided.

2.3 Outstanding Issues

Please see section 1.2.

2.4 Summary of Labeling Recommendations

- Section 2.1 – Administer Omav 1h before eating because the C_{max} of Omav was ~350% higher with food.
- No dose adjustment is required with mild, moderate, or severe renal impairment patients because >92% drug related moieties were excreted via fecal route.
- No dose adjustment is required on the basis of sex, age, race, or body weight.
- Sections 2.5 and 8.6 – A reduced dose of 100 mg QD (or 50 mg QD if adverse events emerge) for Omav in FA patients with moderate hepatic impairment because the AUC_{inf} of Omav was ~1.65-

fold higher in moderate hepatic impairment patients. Although AUCinf of Omav was ~2.17-fold in severe hepatic impairment patients, Omav should be avoided in this population due to concerns about the safety of Omav in this population.

- Sections 2.4 and 7.1 – Omav PK was altered by inhibitors of CYP3A4. If patients with FA can't avoid concomitant use with strong and moderate CYP3A4 inhibitors, FA patients on concomitant moderate CYP3A4 inhibitors can receive Omav at a dose of 100 mg QD. If adverse events emerge, reduce the dose to 50 mg QD. FA patients on concomitant strong CYP3A4 inhibitors can receive Omav at a dose of 50 mg QD. If AEs emerge, concomitant administration with strong inhibitors should be suspended.
- Section 7.2 – Omav is a weak inducer of CYP3A4 and CYP2C8. Concomitant use with SKYCLARYS can reduce the exposure of CYP3A4 and CYP2C8 substrates which may reduce the activity of these substrates. Refer to the prescribing information of substrates of CYP3A4 and CYP2C8for dosing instructions if used concomitantly with SKYCLARYS and monitor for lack of efficacy of the concomitant treatment.
- Section 8.3: Omav is a weak inducer of CYP3A4. SKYCLARYS may decrease the efficacy of hormonal contraceptives. Advise patients to avoid concomitant use with combined hormonal contraceptives (e.g., pill, patch, ring), implants, and progestin only pills. Counsel females using hormonal contraceptives to use an alternative contraceptive method (e.g., non-hormonal intrauterine system) or additional non-hormonal contraceptive (e.g., condoms) during concomitant use and for 28 days after discontinuation of SKYCLARYS.

3. COMPREHENSIVE CLINICAL PHARMACOLOGY REVIEW

3.1 Overview of the Product and Regulatory Background

Omaveloxolone drug product is a 50 mg immediate release oral capsule. The recommended dose is 150 mg once daily 1h before meal. The clinical development program for FA consisted of 4 Phase 1 studies (3 in healthy subjects and 1 in hepatically impaired subjects) and 1 Phase 2 study (MOXIe trial, parts 1 and 2 of study 408-C-1402) with an OLE phase (part 3 of study 408-C-1402) to evaluate the safety, efficacy, pharmacokinetics, and pharmacodynamics of Omav in FA patients.

After the pre-IND interaction (June 2014) and IND submission (August 2014), the Agency allowed the FIH study in FA patients in September 2014. In the Type C meeting in December 2019, the Agency raised concerns on acceptability of a single safety and efficacy study for supporting an NDA submission and stated that a second adequate and well-controlled study is required for independent substantiation of the effectiveness of Omav in FA. The inclusion of mFARS as an intermediate clinical endpoint was deemed acceptable for part 2 of study 408-C-1402 with additional supportive evidence of efficacy from secondary endpoints. The Applicant suggested a post-hoc analysis in the OLE phase (part 3) where the placebo patients switched to Omav at the end of the 48-week double-blind treatment of part 2 of study 408-C-1402.

Based on preliminary review of the results in the "Delayed-start study" of OLE phase, in May 2021, the Agency recommended the Applicant to change their Type C meeting request to a pre-NDA meeting

request. At the pre-NDA meeting in September 2021, several Clinical Pharmacology aspects such as inadequacy of QT prolongation data from cQT analysis (need for a thorough QT study), accounting for nonlinear C_{max} in PBPK modeling, need for a clinical drug interaction study with CYP3A4 inducer, and exposure-response relationships be conducted by including allometry aspects in PPK modeling were discussed and acknowledged by the Applicant.

The Applicant conducted and submitted data for the following clinical studies under this NDA:

Study Identifier	Objective(s) of the Study	Study Design and Type of Control	Test Product(s)/ Dosage Regimen/Route of Administration	Number of Subjects	Healthy Subjects or Diagnosis of Patients	Duration of Treatment
408-C-1805	To assess the PK, mass balance, metabolite profiles, and rates and routes of elimination of [^{14}C]-omaveloxolone and derived metabolites following administration as a single 150 mg (containing approximately 90 µCi) dose to healthy male subjects	Phase 1, open-label, non- randomized, single dose study in healthy male subjects to investigate the AME of omaveloxolone	RTA 408 capsules, 150 mg Single oral dose of 150 mg of [^{14}C]-omaveloxolone containing approximately 90 µCi as a capsule after an overnight fast of at least 10 hours	8	Healthy Subjects	Single-dose, with maximum stay through Day 23
408-C-1804	To assess PK of omaveloxolone following a single dose of omaveloxolone in subjects with mild, moderate, or severe hepatic impairment comparted to health subjects with normal hepatic function.	Phase 1, open-label, non- randomized, parallel-group study to determine the effect of hepatic impairment on PK, safety, and tolerability of a single oral dose of omaveloxolone compared to matched healthy subjects with normal hepatic function	RTA 408 capsules, 50 mg A single dose of RTA 408 (150 mg, 3 capsules) administered to the subjects the morning following an overnight fast of at least 10 hours.	32	2 groups: Subjects with hepatic impairment and Subjects with normal hepatic function	Single dose, with follow-up through Day 15
408-C-1703	Determine the dose proportionality and the effect of food on the pharmacokinetics of RTA 408 in healthy adult subjects.	Part 1 Food Effect: Open label, two period, two- sequence, randomized, cross-over to investigate the effect of food on the PK of RTA 408 Part 2 Dose Proportionality: Open label, randomized phase to access the dose proportionality of RTA 408 PK	RTA 408 Capsules, 50 mg Part 1: Two single doses of RTA 408 (150 mg, 3 capsules) were administered to the subjects in fed (high-fat, high-calorie meal) and fasted states. Part 2: Subjects were randomly assigned to one of the two treatments of RTA 408 (50 mg or 100 mg). A single dose of RTA 408 was administered to the subjects in a fasted state.	Part 1: 16 Part 2: 18 (Total: 34)	Healthy Subjects	Part 1: single-dose each period (fasted or fed) Part 2: single-dose, with confinement for 6 days

408-C-1806	Part 1: Determine impact of multiple oral doses of omaveloxolone on the single oral dose PK of midazolam, repaglinide, metformin, rosuvastatin/digoxin cocktail Part 2: Determine impact of multiple oral doses of gemfibrozil on the single oral dose PK of omaveloxolone Part 3: Determine impact of multiple oral doses of itraconazole on the single oral dose PK of omaveloxolone Part 4: Determined impact of multiple oral doses of verapamil on the single oral dose PK of omaveloxolone	Phase 1, open-label, fixed- sequence, drug-drug interaction study in healthy subjects conducted in 4 parts. Consisting of 1 treatment period only.	RTA 408 capsules, 150 mg Part 1: Single oral doses of 2 mg midazolam, 1 mg repaglinide, 500 mg metformin, 10 mg rosuvastatin/0.25 mg digoxin cocktail, Multiple oral doses of 150 mg omaveloxolone (QD) Part 2: Single oral doses of 150 mg omaveloxolone, multiple oral doses of 600 mg gemfibrozil (QD Part 3: Single oral doses of 150 mg omaveloxolone, multiple oral doses of 200 mg itraconazole (QD) Part 4: Single oral doses of 150 mg omaveloxolone, Multiple oral doses of 120 mg verapamil (QD)	Part 1: 16 Parts 2, 3 and 4: 15 in each part (Total: 61)	Healthy Subjects	Part 1: ~9 weeks total duration of study with QD Omav on Days 12 to 27 Parts 2, 3, and 4: 8 weeks total duration of study with QD Omav on Days 1 and 13
408-C-1402 Part 1	Determine the efficacy and safety of RTA 408 Capsules versus placebo in the treatment of patients with Friedreich's ataxia	Multi-center, double-blind, randomized, placebo- controlled, dose-ranging, efficacy study	RTA 408 5 mg to 300 mg or placebo QD	69	Patients with genetically confirmed Friedreich's ataxia	Treatment: 12 weeks Follow-up: 4 weeks Total Duration: 16 weeks
408-C-1402 Part 2	Determine the efficacy and safety of RTA 408 Capsules versus placebo in the treatment of patients with Friedreich's ataxia	Multi-center, double-blind, randomized, placebo- controlled, dose-ranging, efficacy study	RTA 408 150 mg or placebo QD	103	Patients with genetically confirmed Friedreich's ataxia	Treatment: 48 weeks Follow-up: 4 weeks Total Duration: 52 weeks
408-C-1402 Extension	Determine the efficacy and safety of RTA 408 Capsules versus placebo in the treatment of patients with Friedreich's ataxia	Open label dose-escalation safety evaluation	RTA 408 150 mg QD	149	Patients with genetically confirmed Friedreich's ataxia	Open-label, long-term extended access (Treatment Duration 2.8 years as of 17 August 2021)

3.2 General Pharmacology and Pharmacokinetic Characteristics

Pharmacology	
Mechanism of Action	Omaveloxolone selectively and reversibly binds to Keap1, resulting in the activation of Nrf2, a transcription factor that modulates the expression of genes involved in regulating mitochondrial function, oxidative stress, and inflammation.
Active Moieties	Omav is considered as the active moiety. M22 and M17, the major metabolites of Omav, were pharmacologically inactive in nonclinical studies.
QT Prolongation	The effect of omaveloxolone on the QTc interval has not been adequately characterized. (See QT-IRT Review dated 02/22/2022).
General Information	
Bioanalysis	The concentrations of Omav in human plasma were measured using three validated LC-MS/MS methods. The lower limit of quantification (LLOQ) in plasma was 0.073 ng/ or 0.075 ng/mL. Please refer to Section 4.1 for details.
Healthy Volunteers vs. Patients	MAD study was not conducted in HV. A comparison between FA patients and healthy subjects is not established.
Dose Proportionality	AUC of Omav was dose proportional from 50-150 mg single dose for AUC, and less than dose proportional for C_{max}.
Accumulation	The exposures in FA patients after multiple (QD) dosing of 150 mg shows accumulation ratio (RAC) for C_{max} and AUC to be between 1.7 to 2.3.
Variability	In FA patients, the coefficient of variation (CV%) was approximately 46% for $C_{max,0-24h}$ and 35% for AUC_{0-24h}. The coefficient of variation (CV%) was approximately 34% for $C_{max,ss}$ and 35% for AUC_{ss}.
Absorption	
Bioavailability	The absolute oral bioavailability of Omav was not determined .
T_{max}	The median T_{max} for Omav is 7 to 14 h under fasting condition
Food effect (high-fat meal) GMR relative to fasted state	A high-fat meal increased C_{max} by ~350% and AUC by ~15%.
Distribution	
Volume of Distribution	Based on population PK analysis (Study REAT-PMXOMAV-2081), the typical apparent volume (Vc/F) is 410 L. The typical apparent peripheral volume (Vp/F) is 6951 L.
Plasma Protein Binding	97%
Substrate transporter systems	The following information was concluded from in vitro studies: • Omav is a weak substrate of P-gp. • Omav inhibited OAT1,OCT1, P-gp, and OATP1B3, however IC_{50} values were much greater than clinically relevant concentrations.
Elimination	
Mean Terminal Elimination half-life	Approximately 57 h in healthy subjects (from different Phase 1 studies)
Metabolism	

Primary metabolic pathway(s)	Omav was metabolized majorly by CYP3A4 followed by minor contribution by CYP2C8 and CYP2J2
Inhibitor/Inducer (in vitro)	• Omav has inhibition potential on CYP3A4 and CYP2C8 • Omav is a weak inducer of CYP3A4
Excretion	
Primary excretion pathways	Human mass balance study showed that Omav is primarily excreted in feces. Approximately 92% was recovered in feces (~40% excreted as unchanged Omav and ~90% of radioactivity was recovered in first 96h post-dose). Less than 0.1% radioactivity was recovered in urine (Study 408-C-1805).

3.3 Clinical Pharmacology Review Questions

3.3.1 To what extent does the available clinical pharmacology information provide pivotal or supportive evidence of effectiveness?

The pivotal evidence of effectiveness came from part 2 of a single Phase 2 study 408-C-1402 (also referred to as MOXIe study) in 103 patients with FA (51 in part 1 and 52 in part 2). Supportive evidence of effectiveness included delayed start analysis using data from open label extension (OLE) and propensity matched analysis that includes the FA-COMS natural history data. Finally, biomarker data were provided for additional mechanistic support for efficacy of Omav in FA patients.

Controlled Efficacy data from study 408-C-1402:

Study 408-C-1402 comprised parts 1 and 2. Part 1 was a randomized, placebo-controlled, double-blind, dose-ranging study to evaluate the safety, efficacy, and PD of Omav at 2.5, 5, 10, 20, 40, 80, 160, and 300 mg in 69 FA patients (52 with Omav and 17 with placebo; ~50% were men with mean age of 25.9±6.41 y). The double-blind treatment duration was 12 weeks. In Part 1, there was no statistically significant difference in the primary endpoint, the peak workload on exercise testing at 12 weeks. Although, no dose response was observed in the key secondary endpoint, the modified Friedreich's Ataxia Rating Scale (mFARS), the Applicant conducted post-hoc analysis to rationalize the dose selection for Part 2 of this study. In this analysis, the Applicant asserted greater improvement on mFARS in a subgroup of patients without pes cavus at 160 mg (n=4 on Omav and n=7 placebo) with a nominal p-value of 0.01. This was the basis of selecting the dose of 150 mg and the patient population (patients without pes cavus) for the primary analysis in Part 2 of the study (Note: patients with pes cavus have a musculoskeletal foot deformity and it may represent a different subtype of FA that has a different pathophysiology and clinical phenotype).

It should be noted that Part 1 of the study was a small and short study that doesn't seem to support the effectiveness of Omav. However, this study supported the safety of Omav up to 300 mg. Biomarker data from part 1 of the study were combined with data from part 2 to provide mechanistic support and to rationalize dose selection.

Part 2 was a randomized, double-blind, placebo-controlled (1:1) study to assess the efficacy and safety of Omav (150 mg) in 103 patients with FA (51 with Omav and 52 with placebo) for up to 48 weeks (with 24 adolescent patients). As patients without pes cavus responded better (on change in mFARS score) in part 1, patients in part 2 were stratified by their pes cavus status such that ~80% were without pes cavus.

Per the Applicant's analysis, at Week 48, the change from baseline in mFARS (primary efficacy endpoint) was significantly greater (-2.41 points in patients without pes cavus, p=0.0138) in Omav group relative to placebo (see **Figure 1**). The secondary endpoints, PGIC and CGIC, were not statistically different compared to placebo except FA-ADL which was last the hierarchy. Please refer to the Clinical review by Dr. Veneeta Tandon and Statistics review by Dr. Jinnan Liu for further details on safety and efficacy analyses from part 2.

Figure 1: Change in primary efficacy endpoint (change from baseline in mFARS) with 150 mg dose at week 48.

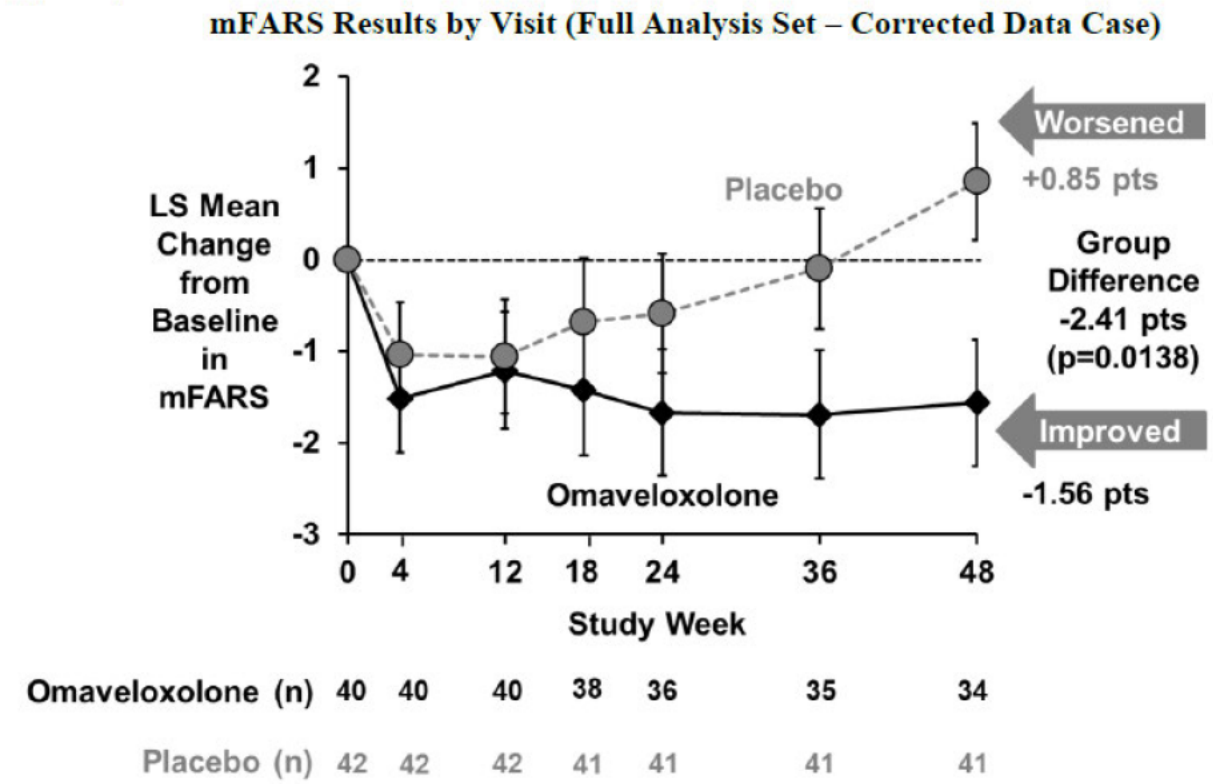

Source: CSR addendum for study 408-C-1402, part 2, page 10 of 700

Supportive Evidence from OLE study:

The Applicant also provided supportive efficacy data for Omav from open-label extension (OLE) study using delayed-start analysis and evaluation of Part 2 and extension study results using a propensity

matched analysis that includes the FA-COMS natural history data. The propensity matched data were submitted late in the review cycle which were considered as a major amendment to the NDA.
For delayed-start analysis, patients in the placebo-Omav group (i.e., patients initially randomized to placebo in study 1402 Part 2 who then initiated treatment with Omav in OLE study) began treatment with Omav 52 weeks after patients in the Omav-Omav group (i.e., patients initially randomized to Omav in study 1402 Part 2 who continued Omav treatment in OLE study). The primary efficacy analysis performed in patients without pes cavus, demonstrate that the difference in mFARS between Omav and placebo groups at the end of the placebo-controlled part 2 was preserved at week 72 of the delayed-start period.

In propensity matched analysis, patients from OLE study were compared to natural history cohort (external controls). Specifically, patients from FA-COMS were matched to Study 1402 Extension patients using propensity scores based on multiple covariates. The change from baseline in mFARS at Year 3 for study 1402 OLE patients compared to the propensity score-matched FA-COMS patients was analyzed as the primary efficacy endpoint using mixed model repeated measures (MMRM) analysis. Change from baseline in mFARS at Year 1 and Year 2 were secondary endpoints. The Applicant reported that Omav treated patients in study 1402 OLE experienced 55% slower progression of mFARS (difference of -3.607) compared to matched FA-COMS external control group at Year 3. Similar trends were observed at Year 1 and Year 2. Refer to Clinical review by Dr. Veneeta Tandon for additional discussion of these data.

Mechanistic Support from Biomarker Data:

In addition to clinical efficacy assessments (reduction in mFARS scores), the Applicant submitted biomarker data from study 408-C-1402 to support the mechanistic activity of Omav as nuclear factor erythroid 2 related factor 2 (Nrf2) activator. Frataxin deficiency in patients with FA causes suppression of Nrf2 and mitochondrial energy production. Since Nrf2 (a nuclear receptor) is down-regulated in FA patients, activation of Nrf2 could be a potential therapeutic target for treatment of FA. Nonclinical and in vitro data submitted by the Applicant suggested that Omav is a Nrf2 activator in vitro. We defer to the non-clinical review by Dr. Chun-Ting Lee for details about the non-clinical studies.

The Applicant submitted clinical data for five biomarkers measured in the plasma of patients treated with Omav in study 408-C-1402 to provide mechanistic support the Nrf2 activation. These biomarkers were the liver enzymes (ALT, AST, GGT), ferritin and creatinine kinase (CK). It should be noted that the detailed methodology on bioanalysis and validation of these biomarkers is not available, thus all biomarker findings discussed should be interpreted with caution.

The review team focused on evaluating whether these biomarkers can serve as pharmacodynamic biomarkers to confirm Nrf2 activation in patients.

Nrf2 is a transcription factor that regulates the expression of over 300 target genes with roles in antioxidant and anti-inflammatory actions, electrophile detoxication, cell metabolism, proliferation differentiation, and general cyto-protection. Based on the known biology of Nrf2 activation, measurement of target gene expression in PBMCs (e.g., NQO1, GCLM, FTH1, FTL), and plasma

glutathione, can provide a direct link for Nrf2 activation and can serve as pharmacodynamic biomarkers to provide direct link to support Nrf2 activation[1]; however, these were not collected in Study 1402.

Alternatively, the Applicant claimed that the 5 biomarkers ALT, AST, GGT, CK and ferritin can also serve as PD biomarkers for Nrf2 activation. Since these biomarkers are not well established to support Nrf2 activation, the review team pursued an extensive literature search to investigate the Applicant's hypothesis on whether the observed increases in these five biomarkers is a downstream effect of Nrf2 activation.

The OCP review team consulted the Division of Applied Regulatory Sciences (DARS) within OCP to get their feedback. The DARS consult response (received on 08/15/2022) concluded that "Based on in vitro, animal and clinical studies, it appears that the increased levels of aminotransferases following omaveloxolone administration is a pharmacodynamic effect related to Nrf2 activation rather than liver toxicity". However, the review team still had concerns about the specificity of these biomarkers to support Nrf2 activation. The Applicant eventually abandoned the endorsement of ALT, AST and CK as a selective downstream biomarker of Nrf2 pathway and proposed that ferritin and GGT should be considered as biomarkers of Nrf2 activation. Thus, the focus was eventually centered on evaluating ferritin and GGT as clinical biomarkers of Nrf2 activation in vivo.

The Agency noted that Literature data indicate that ferritin may also be a marker of other pathological conditions, including liver disease, metabolic syndromes, and abnormal heart conditions or cell damage. An IR was sent to the Applicant to explain why increases in ferritin levels in plasma should be considered a specific pharmacodynamic biomarker for Nrf2 activation in humans. In response (received on 01/12/2023), the Applicant acknowledged that other factors can also influence the serum levels of ferritin. For example, under pathological conditions, elevations in serum ferritin can be significant and may be the direct result of cellular damage, particularly hepatocellular damage. In addition, increased synthesis and/or secretion of ferritin may result from iron overload, infection, inflammation, and metabolic syndrome. However, the Applicant noted that there were no imbalances in adverse events (AEs) or serious adverse events (SAEs) that are reflective of pathological conditions generally associated with elevated serum ferritin levels in Study 1402.

Further, the Applicant cited a literature study in which a dose dependent increase in ferritin-H mRNA was observed in human peripheral blood mononuclear cells 8 hours after initiation of treatment with Omav in an oncology clinical trial [2]. The Applicant also cited studies showing increase in ferritin mRNA in mouse and monkey liver tissues after Omav administration. The Applicant also noted in previous

---

[1] Kerins MJ, Ooi A. The Roles of NRF2 in Modulating Cellular Iron Homeostasis. Antioxid Redox Signal. 2018 Dec 10;29(17):1756-1773. doi: 10.1089/ars.2017.7176. Epub 2017 Sep 21. PMID: 28793787; PMCID: PMC6208163.

[2] Creelan BC, Gabrilovich DI, Gray JE, Williams CC, Tanvetyanon T, Haura EB, Weber JS, Gibney GT, Markowitz J, Proksch JW, Reisman SA, McKee MD, Chin MP, Meyer CJ, Antonia SJ. Safety, pharmacokinetics, and pharmacodynamics of oral omaveloxolone (RTA 408), a synthetic triterpenoid, in a first-in-human trial of patients with advanced solid tumors. Onco Targets Ther. 2017 Aug 29;10:4239-4250. doi: 10.2147/OTT.S136992. PMID: 28919776; PMCID: PMC5587199.

submissions that both GGT and ferritin were transcriptionally regulated by Nrf2 in rodent cells based on Zhang et al[3] (please refer to the non-clinical review for details).

These findings may suggest that the increase in ferritin in the plasma may be related to Nrf2 activation. However, the increase in ferritin due to Omav mediated cell damage can't be ruled out. Finally, the Applicant's rationale for considering GGT as marker of Nrf2 activation remain unproven due to lack of satisfactory literature evidence.

3.3.2 Is the proposed dosing regimen appropriate for the general patient population for which the indication is being sought?

Yes, the Applicant is seeking approval at for 150 mg QD 1h before meal. This dose was well tolerated in the 48-week pivotal Phase 2 study (408-C-1402 part 2). The rationale for dose selection was mainly based on the Applicant's post-hoc analysis of doses tested in Part 1 of the study. In this analysis, the Applicant asserted greater improvement on mFARS in a subgroup of patients without pes cavus at 160 mg (4 on Omav and 7 placebo) with a nominal p-value of 0.01.

Additional supportive biomarker data such as liver transaminases (ALT and AST), GGT, ferritin and creatine kinase were used to select the efficacious dose for part 2. Per the Applicant, these biomarkers demonstrated maximal elevation at doses equal or higher than 160 mg QD in Part 1 of the study.

However, it should be noted that Part 1 was a small study and there was no clear dose response for the clinical endpoints in this part of the study. Although, the 160 mg dose level demonstrated superiority (greatest change in mFARS and biomarker profiles) compared to other dose levels at week-12, the 300 mg dose did not show any improvement in mFARS score and the 5 mg dose level showed comparable reduction in mFARS to the reduction seen with 160 mg dose level.

Although the clinical efficacy and safety data in part 1 of study 408-C-1402 were acquired using 160 mg dose, considering the formulation challenges and dosing feasibility, the 150 mg dose (3 capsules of 50 mg) was selected for the future clinical development program of Omav (part 2 and OLE phase of study 408-C-1402). This difference in dose is <10% and was expected to provide a comparable pharmacologic response.

3.3.3 Is an alternative dosing regimen and/or management strategy required for subpopulations based on intrinsic factors?

Yes, as Omav exposure was increased in subjects with moderate or severe hepatic impairment, dose adjustment or modification are required as described below.

Hepatic Impairment:

---

[3] Zhang H, Liu H, Dickinson DA, et al. Gamma-Glutamyl transpeptidase is induced by 4-hydroxynonenal via EpRE/Nrf2 signaling in rat epithelial type II cells. Free Radic Biol Med. 2006;40:1281-1292.

The effect of hepatic impairment was evaluated in a Phase 1, single-dose (150 mg), open-label, PK study (408-C-1804). No dose adjustment is needed for mild hepatic impairment subjects as Omav exposure were not significantly different than healthy controls. Higher exposure of Omav was observed in subjects with moderate or severe hepatic impairment compared to normal hepatic function.

Compared to healthy controls, subjects with mild hepatic impairment had ~29% higher C_{max}, while the total exposure was comparable. In subjects with moderate hepatic impairment, AUC_{inf}, AUC_{0-t}, and C_{max} values were 65%, 56%, and 83% higher, respectively, compared to healthy controls. Subjects with severe hepatic impairment had 117% increase in AUC_{inf}, 27% increase in AUC_{0-t} and 32% decrease in C_{max} compared to healthy controls. The PK data from severe hepatic impairment cohort should be interpreted with caution due to sample size (n=3 to 5) and PK variability.

The review team recommended lowering the Omav dose to 100 mg QD in patients with moderate hepatic impairment with close monitoring for adverse events. If adverse events persist, a further reduction to 50 mg QD is recommended in these patients. For patients with severe hepatic impairment, Omav should be avoided due to clinical team's concerns about the limited safety data in these patients. No dose adjustment is needed for patients with mild hepatic impairment.

Renal impairment:

The effect of renal function on omaveloxolone was not formally evaluated in the clinical studies. Based on the insignificant contribution of renal elimination pathway to excrete Omav and its metabolites (<0.1% radioactivity in urine from mass-balance study), no dose adjustments are needed for mild, moderate, or severe renal impairment patients (eGFR 30-89 mL/min/1.73m^2). It should be noted that there were 14 patients with eGFR between 60-89 mL/min/1.73m^2 and 89 patients above 89 mL/min/1.73m^2 (total 103 patients studied in part 2 of the pivotal study 1402). Also, there was safety coverage with up to 300 mg QD dosing for 12 weeks (from part 1 of study 1402). Furthermore, renal function status was not identified as a significant covariate in the PPK analysis.

Body weight, age, sex, and race:

The effect of various intrinsic factors, including demographic variables like age, race, sex, and body weight was evaluated in the popPK analysis. Based on covariate analysis, only baseline age (median age in PPK dataset was 34 years; range, 16-71 years) was found to have a significant influence on CL. Although, simulations from PPK analysis showed that mean steady-state C_{max} and AUC in subjects ≥65y are 26% and 24% higher than the mean steady-state C_{max} and AUC of reference subject (34y), these differences between age groups are not clinically meaningful and lie in the range of inter-subject variability. Overall, no dose adjustments are needed in adult FA patients with respect to body weight, age, sex, or race.

3.3.4 Are there clinically relevant food-drug or drug-drug interactions and what is the appropriate management strategy?

Yes. Detailed dosing recommendations for drug interactions and administration with regard to food are described below.

Food Effect:

Food effect was evaluated in a food effect study in healthy volunteers in Study 408-C-1703. Co-administration of Omav with a standard high-fat meal resulted in ~4.5-fold increase in C_{max}. However, AUC was increased by ~15% only.

In the pivotal Phase 2 study (408-C-1402, MOXIe trial), Omav was administered 1h before meal. The dosing proposed by the Applicant matches with the one utilized in the pivotal efficacy study with respect to food intake. Therefore, for the final US prescribing information, the review team recommends the same dosing instruction for administering Omav as used in the Phase 2 study.

Drug-Drug Interactions (DDI):

DDI with CYP450 enzymes

Omav as an inhibitor/inducer of major CYP450 enzymes

In vitro, Omav inhibited CYP3A4 and CYP2C8 and induced CYP1A2 (1.01-fold), CYP2B6 (1.61-fold) and CYP3A4 (2.35-fold) enzymes at clinically relevant concentrations. Based on these *in vitro* DDI data, the Applicant conducted a 4-part clinical DDI study (408-C-1806) – a Phase 1, open-label, fixed-sequence, drug interaction study in healthy adults. Part 1 evaluated the perpetrator potential of Omav (administered at steady state). A total of 16 subjects were enrolled in Part 1 with an aim to achieve 12 evaluable subjects. Omav-mediated inhibition/induction of CYP450 was evaluated with substrates of CYP3A4 (2 mg single oral dose of midazolam administered on Days 1 and 18) and CYP2C8 (1 mg repaglinide administered on Days 2 and 19) with Omav administered at 150 mg QD dosing (Days 12 to 27 to achieve steady state).

The systemic exposure of probe drugs (midazolam and repaglinide) was reduced following co-administration of Omav compared to when administered alone. The GLSM ratio of test:reference (where, test = probe substrate + Omav and reference = probe substrate alone) for AUC_{inf} were 0.55 and 0.65 for midazolam and repaglinide respectively. Similar trend in GLSM ratio was observed for C_{max}. Based on these data, Omav is considered as a weak inducer of CYP3A4 and CYP2C8. See Figure 2 for a graphical representation of DDI data.

Based on these data Omav is not a CYP450 inhibitor but is considered as a weak inducer of CYP3A4 and CYP2C8. Although, the review team recommended no dose adjustment for substrates of CYP3A4/5 and CYP2C8, patients and prescribers should refer to the USPI of substrates of these CYP enzymes when co-administering with Omav. Whereas a potential DDI between Omav and oral hormonal contraceptives

cannot be ruled out. Therefore, labeling language of potential DDI was captured in the proposed label of Omav in sections 7.2 and 8.3.

Omav as a substrate of major CYP450 enzymes

In vitro, Omav was mainly metabolized by CYP3A4 with minor metabolism by CYP2C8 and CYP2J2. Based on these, clinical drug interaction between Omav and inhibitors of CYP3A4 and CYP2C8 was evaluated using itraconazole (Part 2) and gemfibrozil (Part 3) (study 408-C-1806), respectively. The dosing regimen for Parts 2 and 3 are listed below.

Part 2: Single oral doses of 150 mg Omav on Days 1 and 13 with multiple oral doses of 600 mg gemfibrozil BID on Days 10 to 18.

Part 3: Single oral doses of 150 mg Omav on Days 1 and 13 with multiple oral doses of 200 mg itraconazole QD on Days 10 to 18.

Coadministration with itraconazole (strong CYP3A4 inhibitor) resulted in ~4.1- and ~3-fold increase in AUC_{inf} and C_{max} of Omav, respectively. No significant changes in C_{max} and AUC_{inf} of Omav were observed with coadministration of gemfibrozil (strong CYP2C8 inhibitor). See Figure 3 for a graphical representation of DDI data.

Based on these results, no clinically significant DDIs are anticipated when Omav is co-administered with inhibitors of CYP2C8, thus no dose adjustments for Omav are needed with coadministration with CYP2C8 inhibitors. Based on ~4-fold increase in AUC_{inf} of Omav with coadministration of a strong inhibitor of CYP3A4/5, the Applicant proposed contraindicating the use of Omav with CYP3A4 strong and moderate inhibitors. However, the clinical pharmacology team provided dose adjustment recommendations after considering the available dose strength (50 mg capsule) and leveraging available safety information from doses tested up to 300 mg in Part 1 of the registration trial. The team recommended to initially avoid the use of Omav with strong CYP3A4 inhibitors. If coadministration can't be avoided, a 50 mg QD is recommended with close monitoring. If adverse events emerge, coadministration with strong CYP3A4 inhibitors should be discontinued. Although the 50 mg QD dosing is expected to result in increasing the exposure to levels higher than actual dose of ~205 mg which is greater than the recommended dose (150 mg QD), there is sufficient safety coverage from part 1 of study 1402 in FA patients who received doses up to 300 mg QD for 12 weeks without any major or irreversible adverse events. The safety coverage was confirmed by the clinical review division.

The review team also recommended dose adjustment for Omav with concomitant moderate CYP3A4 inhibitor if concomitant use can't be avoided. This was based on PK data in part 4 of study 408-C-1806 (further described below) where verapamil (a moderate CYP3A4 inhibitor) increased AUC_{inf} of Omav by 1.25-fold. However, the review team noted few study-design concerns (timing of dosing and actual dose of verapamil were not in line with the literature and other parts of this DDI study) which limit the ability to completely rely on the results. However, the team used the following rationale to provide dose adjustment recommendations with concomitant moderate CYP3A4 inhibitor.

Although the observed 25% increase in exposure in the verapamil DDI study can be underpredicting the drug interaction with moderate CYP3A4 inhibitors, it's unlikely that the increase will be higher than the increase observed with strong CYP3A4 inhibitors (~4 folds). Also, PBPK modeling suggested up to (b) (4) increase in exposure with the moderate inhibitors, however the PBPK model is not considered adequate because it was not validated and its possible that these predictions are over predicting the true drug

interaction. Refer to PBPK review (section 4.6 of this review) for further discussion of these discrepancies.

Based on these information, the team is recommended dose reduction for Omav to 100 mg QD with close monitoring. A conservative assumption of three-fold increase in exposure upon coadministration with moderate CYP3A4 inhibitors, potential increase in exposure with a 100 mg QD dose may not exceed the exposure from 300 mg dose in the general population. Safety of the 300 mg dose has been established based on results from part 1 of the registration trial. If adverse events emerge, the team recommended lowering the dose further to 50 mg daily.

No dose adjustment for Omav is needed with concomitant administration of weak CYP3A4 inhibitor as the expected change is exposure may not be clinically significant.

DDI with transporters

Omav as a substrate of transporters

In vitro, Omav was found to be a weak substrate of P-gp. Thus, Part 4 evaluated the victim potential of Omav with a clinically relevant P-gp inhibitor (verapamil). (Note: verapamil is also known to be a moderate inhibitor of CYP3A4). The dosing regimen for Part 4 was:
Part 4: Single oral doses of 150 mg Omav on Days 1 and 13 with multiple oral doses of 120 mg verapamil (QD) on Days 10 to 18.
Coadministration with verapamil (P-gp inhibitor and also a moderate CYP3A4 inhibitor) resulted in ~1.25-fold increase in AUC_{inf} and C_{max} of Omav. See Figure 3 for a graphical representation of DDI data from Parts 2, 3 and 4.

Although verapamil (a P-gp inhibitor and a moderate CYP3A4 inhibitor) did not significantly alter PK (C_{max} and AUC) of Omav, the review team noted that dose (120 mg QD) and time of verapamil administration (1h before Omav) in the study were not in line with published DDI studies (as briefly discussed above). However, the inhibition or induction effect of Omav on P-gp is expected to be less than that of CYP3A4 because the cellular permeability of Omav *in vitro* (by measuring transit across human epithelial cell lines such as Caco-2 cell, MDCKII MDR1, and MDCKII-BCRP) was shown to have a low permeability indicating Omav as potentially a weak substrate of P-gp. A literature study had similar results with grapefruit juice on disposition of saquinavir (a CYP3A4 and P-gp substrate) where a greater effect was observed with CYP3A4 inhibition compared to P-gp inhibition[4]. Thus, no dose adjustment for Omav with concomitant P-gp inhibitor is needed.

Omav as an inhibitor of transporters

In vitro, Omav inhibited P-gp, OCT1, and BRCP at clinically relevant concentrations. Thus, Omav-mediated inhibition/induction of transporters was evaluated with probe substrates of BCRP/P-gp (10 mg rosuvastatin/0.25 mg digoxin cocktail administered on Days 5 and 22) and OCT1 (500 mg metformin administered on Days 3 and 20) in a Clinical DDI study (Part 1 of study 408-C-1806). Omav was

[4] Eagling VA, Profit L, Back DJ. Inhibition of the CYP3A4-mediated metabolism and P-glycoprotein-mediated transport of the HIV-1 protease inhibitor saquinavir by grapefruit juice components. Br J Clin Pharmacol. 1999 Oct;48(4):543-52. doi: 10.1046/j.1365-2125.1999.00052.x. PMID: 10583025; PMCID: PMC2014377.

administered at 150 mg QD dosing (Days 12 to 27 to achieve steady state). PK sampling for rosuvastatin/digoxin cocktail was performed on Days 5 (pre Omav dosing) and 22 (post Omav dosing) and for metformin on Days 3 (pre Omav dosing) and 20 (post Omav dosing).

The systemic exposure of probe drugs (metformin, rosuvastatin and digoxin) was reduced/unchanged following co-administration of Omav compared to when administered alone. The GLSM ratio of test:reference (where, test = probe substrate + Omav and reference = probe substrate alone) for AUC_{inf} were 1.03, 0.70 and 0.97 for metformin, rosuvastatin and digoxin, respectively. Similar trend in GLSM ratio was also observed for C_{max} values too. See Figure 2 for a graphical representation of DDI data.

Based on these data, rosuvastatin PK was not increased but rather slightly decreased when co-administered with Omav. As rosuvastatin is also an OATP1B substrate, it is not possible to attribute whether the observed rosuvastatin PK changes are due to induction of BCRP and/or OATP1B. As transporter induction studies are not usually reported on the USPIs for drug products and because the observed decrease in the exposure was not major, there will be no labeling recommendations about dose adjustments with BCRP and OATP1B substrates. Also, no dose adjustments are recommended for coadministration with P-gp and OCT1 substrates.

These clinical DDI data with CYP450 enzymes and transporters and associate labeling recommendations are discussed in sections 2.4, 7.2 and 12.3 of the label.

Figure 2: Forest plot illustrating the degree of drug interaction with of Omav as a Drug Interaction Perpetrator

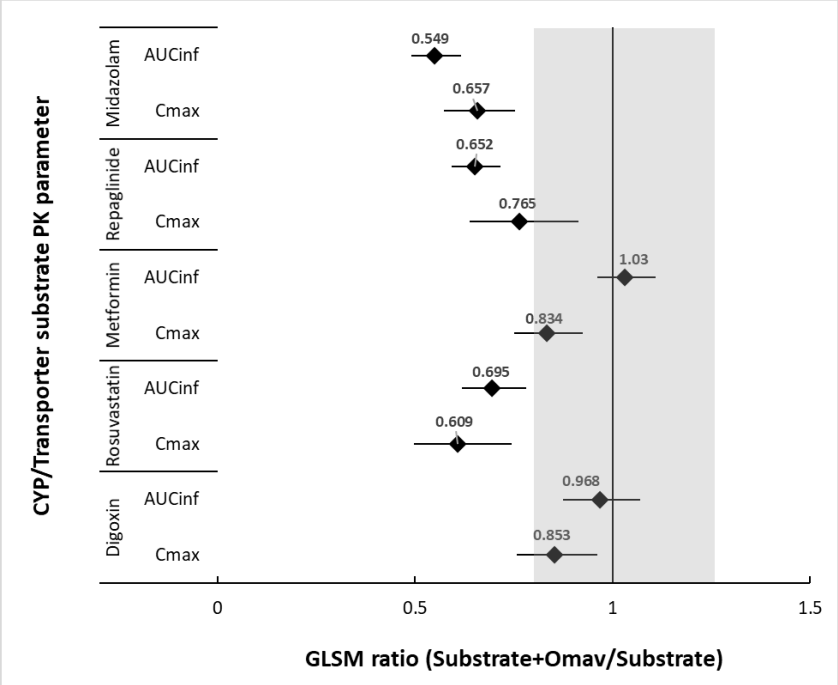

Source: Reviewer generated. Shaded region represents 0.80 to 1.25 CI
Error bars represent 90% CI

Figure 3: Forest plot illustrating the degree of drug interaction with of Omav with as a Drug Interaction Victim

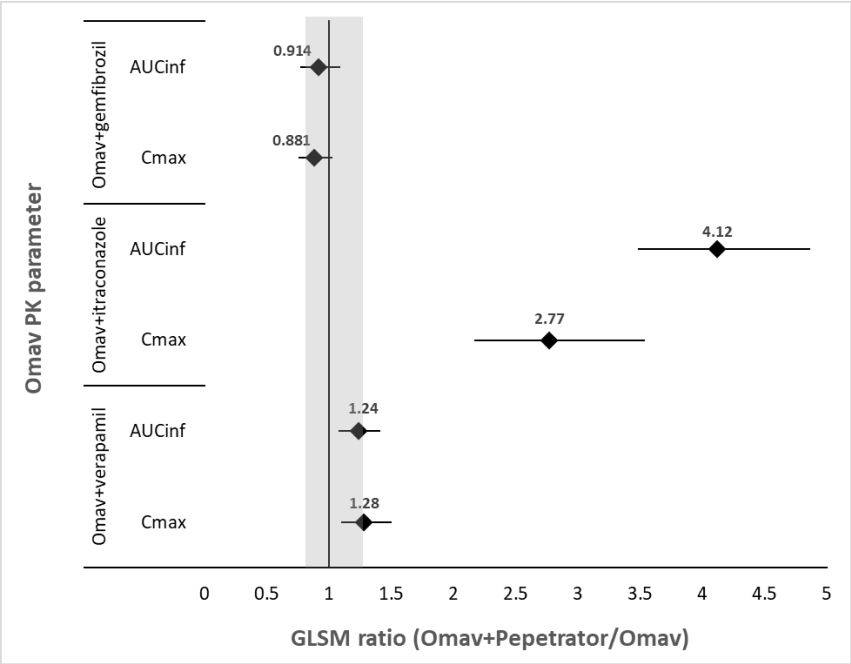

Source: Reviewer generated. Shaded region represents 0.80 to 1.25 CI
Error bars represent 90% CI

3.3.5 Is the to-be-marketed formulation the same as the clinical trial formulation, and if not, are there bioequivalence data to support the approval of the to-be-marketed formulation?

Yes. The Applicant used the to-be-marketed (TBM) formulation in the pivotal Phase 2 safety and efficacy study in FA patients, thus no additional bioequivalence studies were necessary.

4. APPENDICES

4.1 Summary of Bioanalytical Method Validation and Performance

PK analysis of Omav was performed with plasma concentrations measured using three validated liquid chromatography with tandem mass spectrometric detection (LC-MS/MS) assays (Method 1 (b) (4)), (Method 2 (b) (4)) and (Method 3 (b) (4)) (**Table 1: Summary of Bioanalytical Methods**).

Table 1: Summary of Bioanalytical Methods

Method ID	Matrix	LLOQ (ng/mL)	ULOQ (ng/mL)	Method Validation Report	Clinical Studies Using This Method
Method 1 (b) (4)	Plasma	0.073	36.9	(b) (4) 1402484	408-C-1402 (Part 1) 408-C-1403
Method 2 (b) (4)	Plasma	0.075	40	161546VEA_RIT_R1	408-C-1402 (Part 2) 408-C-1403 408-C-1703 408-C-1804
Method 3 (b) (4)	Plasma	0.075	75	8400495	408-C-1805 408-C-1806

The OCP review team noted that the bioanalytical methods for quantification of Omav were adequately validated in accordance with FDA Guidance for Industry, Bioanalytical Method Validation (May 2018). The method performance characteristics, including linear range, precision, accuracy, stabilities, recovery, are provided in **Table 2**.

Table 2: Summary of Bioanalytical Method Validation Information

Validation Parameters	**Method 1[a]**	**Method 2[b]**	**Method 3[c]**
Linear Range (ng/mL)	0.0734 to 36.9	0.075 to 40	0.075 to 75
Stock solution solvent	Methanol	Methanol	Methanol
Matrix	Human plasma	Human plasma	Human plasma
Dilution linearity (ng/mL)	0.0734, 0.184, 0.459, 1.15, 1.91, 3.19, 5.31, 8.86, 14.8, and 36.9	0.075, 0.150, 0.500, 2.00, 10.00, 30.00, 37.50, and 40	0.075, 0.150, 0.500, 2.00, 8.00, 30.00, 64.00, and 75.00
Recovery (%)	23.5 to 31.7	67 to 72	55.2 to 57.8
LLOQ (ng/mL)	0.073	0.075	0.075
ULOQ (ng/mL)	36.9	40	75
Specificity	NR	NR	Tested for hemolysis and hyperlipidemia. Met acceptance criteria (% CV values were ≤15.0% and mean bias values were within ±15.0% of the nominal concentration for each QC level).
Selectivity	Met acceptance criteria (100% of blank samples had peak areas less than 20% of the average peak area of the LLOQ without ISTD; 100% of blank samples had ISTD peak areas less than 5% of the ISTD peak area of the LLOQ standard).	Met acceptance criteria (at least 80% of the assessed lots had no interference >20% of mean response ratio of LLOQ standards; no interference observed for ISTD in individual blank matrix lots or for ISTD in matrix spiked with analyte and ISTD at ULOQ).	Met acceptance criteria (all 6 individual matrices tested demonstrated lack of significant interference with ≤20.0% of the mean acceptable LLOQ calibration standard response and ≤5.0% of ISTD response in the control zero sample in the chromatographic regions of the analyte and ISTD; at least 5 individual matrices generated individual concentration (mean for each matrix sample with more than 1 replicate) values within ±20.0% bias of the nominal concentration. The mean concentration for the 6 matrices generated overall mean bias and precision values of ±20.0% from nominal and CV ≤20.0%, respectively.
Intra-day/batch/run accuracy (%)	≤15.6 (LLOQ); ≤ -7.3 (ULOQ)	≤13.1	≤8.7
Intra-day/batch/run precision (%)	≤19.8 (LLOQ); ≤27.6 (ULOQ)	≤5.9	≤6.6

Validation Parameters	Method 1[a]	Method 2[b]	Method 3[c]
Inter-day/batch/run accuracy (%)	6.7 (LLOQ); -1.3 (ULOQ)	≤3.9	≤4.9
Inter-day/batch/run precision (%)	12.2 (LLOQ); 12.4 (ULOQ)	≤8.3	≤5.8
Dilution QC evaluation	CV: 4.5%; MB=-4.6%	Inter CV: ≤4.2%; RE: ≤6.0%; Intra CV: 4.1%; RE: 2.9%	CV: 2.6%; MB: -8.5%
Stock solution stability at room temperature	Room Temperature: 1 day, 18h Refrigerated: 13 days	Room Temperature: 22h 4°C: 100 days	Room Temperature: 6h
Matrix benchtop stability / short-term stability	At least 69h at 10°C	24h at room temperature	24h at room temperature
Autosampler stability at 10°C	At least 62 hours in an autosampler, setpoint 10°C	96 hours at 10°C	NR
Freeze-thaw stability at -20°C	At least 6 cycles	5 cycles	5 cycles
Freeze-thaw stability at -70°C for up to 5 cycles	NR	5 cycles	5 cycles
Long-term storage stability at -20°C	15 days	577 days	120 days
Long-term storage stability at -70°C	NR	577 days	120 days

Source: Module 2.7.1 Summary of Biopharmaceutics and Associated Analytical Methods, pages 23 and 24

For study 408-C-1402 part 1, the OCP reviewer noted a discrepancy in the long term storage stability at -20 ^{0}C between the bioanalytical report (408-c-1402-pt1-study-report.pdf) and the one summarized in module 2.7.1 and Clinical Pharmacology Summary Aid documents. The Applicant confirmed (IR response received on 06/15/2022) that long term storage stability of Omav at -20 ^{0}C was evaluated up to 1440 days in Method 1 (b) (4) which covers the duration of storage for study samples for study 408-C-1402 part 1.

4.2 *In Vitro* Studies

CYP metabolism (study RTA408-P-1208) In human liver microsomes, extensive turnover of Omav was observed, with <3% Omav remaining after 60-min incubation.

CYP phenotyping (study RTA408-P-1212) Using recombinant CYP450s (supersomes), Omav was confirmed to be extensively metabolized by CYP3A4 followed by CYP2C8 and CYP2J2. Metabolism (substrate loss) of Omav (1 and 10 µM) was observed with rCYP2C8 (45% and 27% loss, respectively), rCYP2J2 (43% and 33% loss, respectively) and rCYP3A4 (80% and 59% loss, respectively). This finding was confirmed in human liver microsomes using specific direct chemical inhibitors of CYP3A4/5 (ketoconazole) and CYP2C8 (gemfibrozil glucuronide) isozymes. The disappearance of Omav at 1 and 10 µM was inhibited (up to 99%) by the direct CYP3A4/5 inhibitor, and partially inhibited (up to 24%) with the metabolism-dependent CYP2C8 inhibitor. Incubation with UDPGA-fortified human liver suggested that UGT enzymes do not play a role (neither primary nor secondary glucuronidation) in Omav metabolism.

CYP inhibition (study RTA408-P-1106) The potential for Omav to inhibit CYP450 enzymes in human liver microsomes (CYP1A2, CYP2B6, CYP2C8, CYP2C9, CYP2C19, CYP2D6, and CYP3A4/5 [using two different substrates]) was evaluated. Omav directly inhibited CYP2C8 with an IC50 value of 0.67 µM and CYP3A4/5 (midazolam 1'-hydroxylation) with IC50 values of 0.7 µM and 0.8 µM. The data revealed that Omav was a mixed inhibitor of CYP2C8 and CYP3A4/5 (midazolam 1'-hydroxylation) with K_i values of ~ 0.5 µM for each enzyme. Omav caused no or slight metabolism-dependent inhibition of CYP1A2, CYP2B6, CYP2C8, CYP2C9, CYP2C19, CYP2D6, or CYP3A4/5.
To support the observed steady-state C_{max} at the therapeutic dose (i.e., 150 mg), Omav was incubated at higher conc. (up to 10 µM) with human liver microsomes (study RTA-P-17011). Omav directly inhibited CYP2C9 and CYP3A4/5 with IC_{50} values of 4.8 and 4.9 µM, respectively. However, these IC_{50} values >> than unbound steady state C_{max} at therapeutic dose.

CYP inhibition activity of metabolites (study RTA-P-20022): Two major metabolites (i.e., >10% of total AUC) in human plasma were identified in the single oral dose [14C]omaveloxolone human ADME study. M22 (TX304579, 1,2-dihydro-30-COOH omaveloxolone) and M17 (TX304571, 1,2-dihydro-29-OH omaveloxolone) accounted for 18.6% and 10.9% of total plasma radioactivity, respectively. Neither M17 nor M22 possessed any meaningful CYP inhibition activity.

Plasma protein binding (study RTA408-P-1124) Omav is 97% bound to protein in human plasma, the blood-to-plasma ratio in human was 0.694 over the concentration range 10 to 2000 ng/mL, and no concentration dependence was observed for blood-to-plasma partitioning.

CYP induction (study RTA408-P-1107) Omav at conc. ≤3 µM were well tolerated and caused little or no change in CYP1A2, CYP2B6, or CYP3A4/5 enzyme activity. Whereas Omav caused ~4-fold increase in CYP3A4/5 activity in a single culture at conc. of 5 µM.

Transporter inhibition (study RTA408-P-1209 and study RTA-P-17012) Omav displayed little to no inhibitory effects on the systemic transporters BCRP, BSEP, OAT3, OATP1B1, and OCT2. Omav inhibited the systemic transporters MDR1 and OCT1 with estimated IC_{50} values of 0.706 and 0.945 µM, respectively. Omav inhibited the renal transporter OAT1 with an estimated IC_{50} value of 2.27 µM, and the hepatic transporter OATP1B3 with an estimated IC_{50} value of 3.47 µM. No significant inhibition was observed for BCRP, MATE1, or MATE2-K human transporters (study RTA-P-17012).

Reviewer's comments:

1. The Applicant did not conduct CYP2C induction assay.

4.3 Clinical PK Assessments

4.3.1 Food Effect and dose proportionality (study 408-C-1703)

Food effect Study Design (Part 1):

Study 408-C-1703 was a Phase 1, open-label, food effect, and dose proportionality study with Omav in healthy volunteers. The study was conducted in 2 parts simultaneously. Part 1 was to assess the food effect, while part 2 was to assess dose proportionality. In part 1, two single doses of Omav (150 mg) were administered to the subjects in fed and fasted states (overnight fast, ~10h prior to dosing) in a crossover fashion. The washout between periods was 14 days. A total of 16 subjects received a single dose of Omav in the fasted state and 15 subjects received in the fed state.

Figure 4: Design of Study 408-C-1703

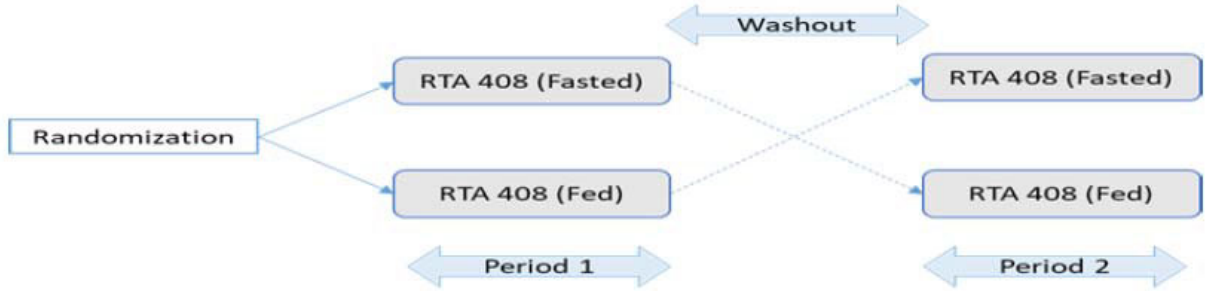

Subjects were confined to the site beginning on Study Day -1 through the last PK blood draw on Study Day 6 during Period 1, and from Study Day 14 through the last PK blood draw on Study Day 20 during Period 2. There was a 1-week washout period between Period 1 and Period 2. PK blood sampling for omaveloxolone was performed pre-dose (0 hour), and at 0.5, 1, 2, 3, 4, 5, 6, 8, 10, 12, 18, 24, 36, 48, 72, 96, and 120 h following Omav administration. All subjects were included in the PK population.

The meal provided approximately 800 to 1000 calories and 50% of its total caloric content from fat such that 150, 250, and 500 to 600 calories from protein, carbohydrate, and fat, respectively. The drug was administered 30-min after meal.

To assess effect of food on PK of Omav PK, the C_{max} and AUCs (AUC_{0-t} and $AUC_{0-\infty}$) of Omav were compared between fed and fasted states using an analysis of variance (ANOVA) model for the natural logarithm-transformed C_{max} and AUCs. Lack of an effect of food on PK of Omav was concluded if the calculated 90% confidence intervals for resulting point estimates (geometric least squares means) and their ratios (fed vs. fasting) were contained within the 80.00% to 125.00% range.

Results:

Figure 5: PK concentration time profile for Omav [(50 mg (fasted), 100 mg (fasted) and 150 mg (fasted and fed)]

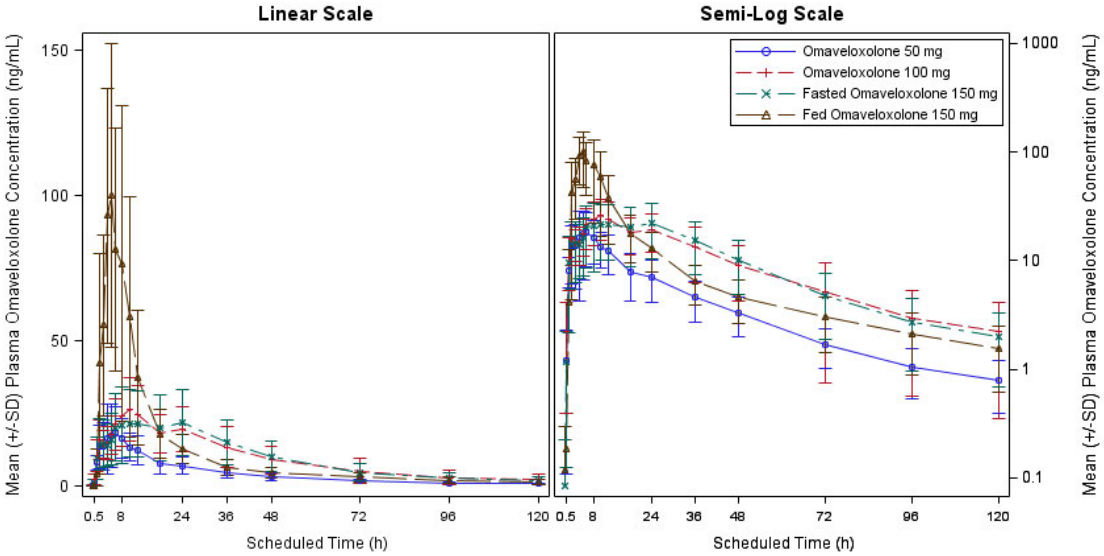

Source: CSR Study 408-C-1703, page 56 of 327

Table 3: PK Parameters for Omav

PK Parameter Statistic	RTA-408			
	50 mg Fasted (N=10)	100 mg Fasted (N=8)	150 mg Fasted (N=16)	150 mg Fed (N=15)
C_{max} (ng/mL)				
n	10	8	16	15
Mean (SD)	21.1 (11.7)	27.7 (9.72)	28.2 (13.0)	129 (51.1)
GM (CV%)	18.8 (52.9)	26.1 (38.5)	25.4 (51.3)	119 (45.6)
T_{max} (h)[1]				
n	10	8	16	15
Median (min, max)	5.5 (1.0, 8.0)	10.0 (8.0, 12.0)	11.0 (3.0, 24.0)	5.0 (2.0, 8.0)
AUC_{0-t} (h*ng/mL)				
n	10	8	16	15
Mean (SD)	483 (188)	1110 (498)	1140 (526)	1340 (557)
GM (CV%)	456 (35.1)	1030 (43.3)	1030 (47.0)	1220 (48.1)
AUC_{0-inf} (h*ng/mL)				
n	9	8	16	15
Mean (SD)	545 (215)	1230 (614)	1230 (583)	1440 (633)
GM (CV%)	513 (36.4)	1120 (46.4)	1120 (48.4)	1310 (49.8)
$T_{½}$ (h)				
n	9	8	16	15
Mean (SD)	34.6 (7.3)	33.7 (7.0)	31.5 (5.6)	42.2 (10.6)
λ_z (1/h)				
n	9	8	16	15
Mean (SD)	0.021 (0.004)	0.021 (0.004)	0.023 (0.004)	0.018 (0.005)
CL/F (L/h)				
n	9	8	16	15
Mean (SD)	102 (32.5)	95.9 (36.0)	148 (71.9)	128 (73.0)
V_z (L)				
n	9	8	16	15
Mean (SD)	5080 (1950)	4520 (1790)	6630 (3240)	7300 (3260)

[1] T_{max} is expressed as median and range (min, max)

Source: CSR Study 408-C-1703, page 57 of 327

Table 4: Statistical Analysis Results for the Assessment of Food Effect for Omav

PK Parameter	GLSM[a] 150 mg (n) Omaveloxolone Fasted	GLSM[a] 150 mg (n) Omaveloxolone Fed	Ratio (Fed/Fasted) GLSM (90% CI)[b]
C_{max} (ng/mL)	26.7 (15)	121 (15)	451 (362 - 562)
AUC_{0-t} (h*ng/mL)	1070 (15)	1240 (15)	116 (100 - 134)
AUC_{0-inf} (h*ng/mL)	1160 (15)	1330 (15)	115 (99.5 - 132)

[a] GLSM were the least square means from the ANOVA model presented after back transformation to the original scale.
[b] The 90% CIs were presented after back transformation to the original scale.

Source: CSR Study 408-C-1703, page 59 of 327

Conclusion:

Following a single oral dose of 150 mg, plasma exposure, namely C_{max}, AUC_{0-t} and AUC_{0-inf}, of Omav increased by ~450%, 16% and 15%, respectively, in the fed state relative to the fasted state. Based on these data, Omav was recommended to be administered 1h before eating.

Dose proportionality study design (Part 2):

This was an open-label, randomized phase to assess the dose proportionality of Omav. Subjects were randomly assigned to 1 of 2 treatments. A single dose of omaveloxolone was administered to the subjects in a fasted state. To assess proportionality of the 50-mg, 100-mg, and 150-mg doses of Omav, data from all subjects during the fasted period of Part 1 were included in Part 2 analyses.

The PK sampling scheme was similar to the food effect study design. The PK parameters of 50 mg and 100 mg doses are summarized in Table 1. To assess the dose proportionality of Omav, the plasma PK parameters (C_{max} and AUCs) of 50 mg, 100 mg, and 150 mg in fasted state in part 1 and part 2 were assessed with a power model. The power model is described as: $y = \alpha * Dose^{\beta}$, where y denoted the PK parameters. Dose proportional PK was implied if $\beta=1$ and it was assessed by estimating β along with its 90% confidence interval. The exponent, β, in the power model was estimated by regressing the ln-transformed PK parameter on ln-transformed dose.

Results:

The total plasma exposure for Omav (AUC_{0-inf} and AUC_{0-t}) increased dose proportionally from 50 mg to 150 mg, however the C_{max} increased in a less than dose proportional manner.

In CSR for study 408-C-1703, the wash out duration between the two periods (fasted arm and fed arm) was listed as 1 week. However, the OCP reviewer confirmed that Omav was administered 14 days apart in the two periods.

4.3.2 Hepatic impairment (Study 408-C-1804)

This study was a Phase 1, open-label, non-randomized, parallel-group study in adult men and women patients aged 18 to 70 years (inclusive) with a BMI between 18 kg/m^2 and 38 kg/m^2 (inclusive) to determine the effect of hepatic impairment on the PK, safety, and tolerability of a single oral dose of omaveloxolone compared to matched healthy subjects with normal hepatic function. Patients were grouped at the screening into 4 groups –

- Group 1: matched healthy controls (N=12)
- Group 2: patients with mild hepatic impairment (Child-Pugh Class A [score of 5-6]) (N=8)
- Group 3: patients with moderate hepatic impairment (Child-Pugh Class B [score of 7-9]) (N=7)
- Group 4: patients with severe hepatic impairment (Child-Pugh Class C [score of 10-14]) (N=5)

Following administration of a single oral dose of 150 mg Omav, the PK profiles for the normal function and moderate and severe hepatic impairment groups were each characterized by a slow absorption phase (median T_{max} values of 7.00 hours, 8.00 hours, and 6.00 hours, respectively). For the mild hepatic impairment group, the absorption phase was rapid (median T_{max} 2.00 hours).

The geometric mean $t_{1/2}$ values of Omav were similar for normal function and mild hepatic impairment groups ([range] = 90 [57-152] h and 86 [26-151] h, respectively), and longer for moderate and severe hepatic impairment groups (107 [71-142] h and 190 [138-331] h, respectively). Geometric mean CL/F values were lower for moderate and severe hepatic impairment groups (60.2 L/h and 58.8 L/h, respectively) than for normal function and mild impairment groups (92.1 L/h and 87.8 L/h, respectively).

Patients with mild hepatic impairment (n=8) had approximately 21% higher C_{max}, while the total exposure was comparable, compared to subjects with normal hepatic function (n=12).

Patients with moderate hepatic impairment (n=7) had 65% and 83% higher AUC_{inf} and C_{max} values, respectively, compared to subjects with normal hepatic function.

Patients with severe hepatic impairment (n=3 to 5) had 117% increase in AUC_{inf} compared to the normal hepatic function group. Interestingly, C_{max} was 31% lower for the severe impairment group compared to subjects with normal hepatic function.

Few important study design and data analysis considerations should be noted for this study:

1. The Applicant selected PK data for comparisons between hepatic impairment cohorts after matching to normal healthy controls. However, the review team noted that the Applicant had already enrolled subjects in the study based on prespecified criteria of body weight ±10 kg and BMI ±20%. Also, as Omav is dosed at a fixed dose of 150 mg QD irrespective of body weight, the review team reanalyzed PK data considering all subjects from normal healthy controls and hepatic impairment cohorts.

2. Although major differences between the Applicant's (117% increase in AUC_{inf}) and review team's (56% increase in AUC_{inf}) analysis were noted only for the severe hepatic impairment cohort, due to limited sample size and inherent PK variability of Omav, dosing recommendations for moderate and severe hepatic impairment cohorts were based on a conservative approach of maximum increase observed with the Applicant's analysis.

3. Omav was recommended to be avoided in moderate and severe hepatic impairment patients. However, if avoiding is not possible, then a reduced dose of 100 mg QD for moderate hepatic impairment patients was recommended based on the observed PK data. Patients with severe hepatic impairment should avoid Omav due to added risk of adverse hepatic events which could be difficult to attribute to either the overexposure of Omav or the pathological condition itself.

4.3.3 Human mass balance study (study 408-C-1805)

This was an open-label, non-randomized, single-dose study in healthy male subjects to investigate the absorption, metabolism, and excretion of Omav. The primary objective of the study was to assess the PK, mass balance, metabolite profiles, and rates and routes of elimination of [^{14}C]-omaveloxolone and derived metabolites following administration as a single 150-mg (containing approximately 90 µCi) dose to healthy male subjects. A total of 8 subjects entered and completed the study.

A median T_{max} (min-max) of 9.00 (4.00-36.00) hours in plasma. After reaching C_{max}, plasma concentrations appeared to decline in a generally biphasic manner, with geometric mean $t_{1/2}$ of 48.4 h and individual estimates ranging from 32.4 to 68.9 h. The geometric mean $AUC_{0\text{-}inf}$ for Omav in plasma was ~31% of that for total radioactivity in plasma. The geometric mean $t_{1/2}$ of total radioactivity (~54 h) was slightly higher than Omav (~48.4 h).

With metabolite profiling, plasma, urine, and fecal homogenate samples indicated that ^{14}C-Omav underwent moderate metabolism in human subjects to produce 30 metabolites, of which seven were identified. Omav was a major (>10% of total plasma radioactivity) circulating component, with 10.5% of total plasma radioactivity exposure. Metabolites M22 (TX304579) and M17 (TX304571) were major plasma metabolites that accounted for 18.6% and 10.9% of total plasma radioactivity, respectively. Plasma metabolites M28 (TX64094), M14 (TX304574), M15 (TX304575), and M23 (TX304576) were minor (<10% of total plasma radioactivity exposure) and accounted for 8.35%, 2.86%, 2.14%, and 1.77% of total plasma radioactivity exposure, respectively.

Of the dose excreted in feces, at 0 to 144 hours post-dose, Omav accounted for ~40% of the dose. At 96 h post-dose, ~91% radiolabeled material with 92.4% radioactivity recovered in the feces by 528 h post-dose, suggesting fecal elimination was the primary route of elimination. Urinary excretion accounted for <0.1% radioactivity at 528 h post-dose. Elimination of metabolites was predominant in feces and cumulatively accounted for 42.1% of dose. Metabolite M29 (TX63647) was the major metabolite in feces, accounting for 35.9% of dose, while metabolite M28 (TX64094) was minor, accounting for 6.21% of dose.

4.4 Population PK Analyses

The Applicant submitted report reat-pmx-omav-2081-study-report.pdf, titled "*Population Pharmacokinetic and Exposure-Response Modeling of Omaveloxolone*" to module 5335 in sequence 0001. The population PK analysis objective was to identify the intrinsic and extrinsic factors that affect omaveloxolone concentrations in plasma in adult healthy subjects and patients with FA. Applicant conducted simulations to predict the effect of age on omaveloxolone PK.

4.4.1 PPK Modeling

The data used in the population PK analyses came from studies 408-C-1402 Part 1, 408-C-1402 Part 2, 408-C-1403, 408-C-1703, 408-C-1804, and 408-C-1806. There were 3310 measurable (non-blq) omaveloxolone concentrations from n=253 subjects available for analyses. Details regarding the PK sampling schedule for these studies can be found in the table below.

Table 5: Clinical Studies included in the Population PK Analyses

Study Number, Phase, Type	Subject Population	Drug Dose and Regimen	PK Sampling
408-C-1402 Phase 2 Safety, PK, and efficacy	Patients with Friedreich's ataxia (N=172)	Part 1: Placebo, 2.5, 5, 10, 20, 40, 80, 160, and 300 mg QD Part 2: Placebo, 150 mg QD	PK: Part 1, Cohort 1: Predose and 1, 2, 4, and 8 hours postdose on Days 14 and 56, and predose on Day 84 Part 1, all other cohorts: Predose and 1, 2, 4, and 8 hours postdose on Day 14 and predose on Day 84 Part 2: Predose and 1, 2, 4, and 8 hours postdose on Day 14 and predose on Days 84, 168, and 336 Efficacy: Part 1: Screening and on Days 1, 28, 56, and 84 Part 2: Screening and on Days 1, 28, 84, 126, 168, 252, and 336
408-C-1403 Phase 2 PK	Patients with mitochondrial myopathy (N=53)	Placebo, 2.5, 5, 10, 20, 40, 80, and 160 mg QD	PK: Predose and 1, 2, 4, and 8 hours postdose
408-C-1703 Phase 1 Food effect and dose proportionality	Healthy subjects (N=34)	50, 100, and 150 mg, single dose	PK: Predose and 0.5, 1, 2, 3, 4, 5, 6, 8, 10, 12, 18, 24, 36, 48, 72, 96, and 120 hours postdose
408-C-1804 Phase 1 Hepatic impairment	Subjects with hepatic impairment and normal hepatic function (N=48)	150 mg, single dose	PK: Predose and 0.5, 1, 2, 3, 4, 5, 6, 8, 10, 12, 24, 36, 48, 72, 96, 120, 168, 216, 264, 312, and 336 hours postdose
408-C-1806 Phase 1 Drug-drug interaction	Healthy subjects (N=61)	150 mg, single dose (Only Day 1 data from Parts 2, 3, and 4 were used when no interacting drugs were present. Part 1 did not include PK data on a study day when interacting drugs were not present.)	PK: Predose and 0.5, 1, 1.5, 2, 3, 4, 6, 8, 12, 16, 24, 36, 48, 72, 96, 120, 144, 168, 192, 216, and 240 hours postdose on Day 1 only

Source: sequence 0001, module 5335, reat-pmx-omav-2081-study-report.pdf, pages 21-22

The structural model utilized two compartments, first order absorption, and linear clearance. The Applicant assessed alternative absorption models (zero-order, sequential zero- plus first- order, and parallel zero- plus first- order) and did not improve the model fit based on diagnostic plots and Cmax prediction performance. PK parameters include apparent clearance (CL/F), apparent central volume of distribution (Vc/F), apparent intercompartmental clearance (Q/F), apparent peripheral volume of distribution (Vp/F), and absorption rate constant (Ka).

Interindividual Variability: exponential
Residual Variability: proportional
Covariates: Age and alanine phosphatase are covariates on apparent clearance. Healthy subjects (versus patient as a categorical covariate) and food are covariates on the absorption rate constant (Ka). Food is a covariate on bioavailability.

Parameter estimates for the final population PK model are shown in the table below.

Table 6: Parameter Estimates for the Final Omaveloxolone Population PK Model

Parameters	Estimates	%RSE	95% CI	
Apparent clearance (CL/F, L/h)	108.8	3	102.5 – 115	
Baseline age effect on CL	$CL_i = \left({Age_i}/{34}\right)^{-0.2767}$	29	-0.4354 – -0.1179	
Baseline ALP effect on CL	$CL_i = \left({ALP_i}/{69}\right)^{-0.3393}$	30	-0.5381 – -0.1404	
Apparent central volume of distribution (Vc/F, L)	409.7	11	323.9 – 495.5	
Apparent intercompartmental clearance (Q/F, L/h)	81.88	13	60.47 – 103.3	
Apparent peripheral volume of distribution (Vp/F, L)	6951	12	5355 – 8547	
Absorption rate constant (Ka, 1/h)	0.1001	18	0.06386 – 0.1363	
Healthy subject effect on absorption (KAINDIC)	Ka*(1 – 0.5559)	13	-0.703 – -0.4089	
Food effect on absorption (KAFED)	Ka*(1 + 5.081)	29	2.181 – 7.981	
Food effect on relative bioavailability (F1FED)	F*(1 + 0. 2394)	50	0.005933 – 0.473	
Random effects	**Estimates (%CV)**	**%RSE**	**95% CI**	**Shrinkage (%)**
IIV on Vc	79	8	0.4424 - 0.8198	24
ηVc-ηCL correlation	-	r=0.0333		
IIV on CL	42	6	0.1352 - 0.2152	5
ηVc-ηVp correlation	-	r=0.0481		
ηCL-ηVp correlation	-	r=0.0478		
IIV on Vp	98	9	0.6226 - 1.293	12
ηVc-ηQ correlation	-	r=0		
ηCL-ηQ correlation	-	r=0.0361		
ηVp-ηQ correlation	-	r=0.0178		
IIV on Q	84	13	0.3462 - 1.08	12
IIV on Ka	47	10	0.1069 - 0.2492	27
Residual error	**Estimates**	**%RSE**	**95% CI**	
Proportional error	34.47	3.0	32.5 - 36.45	

η=eta; %CV=percentage of coefficient of variation; %RSE=percentage of relative standard error; ALP=alkaline phosphatase; CI=confidence interval; CL=clearance; F=bioavailability; IIV=interindividual variability; Ka=absorption rate constant; Q=intercompartmental clearance; Vc=central volume of distribution; Vp=peripheral volume of distribution.

Source: sequence 0001, module 5335, reat-pmx-omav-2081-study-report.pdf, page 62

Key diagnostic plots are shown in the figures below.

Figure 6: Goodness of Fit Plots for the Final Population PK Model

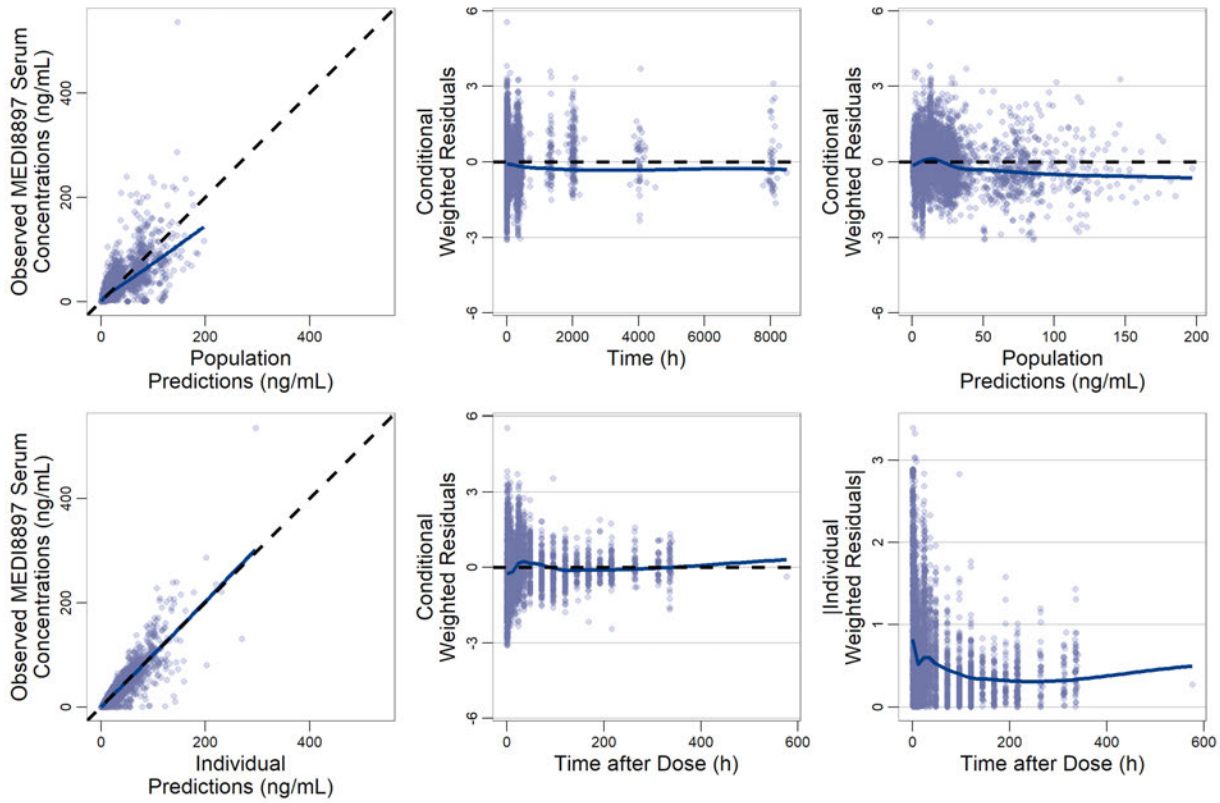

Dots are individual data. Solid red lines are smoothed LOESS lines. Dashed lines are lines of identity. Abbreviations: GOF=goodness-of-fit; LOESS=locally weighted scatterplot smoothing.

Source: sequence 0001, module 5335, reat-pmx-omav-2081-study-report.pdf, page 63

Figure 7: Prediction Corrected Visual Predictive Check

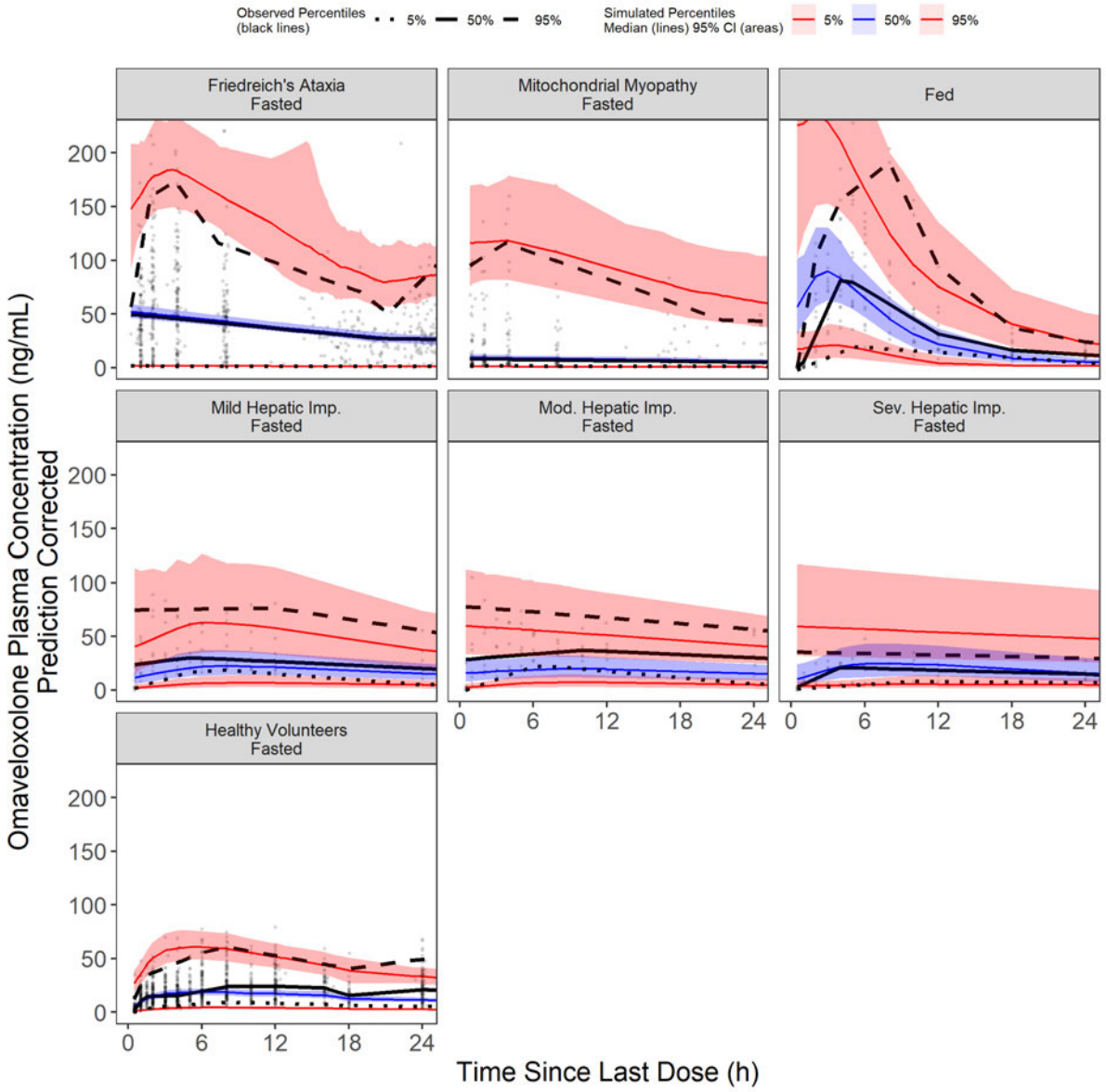

CI=confidence interval; VPC=visual predictive check.

Source: sequence 0001, module 5335, reat-pmx-omav-2081-study-report.pdf, page 185

[*Reviewer comment: The diagnostics presented in Figure 6 suggest performs best when predicting concentration values up to ~50 ng/mL. The model is used to discuss the effect of age, race, gender, and body weight on PK in label. Overall, the model is acceptable for characterizing the effect of these covariates in the label. The reviewer agrees that the PPK analyses suggest race, sex, and body weight do not affect omaveloxolone PK for the labelled population of FA patients age 16 years and older. While inclusion of patient status (healthy volunteer versus FA patient) on absorption rate constant improved the model fit, this covariate relationship is unexpected and there is no apparent mechanistic basis. The effect of age on omaveloxolone is discussed in the next section.*]

4.4.2 PPK Simulation

The final PPK model includes age as a covariate on omaveloxolone clearance (see 4.4.1 PPK Modeling for details on the for details on the final population pharmacokinetic model). The Applicant conducted PK simulations to quantify the effect of age on omaveloxolone C_{max} and AUC_{tau} at steady state. The simulations were conducted for a typical subject in fasted state. The PK was summarized within age bins of 6 to < 12 years, 12 to < 16 years, 16 to < 40 years, 40 to < 65 years, and ≥ 65 years. For each age group in the virtual population, 2000 virtual subjects were generated. The median age of the subjects in the dataset, 34 years, was used as a reference. The results of these simulations for the proposed dose of 150 mg once daily are shown below.

Figure 8: Simulated Cmaxss and AUCtau,ss for 150 mg Once Daily By Age Group

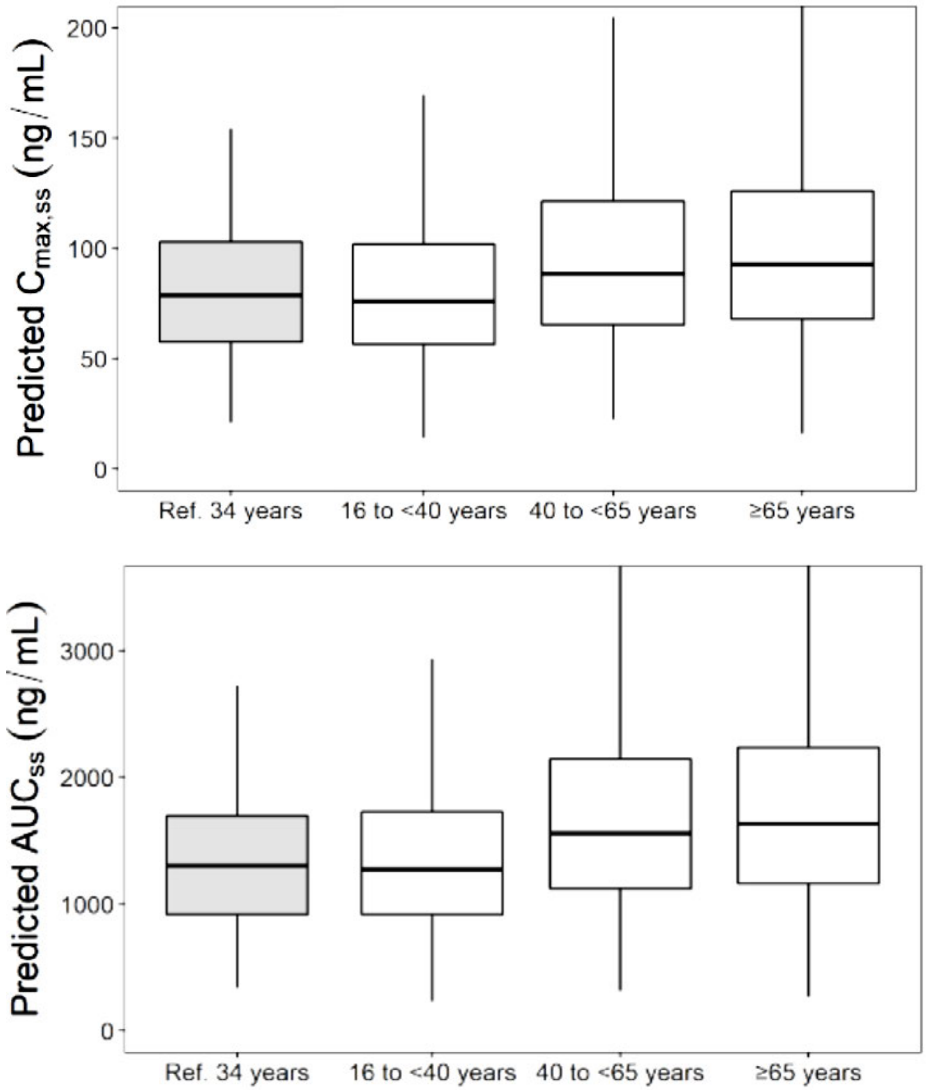

2000 virtual subjects were simulated for every age group in the virtual population. Simulated profiles for 34 years old virtual subjects (median age of the population PK analysis dataset) were pooled to serve as a reference group. AUCss=steady-state area under the plasma concentration-time curve; PK=pharmacokinetic; QD=once daily.

Source: sequence 0001, module 5335, reat-pmx-omav-2081-study-report.pdf, page 96-97

Table 7: Simulated C_{maxss} and $AUC_{tau,ss}$ for 150 mg Once Daily By Age Group

Dose		Ref. 34 years (N=88)	6 to <12 years (N=2000)	12 to <16 years (N=2000)	16 to ≤40 years (N=2000)	40 to ≤65 years (N=2000)	≥65 years (N=2000)
150 mg				AUC_{ss} (hr·ng/mL)			
	Mean (SD)	1430 (712)	1040 (516)	1160 (570)	1420 (734)	1710 (823)	1820 (928)
	Median [min, max]	1300 [336, 4140]	936 [192, 4220]	1050 [181, 5220]	1270 [230, 5750]	1560 [316, 8370]	1630 [267, 10000]
				$C_{max,ss}$ (ng/mL)			
	Mean (SD)	85.1 (38.5)	66.7 (33.1)	71.7 (33.4)	84.1 (41.2)	97.9 (45.1)	103 (49.4)
	Median [min, max]	78.6 [21.0, 193]	59.4 [13.5, 312]	65.6 [12.0, 340]	75.7 [13.9, 395]	88.5 [22.4, 366]	92.6 [15.9, 502]

2000 virtual subjects were simulated for every age group in the virtual population. Simulated profiles for 34 years old virtual subjects (median age of the population PK analysis dataset) were pooled to serve as a reference group. Abbreviations: AUCss=steady-state area under the plasma concentration-time curve; Cmax,ss=maximum steady-state plasma concentration; PK=pharmacokinetic; max=maximum; min=minimum; N=number of subjects with available information; Qu=quartile; SD=standard deviation.

Source: sequence 0001, module 5335, reat-pmx-omav-2081-study-report.pdf, page 98

The simulations indicate that compared to the reference group of 34-year-old subjects, subjects ≥ 65 years of age will have 25% higher $AUC_{tau,ss}$ (based on median values of 1300 hr*ng/mL versus 1630 h*nr/mL) and 18% higher $C_{max,ss}$ (based on median values of 78.6 ng/mL versus 92.6 ng/mL), respectively.

The Applicant concludes that though systemic exposure was predicted to be higher in older subjects, that there are no meaningful differences in systemic exposure between the age groups. The Applicant's proposal is that no dose adjustment is needed based on age.

[*Reviewer comment: The reviewer agrees that no dose adjustment is needed based on age for the proposed population of FA subjects age ≥ 16 years.*]

4.5. Exposure-response analyses

The Applicant submitted report reat-pmx-omav-2081-study-report.pdf, titled "*Population Pharmacokinetic and Exposure-Response Modeling of Omaveloxolone*" to module 5335 in sequence 0001. The objective was to perform E-R modeling with the modified Friedreich's ataxia rating scale (mFARS) scores, aminotransferase levels, cardiac adverse events (AEs), and infections and infestations AEs.

The analyses were conducted with data from Study 408-C-1402 Part 1 and Part 2 only. The final population PK model was used to predict PK profile based on posterior Bayes estimates. Steady-state AUC ($AUC_{tau,ss}$) and steady-state C_{max} ($C_{max,ss}$) were generated based on these predictions.

The relationship between omaveloxolone exposure and ALT, AST, or mFARS (continuous PD measures) and using the nonlinear regression method from the nlme package in R. Based on this exploratory analysis, linear structural models with various interindividual terms were assessed for their capacity to sufficiently characterize the exposure-response relationship.

Logistic regression analyses were employed to analyze 2 different AEs from patients with FA in Study 408-C-1402 Part 1 and Part 2: cardiac events and infections and infestations events.

Variables screened for use as covariates include concomitant medication, age or age group, sex, race, baseline mFARS, and pes cavus status. For exposure-response model, the initial model fit for each clinical endpoint included $AUC_{tau,ss}$, $C_{max,ss}$, and all the potential covariates. Backward elimination was applied using the step Akaike information criterion (stepAIC) function from the Modern Applied Statistics with S (MASS) package in R. This function will iteratively eliminate variables to minimize the Akaike information criterion (AIC). Bivariate interaction terms were assessed between remaining explanatory variables provided that such interactions had a plausible clinical or biological interpretation. Finally, model terms that were retained through the statistical evaluation but were not considered biologically plausible were considered for removal from the model.

4.5.1 Cardiac Events

The dataset included 171 patients, 27 which experienced a cardiac event and 144 that did not experience a cardiac event. Univariate analysis of exposure metrics ($AUC_{tau,ss}$, $C_{max,ss}$, and dose level) indicated that $C_{max,ss}$ was the strongest predictor of cardiac events. Prior to initiation of the backward elimination process, the full model included age, body weight, baseline mFARS, sex, PPI, moderate CYP3A4 inhibitor, and race. After backward elimination, the final model retained no significant predictors. To assess the potential impact of $C_{max,ss}$ on cardiac events, the Applicant utilized the initial model with $C_{max,ss}$ as a predictor of cardiac events. The parameter estimates of the final model, a logistic regression model with $C_{max,ss}$ as the only predictor are presented in the table below.

Table 8: Parameter Estimates for the Final Cardiac Event Exposure-Response Model

Parameter	Estimate	RSE (%)	95% CI
Intercept	-1.75	27.2	-2.32 – -1.25
C_{max} slope	0.00196	0.4	-0.00654 – 0.00958

CI=confidence interval; Cmax=maximum plasma concentration; RSE=relative standard error. The intercept is the probability of event for a reference individual on the logit scale (14.8%)

Source: sequence 0001, module 5335, reat-pmx-omav-2081-study-report.pdf, page 72

The observed cardiac event data are overlayed with the simulated $C_{max,ss}$ values and the exposure-response model prediction of cardiac event probability are presented in the figure below.

Figure 9: Observed and Predicted Cardiac Events for PBO and 150 mg Omav

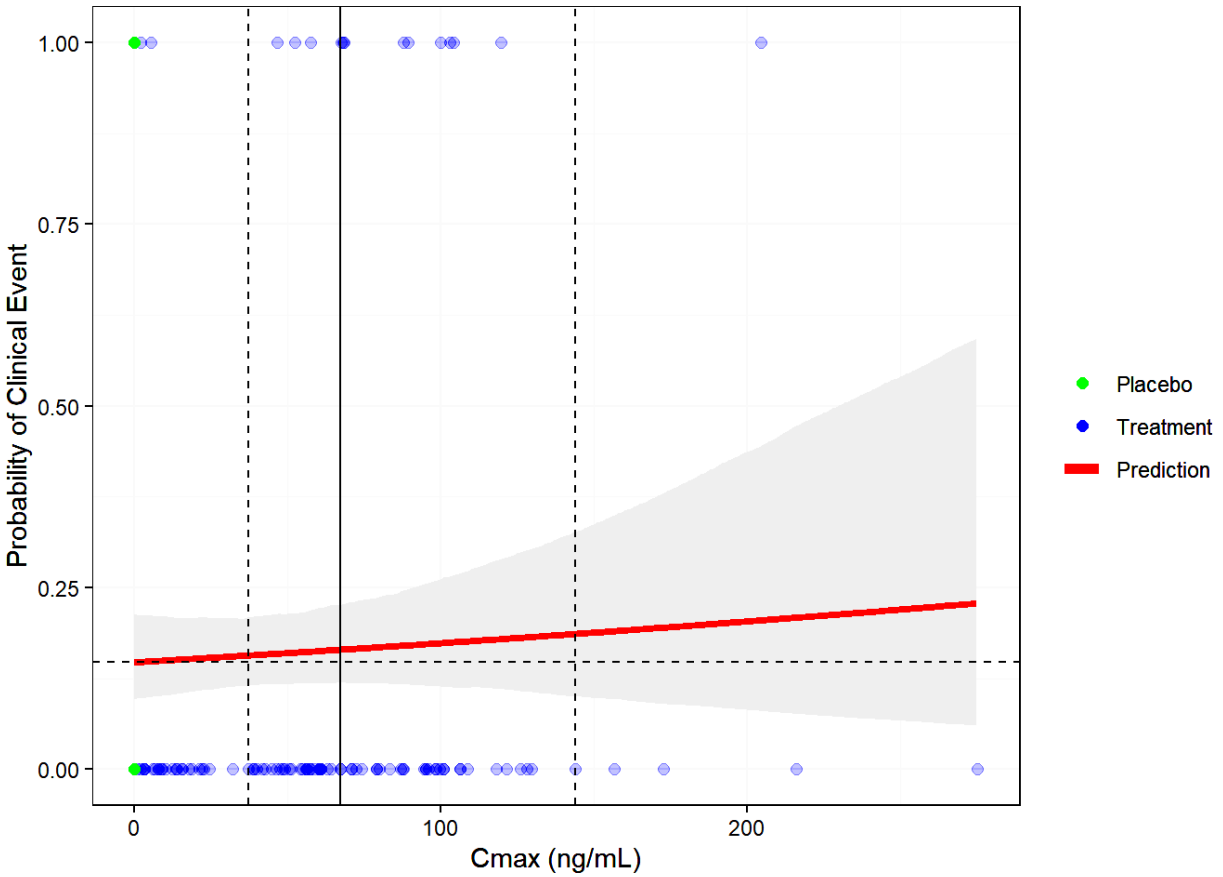

The solid red line is the predicted probability of experiencing a cardiac event. The gray-shaded area is the 95% CI of the model prediction. The 2 vertical dashed lines are the minimum and maximum Cmax for the 150-mg dose level. CI=confidence interval; Cmax=maximum plasma concentration.

Source: sequence 0001, module 5335, reat-pmx-omav-2081-study-report.pdf, page 73

The Applicant provides the following observations from these analyses:

- The probability of a cardiac event is correlated with increasing Cmax.
- The model predicted mean probability of a cardiac event for a subject receiving the 150 mg dose was 16.5% compared to 14.8% for placebo.
- The 95% CI for the effect of Cmax on cardiac event includes 0 for slope, indicating that Cmax is not significant.

[*Reviewer comment: The Applicant reports that the slope of $C_{max,ss}$ on cardiac event probability contains zero. However, limitations to this analysis include 1) pooling various types of cardiac events that otherwise may be too infrequent to model, and 2) exclusion of time of cardiac event AE with respect to Tmax. Overall, the relationship of omaveloxolone PK to cardiac risk is not clear. Please refer to the review of Dr. Veneeta Tandon for discussion on pharmacovigilance and post-marketing requirements for TQT assessment. .*]

4.5.2 Infections and Infestations

The Applicant reports the rate of treatment emergent infections and infestations rates in placebo and 150 mg omaveloxolone arms to be 57.7% and 66.7%, respectively (iss-report-body-1.pdf, page 162). Based on discussions with the Clinical team, considering the magnitude of infections and infestations incidence in the placebo arm, the Clinical team is not significantly concerned about the effect of omaveloxolone on infection and infestation risk. As such, the exposure-response relationship for infections and infestations will not be reviewed.

4.5.3 ALT and AST

OCP has concluded that the levels of ALT and AST do not provide substantive and/or direct evidence to support omaveloxolone pharmacological effect for treatment of FA (please refer to 3.3.1 To what extent does the available clinical pharmacology information provide pivotal or supportive evidence of effectiveness? for details). As such , the exposure-response analyses for AST and ALT were not reviewed.

4.5.4 mFARS

The observed mFARS measurements stratified by dose level in Study 1402 are presented in the figure below.

Figure 10: Observed mFARS Measurements By Dose Level in Study 1402

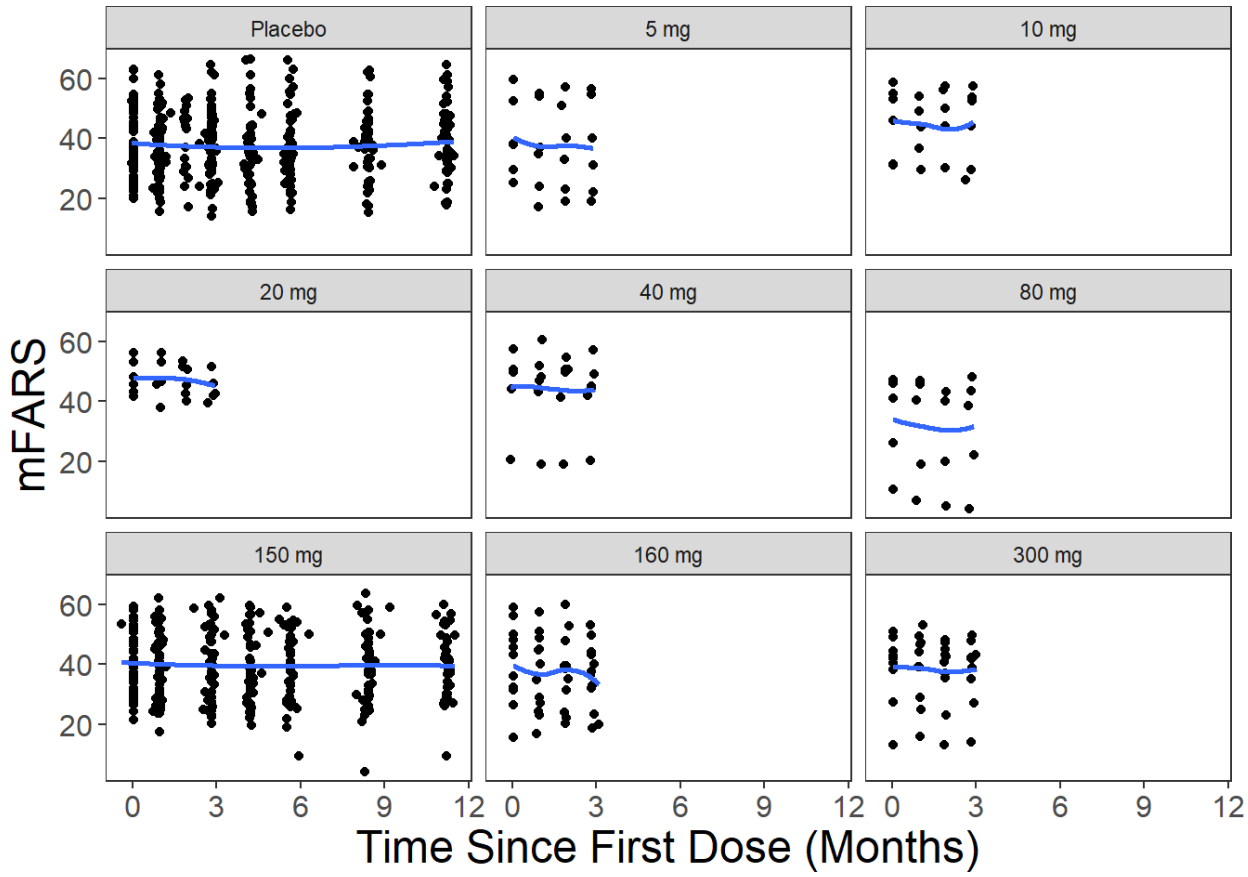

mFARS=modified Friedreich's ataxia rating scale.

Source: sequence 0001, module 5335, reat-pmx-omav-2081-study-report.pdf, page 88

The Applicant initially generated a structural model of the placebo arm to assess the disease progression in the absence of omaveloxolone. Applicant determined that a delayed linear model described the data better than a linear model. The final placebo model included a linear disease progression function of SLOPE*t, a time delay function (modeled with a sigmoid E_{max} function), and a random effect on baseline mFARS. The Applicant indicates that the time delay function describes the time delay between placebo administration and the elevation in mFARS. The model for the disease progression in the placebo arm is:

$$\text{mFARS} = BASELINE\ \text{mFARS} + Disease\ Prgression$$

$$\text{mFARS} = BASELINE + \frac{t^H}{T50^H + t^H} * SLOPE * t$$

where *BASELINE* is the baseline mFARS at time 0, *SLOPE* is the disease progression, *H* is the Hill coefficient, T_{50} is the time (in days) to 50% of maximum mFARS, and *t* is time in days. The figure below shows the observed (mean ± standard deviation) mFARS overlayed with the predicted mean mFARS for the placebo arm.

Figure 11: Observed and Model-Predicted mFARS Following Placebo Versus Time

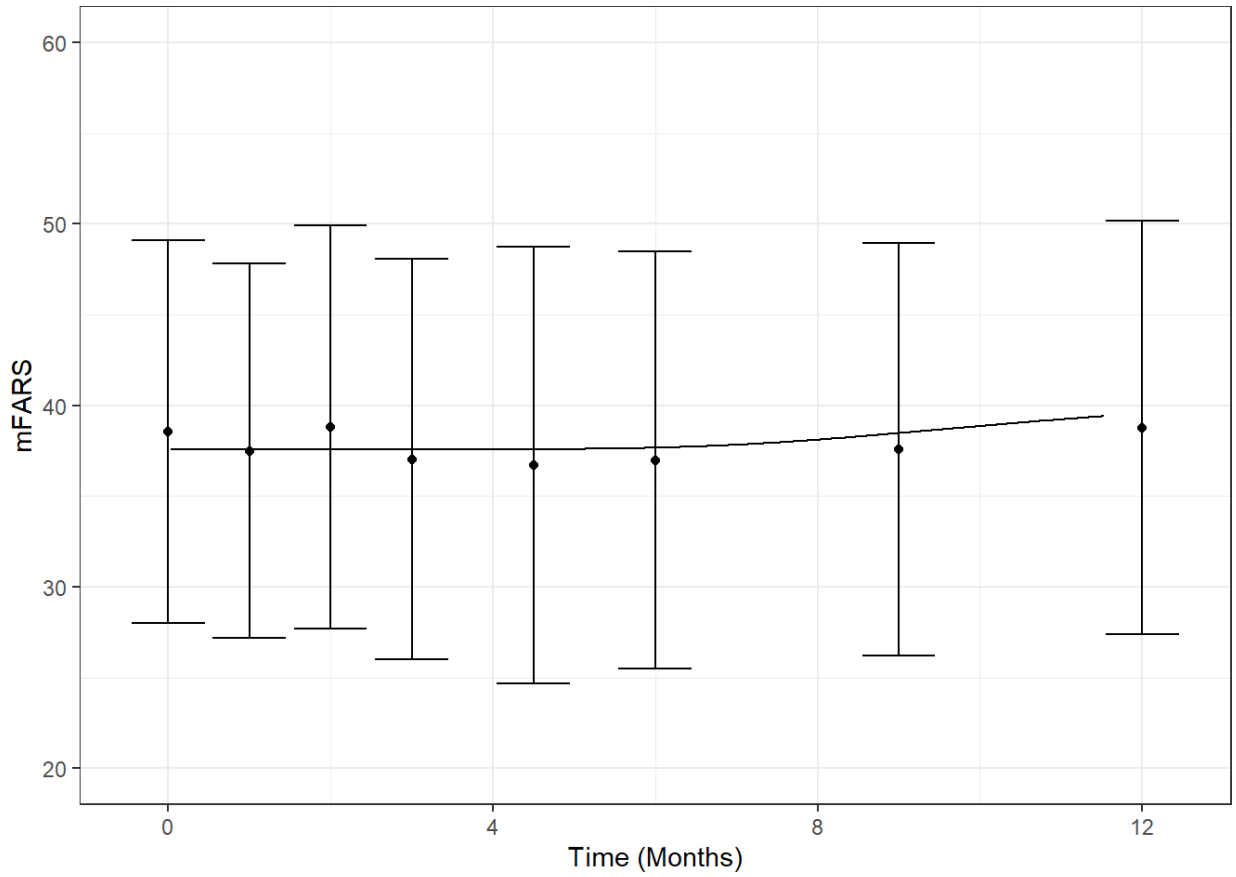

Black dots and whiskers are observed mean ± standard deviation. Black line is the model predicted mFARS following placebo dosing. mFARS=modified Friedreich's ataxia rating scale.

Source: sequence 0001, module 5335, reat-pmx-omav-2081-study-report.pdf, page 90

The Applicant used a treatment effect to model the omaveloxolone effect on disease progression. The treatment effect is active for any subject in the treatment arm and inactive for every subject in the placebo arm. The effect of treatment on disease progression was assessed two ways; as a proportional change or as an additive change in disease progression. The final structural model utilized an additive drug effect with a random effect on baseline mFARS and a random effect on slope. The disease progression model with a treatment effect is:

$$\text{mFARS} = BASELINE + \frac{t^H}{T50^H + t^H} * SLOPE * t + EFF * t * Treatment$$

where *BASELINE* is the baseline mFARS at time 0, *SLOPE* is the change in mFARS over time due to disease progression, *EFF* is the change in mFARS due to treatment, *Treatment* is placebo or treatment (0 or 1), *H* is the Hill coefficient, T_{50} is the time (in days) to half-maximum mFARS, and *t* is time in days.

The covariate analysis included assessment of the influence of age, baseline body weight, baseline mFARS, sex, and pes cavus status baseline mFARS and drug effect. Covariates in the final model are the effect of pes cavus on the treatment effect and baseline mFARS on the T_{50} of effect delay. The parameter estimates for the final model (mod44) are shown in the table below.

Table 9: Parameter Estimates for the Final mFARS disease progression Model (mod44)

Parameter	Description	Estimate	95% CI
BL	Baseline mFARS	39.100	(37.4 – 40.8)
εBL	Random effect on baseline mFARS (%CV)	28%	
T50	Time to half-maximum mFARS (presented in years)	0.463	(0.369 - 0.557)
SLOPE	Change in mFARS over time due to disease progression	0.007	(0.005- 0.01)
EFF	Change in mFARS due to treatment	-0.011	(-0.015 - -0.007)
PESCAV	Effect of pes cavus status on change in mFARS due to treatment	0.011	(0. 004 - 0.0176)
H	Hill coefficient that describes the sharpness of change in slope	18.340	(-27.108 - 63.78)
β	Scaling parameter for baseline mFARS effect on T50	-1.244	(-1.813 - -0.676)

%CV=percentage of coefficient of variation; CI=confidence interval; mFARS=modified Friedreich's ataxia rating scale.

Source: sequence 0001, module 5335, reat-pmx-omav-2081-study-report.pdf, page 92

The figure below displays the key diagnostic plots.

Figure 12: Goodness of Fit Plots for the final mFARS Disease Progression Model

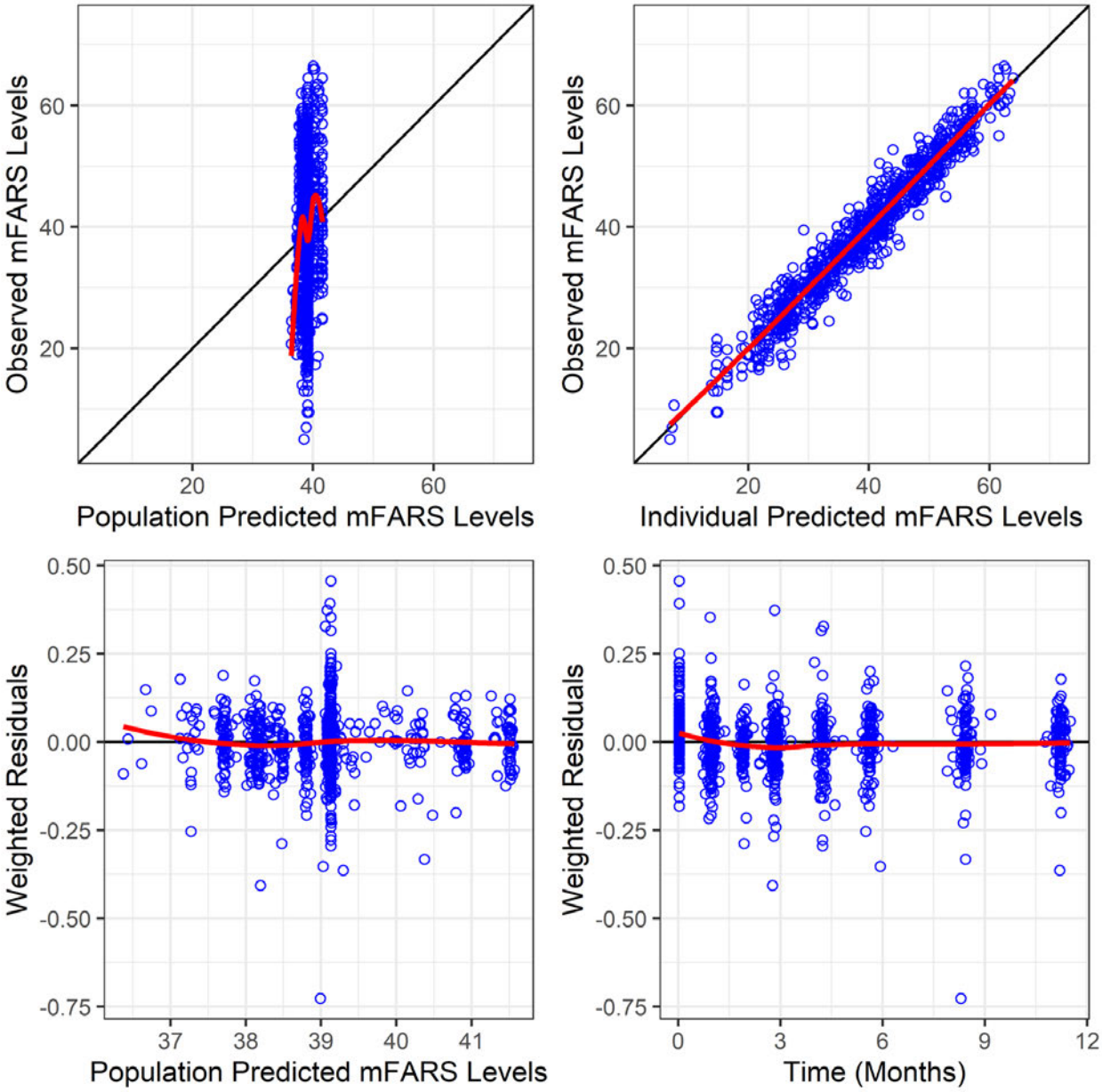

GOF=goodness-of-fit; mFARS=modified Friedreich's ataxia rating scale.

Source: sequence 0001, module 5335, reat-pmx-omav-2081-study-report.pdf, page 93

The Applicant points out that the goodness of fit plots suggest that the population parameters do not describe the variability in observed mFARS values (see top left panel of Figure 12). The Applicant points out that the population predictions use the typical baseline mFARS value and thus does not reflect the variability in individual baseline values (which range from 10.7 to 63.0).

The results of the visual predictive checks (VPCs) are shown in the figures below.

Figure 13: Visual Predictive Check for the final mFARS Disease Progression Model – All Arms

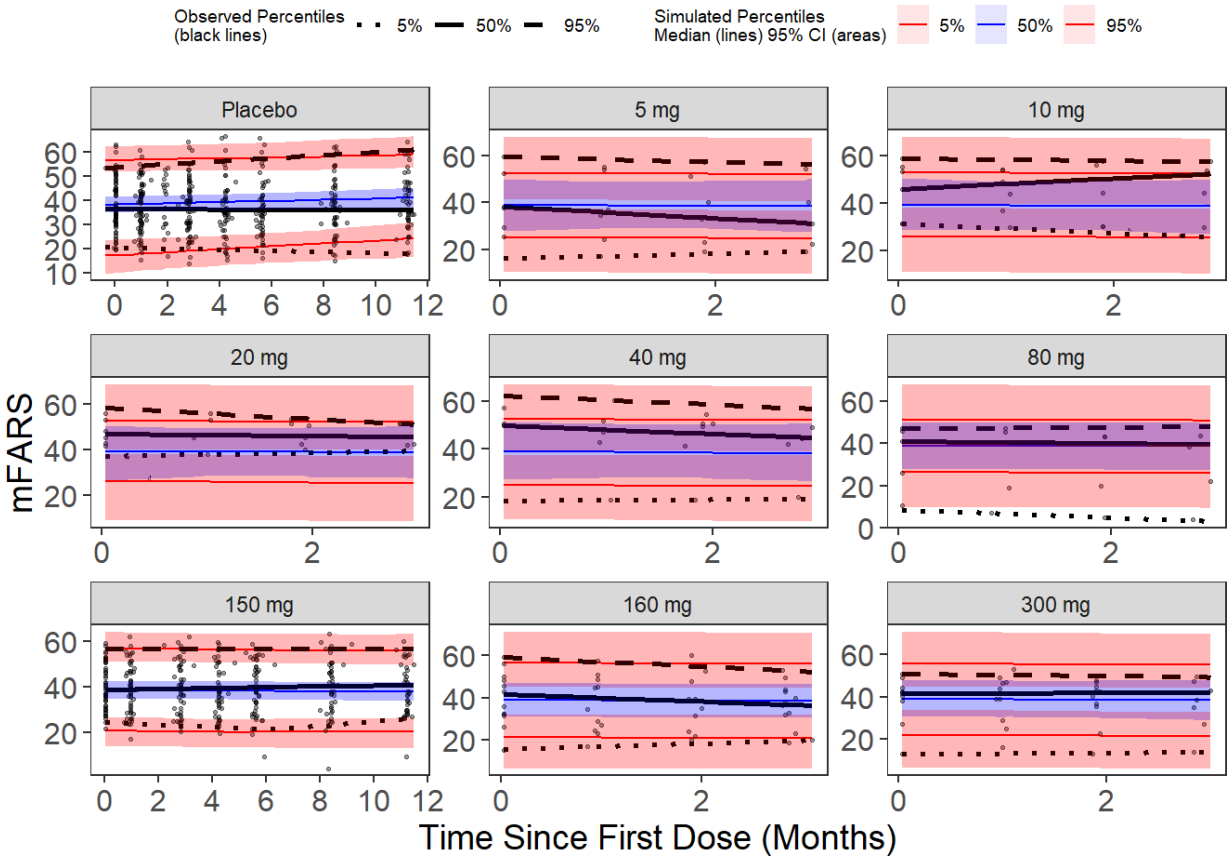

CI=confidence interval; mFARS=modified Friedreich's ataxia rating scale.

Source: sequence 0001, module 5335, reat-pmx-omav-2081-study-report.pdf, page 95

Figure 14: Visual Predictive Check for the final mFARS Disease Progression Model – Placebo, 150 mg Arms

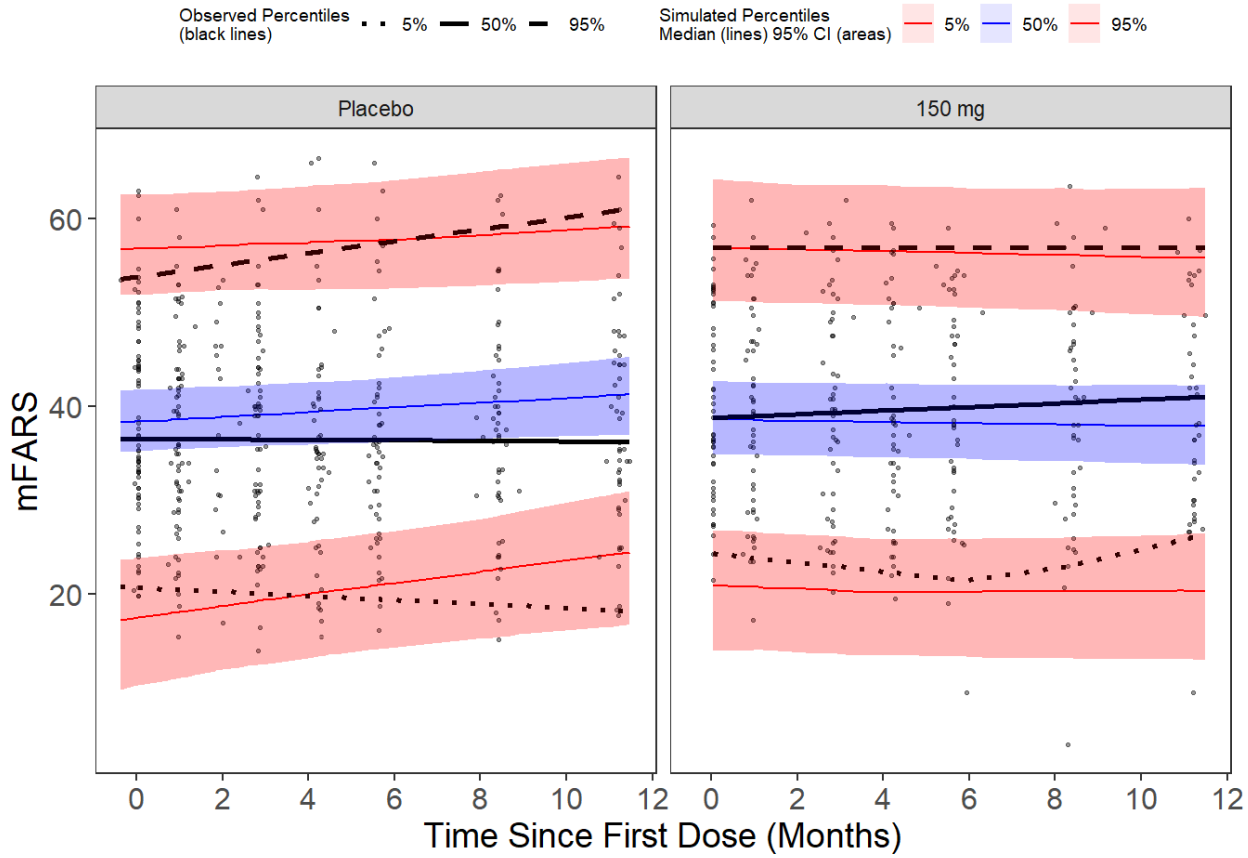

CI=confidence interval; mFARS=modified Friedreich's ataxia rating scale.

Source: sequence 0001, module 5335, reat-pmx-omav-2081-study-report.pdf, page 250

Applicant provides the following comments regarding the VPCs:

- The model provides good characterization of the central tendency of the observed data
- Prediction Cis are wide for most dose levels likely due to the sparsity of the observed data for most dose levels
- there is a slight trend towards over-prediction for placebo that is more likely due to the static inclusion of random effects on estimated baseline.
- The observed placebo baseline is lower than the model predicted baseline which inflates the difference from observed and model predicted median mFARS.

Applicant provides the following key findings and conclusions:

- higher baseline mFARS (corresponding to more advanced disease) is associated with shorter time until mFARS begins to increase (corresponding to worsening of neurological function).
- Having pes cavus is associated in a 1.1% decrease in treatment effect
- Population parameters do not describe the variability in observed mFARS value. However, when individual baseline values are included, predictions alight with observations. Individual plots with observed data, IPRED and PRED suggest that the models could adequately predict individual mFARS measurements.
- The model is fit for purpose.

[*Reviewer comment: The reviewer agrees with the applicant that the mFARS disease progression model does not describe the variability in mFARS values when using a fixed baseline mFARS value. When individual baseline mFARS values are utilized, the model performance improves.*

The visual predictive check (Figure 13) shows that the model performs best describing the placebo group and the 150 mg group. This finding is likely due to the higher number of subjects in these two arms compared to the number of subjects in other arms.

The E-R model supports mFARS benefit of omaveloxolone at the included dose levels compared to placebo.]

4.6 Physiologically based Pharmacokinetic Modeling and Simulation Review

Primary PBPK Reviewer	Manuela Grimstein, M.Sc., Ph.D.
Secondary PBPK Reviewer	Yuching Yang, Ph.D.

Executive Summary

The objective of this review is to evaluate the adequacy of the Applicant's Physiologically based Pharmacokinetic (PBPK) analyses to predict the DDI liability of omaveloxolone as a victim of CYP3A4-mediated interaction by strong and moderate CYP3A inhibitors and inducers.

The Division of Pharmacometrics has reviewed the PBPK submission (Report AG-48-PBPK-001, model files, responses to FDA's request for information) to conclude the following:

- The PBPK analysis was inadequate to predict the effect of CYP3A inhibitors and inducers on the exposure of omaveloxolone mainly because of uncertainties of the contribution of CYP3A4 to omaveloxolone clearance.

1. Methods

1.1 Model Development

The PBPK analyses were performed using the software Simcyp® version 18 release 2.

(b) (4)

[redacted]

2 Pages have been Withheld in Full as b4 (CCI/TS) immediately following this page

[redacted] (b) (4)

1.2 Model Application

The PBPK analysis was used to predict the PK of omaveloxolone following 150 mg single dose (SD) and 150 mg once daily dose (QD) in the presence of the following CYP3A modulators:

- Strong CYP3A4 inhibitor, itraconazole (200 mg QD for 14 days)
- Moderate CYP3A4 inhibitor fluconazole (600 mg QD for 14 days)
- Strong CYP3A4 inducer rifampin (600 mg QD for 14 days)
- Moderate CYP3A inducer efavirenz (600 mg QD for 14 days)

The default compound models (software's library, V18) for efavirenz, fluconazole, gemfibrozil, itraconazole (capsule formulation), midazolam, rifampin, and verapamil were used in the simulations for the respective DDIs.

The virtual population model "North European Caucasian (NEC)" was used to represent both healthy and patient populations. For healthy subjects, ten virtual trials of similar number of subjects (n) with age ranges and proportion of females matching the demographics of the respective study/dosing groups were simulated. For patient population, ten virtual trials of fixed individual trial design (where height, weight, age, and albumin were matched to subjects in clinical studies) were simulated. [redacted] (b) (4) All simulations were conducted under fasting conditions.

Additional comments: The rationale or potential mechanisms for the observation of higher Cmax in patients compared to healthy volunteers have not been discussed by the Applicant.

A list of the clinical studies used for model development and verification is shown in **Figure 15**.

Figure 15: Schematic representation of model development, verification, and application for omaveloxolone

2. Results

Q1. Can the PBPK model adequately describe the PK profiles of omaveloxolone?

The PBPK model of omaveloxolone did not adequately capture the observed PK profile following oral administration of single-doses of 50 to 150 mg in healthy subjects [Studies 408--C-1703, -C-1804, and -C-0806-control groups] and multiple-doses of 80 to 300 mg QD in the patient population [Study C-1402-Part I and Part II] (Figure 16 and Table 10).

1 Page has been Withheld in Full as b4 (CCI/TS) immediately following this page

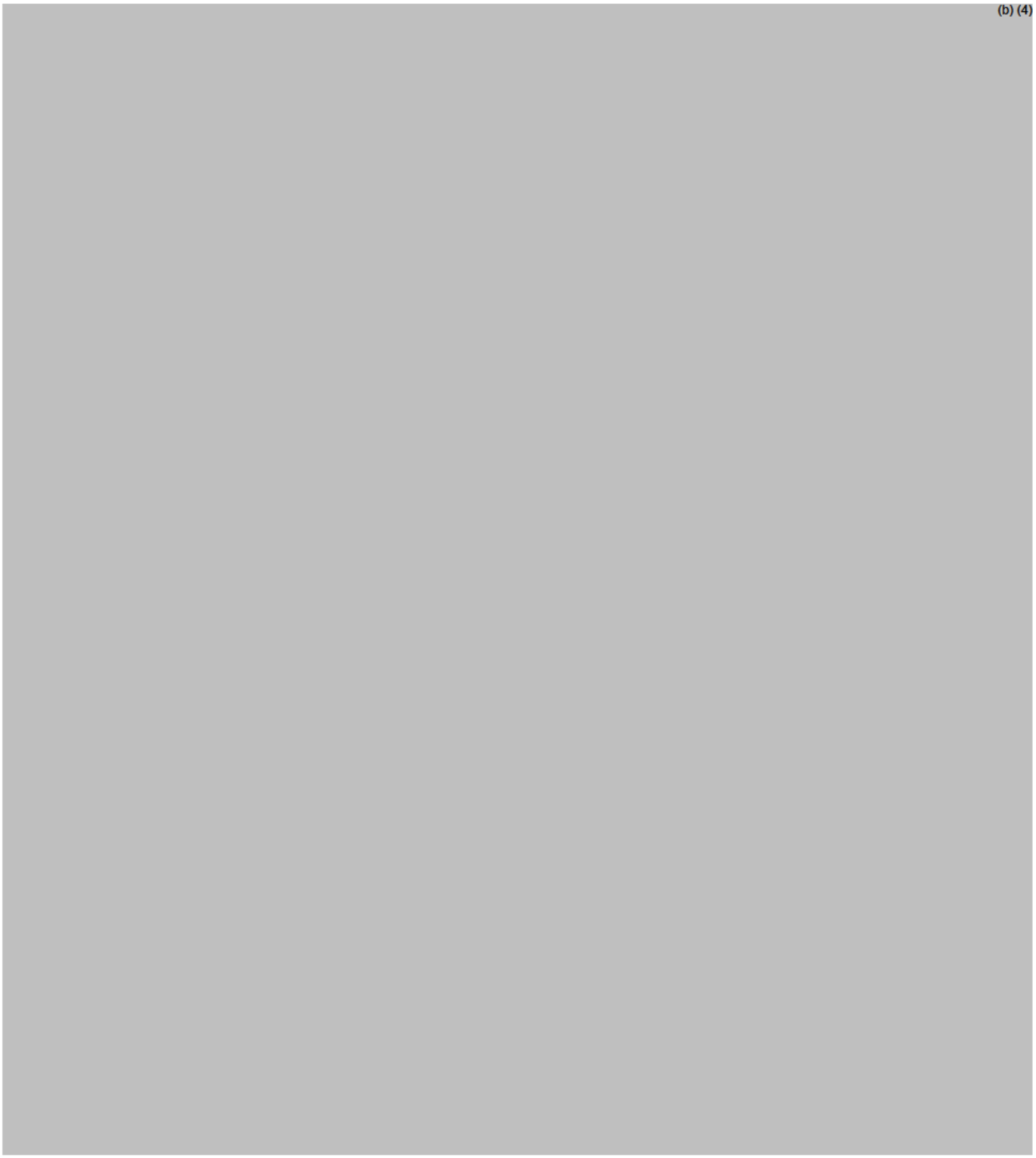

FDA Reviewer's Assessment

In the absence of intravenous ADME data, there is uncertainty whether the 40% unchanged omaveloxolone in feces following oral administration, as reported in the human ADME study, was due to biliary clearance (b) (4) and/or incomplete absorption/gut efflux (b) (4) The Applicant's model of omaveloxolone assumed incomplete absorption (b) (4) and no biliary clearance. However, an apparent clue that would be suggestive of a meaningful contribution of

biliary clearance and enterohepatic circulation (EHC) was the presence of multiple peaks in the single-dose PK profile of omaveloxolone, including at late time points post-dose. Additionally, in vitro data suggested that omaveloxolone may be a substrate of P-gp, although not a substrate of BCRP. It was not evaluated in vitro whether omaveloxolone is a substrate of MRP2 and/or BSEP. Thus, the Reviewer investigated the potential for biliary clearance to omaveloxolone disposition because misrepresentation of this clearance pathway would impact the estimations of the percentage contribution of CYP3A4 to the total clearance (fmCYP3A value in the model), and subsequent model application (i.e., predictions of the interaction effects of CYP3A modulators on omaveloxolone PK). Of note, an adequate verification of the fmCYP3A value was not provided in the current omaveloxolone model, based on Reviewer's assessment (refer to section 2. Results, Q2).

The Reviewer evaluated the potential for biliary clearance of omaveloxolone, using available nonclinical and clinical pharmacology data, to conclude there was not strong evidence of major biliary excretion and EHC of omaveloxolone. Reasons are:

- Omaveloxolone has low solubility and low permeability
- Moderate metabolism could be inferred based on total radioactivity exposure in plasma for all metabolites (54%) compared to parent (10%); consequently, major biliary excretion (~40% of total clearance) may be ruled out.
- The secondary peak in omaveloxolone PK profile was not affected by coadministration of the P-gp inhibitors itraconazole and verapamil suggesting minor role of P-gp-mediated disposition.
- No glucuronide metabolites (primary or secondary) were reported in vitro neither in vivo (human ADME study). Thus, EHC of omaveloxolone from back-conversion of such metabolites may be ruled out.
- Nonclinical ADME study showed no evidence of biliary excretion of omaveloxolone. Omaveloxolone was not quantified in bile after oral dose in bile-duct cannulated monkeys, while five metabolites of omaveloxolone were quantified in bile. Omaveloxolone was not quantified in feces after an IV dose.

Therefore, the assumption of negligible biliary clearance of omaveloxolone was supported and its impact on the estimation of fmCYP3A value in the model should be insignificant.

Further, the Reviewer concluded that there are evidence suggesting that the secondary peak in the PK profile of omaveloxolone is related to absorption:

- Omaveloxolone has low permeability and low solubility
- The secondary peak in the PK profile of omaveloxolone was not prominent in the fed state compared to fasted state. Food significantly increased the Cmax (350%) of omaveloxolone, but minimal effect on AUC. This observation suggested that solubility in bile acid may contribute significantly to the absorption of omaveloxolone. In the absence of food, omaveloxolone absorption seems delayed.

The mechanistic reason for the double peak phenomenon remains unknow. Possible mechanisms may be drug storage and subsequent release from a post-absorptive depot; variable absorption rates along the gastrointestinal tract; and/or discontinuous absorption.

The current model structure of omaveloxolone related to its absorption (first-order absorption model) do not mechanistically address neither recover the observed secondary peak.

Q2. Can PBPK analyses predict the effect of a CYP3A modulator on the PK of omaveloxolone?
No, the PBPK analysis was considered inadequate to estimate the interaction effects of CYP3A modulators on the PK of omaveloxolone. Validation of the contribution of the CYP3A4 pathway to omaveloxolone clearance is crucial to allow prediction of the effect of CYP3A modulators on the PK of omaveloxolone. However, the Reviewer considered that the fmCYP3A4 value was not adequately validated by the Applicant's PBPK analysis.

(b) (4)

FDA Reviewers' Assessment

The verapamil dosing regimen of 120 mg QD for 9 days in the DDI study with omaveloxolone was different from those usually used in other DDI studies in literature, 240 mg daily as BID or TID dosing regimens. The Reviewer conducted DDI simulations to evaluate the impact of verapamil dosing regimen on the reported DDI effect with midazolam[2]. Similar DDI effect on midazolam with 80 mg TID or 120 mg QD verapamil dosing was predicted (Table 12). The verapamil 120 mg QD dose resulted in higher fluctuation and lower Ctrough values of verapamil and norverapamil compared to 80 mg TID. However, both dosing regimens of verapamil yielded around 45% of active CYP3A4 remaining by the time of administration of midazolam, based on model predictions of CYP3A4 activity and time-dependent inhibition effect of verapamil and norverapamil.

Table 12: Predicted DDI effect of verapamil on the PK of midazolam (MDZ) based on verapamil dosing

	Verapamil dose regimen, MDZ dose	MDZ AUC ratio	MDZ Cmax ratio
Observed	80 mg TID 2 days (5 doses), MDZ 15 mg SD on day 2	2.92	1.97
Predicted	80 mg TID 2 days (5 doses), MDZ 15 mg SD on day 2	(b) (4)	
Predicted	120 mg QD 9 days, MDZ 15 mg SD on day 4		

Observed: Backman et al 1994; Predicted values using population representative. Analysis conducted by the Reviewer using Simcyp workspaces file, with modification of verapamil dosing.

The Applicant acknowledged other potential reason for inconsistency between the observed and predicted DDI effect of verapamil on omaveloxolone PK (b) (4)

As the Applicant also acknowledged, the evaluation of DDI predictive performance of verapamil PBPK model as a CYP3A inhibitor (software's library V18r2) was limited to one clinical DDI dataset. Additionally, in general, clinical interaction effect of a strong CYP inhibitor has higher sensitivity and utility for fmCYP value verification compared to clinical DDI data of a moderate CYP inhibitor.

In conclusion, the observed DDI effect of verapamil on omaveloxolone could not be explained by the current PBPK analysis using the Applicant's omaveloxolone model.

The Reviewer then conducted exploratory analysis of the PBPK model structure of omaveloxolone to evaluate the impact of model uncertainties on the predicted DDI effect of CYP3A inhibitors.

The Applicant's first-order absorption model was replaced by a mechanistic absorption model, which incorporated in vitro solubility data and predictions of bile micelle partition coefficients, aiming to recovery the dose-dependent trend of Cmax decrease reported following single-dose [Study 408-C-1703]. Subsequently, SA was undertaken to evaluate the impact of the values of first-pass metabolism (Fg.Fh), fmCYP3A4 and fraction unbound in enterocytes (fugut) on the changes of exposure to omaveloxolone when co-administered with CYP3A inhibitors. The results showed that fugut, Fg and fmCYP3A4 were sensitive model parameters for the purpose of DDI predictions. These results were also supported by the observation of minor change in omaveloxolone half-life in the presence of itraconazole suggesting that inhibition of first-pass gut metabolism of CYP3A4 appears to be the main mechanism of interaction with itraconazole.

The Reviewer considered that the model predicted effect of CYP3A4 auto-induction on omaveloxolone AUC and CL/F seems rather overestimated compared to patient data. Misrepresentation of CYP3A4 auto-induction by omaveloxolone could impact modeling predictions of the DDI effects of CYP3A modulators on omaveloxolone PK at steady state.

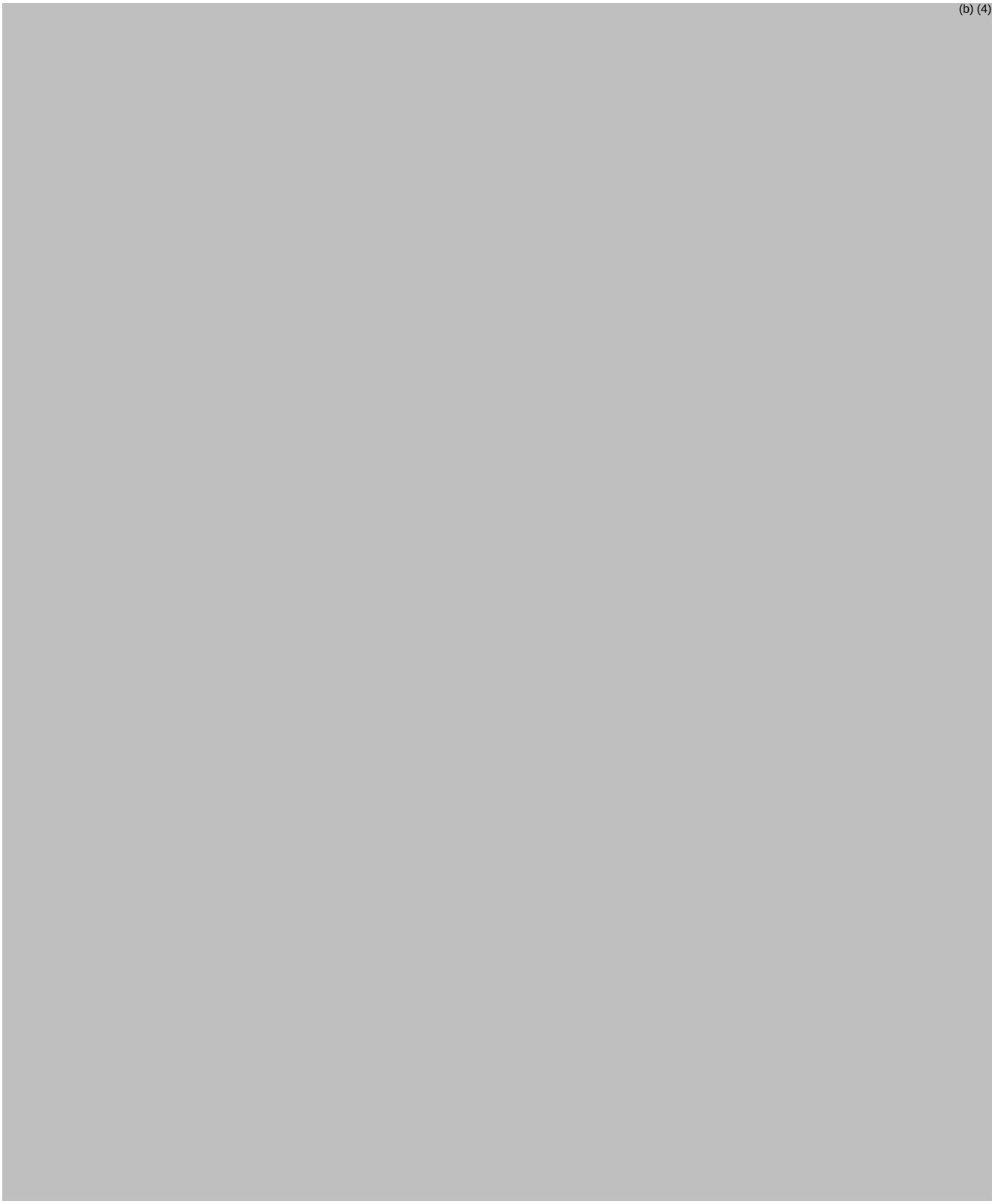

In conclusion, the current model structure of omaveloxolone related to its absorption and uncertainties of key model parameters for DDI predictions (i.e., fmCYP3A4, Fg) precluded the

acceptance of the model for the intended purpose, i.e., prediction of changes on omaveloxolone exposure in the presence of CYP3A inhibitors or inducers.

Additionally, The Applicant claimed that the clinical DDI effect of itraconazole [Study 408-C-1806] was used as the pivotal data for model development and verification. The Reviewer noted that a single clinical DDI dataset cannot be used to both develop and verify model parameters (e.g., Fg and fmCYP3A4 values), considering the context of use and model risk for omaveloxolone (see section 3).

3. Model Performance and Credibility Assessment

Context of use: The PBPK modeling analysis was used to predict the effect of CYP3A modulators, including fluconazole, efavirenz and rifampin, on the PK of omaveloxolone, and be the regulatory basis for avoidance and/or dosage modification language in the prescribing information.

3.1 Model influence

The Reviewer considered the model influence high because PBPK prediction will be used in lieu of clinical DDI studies and will provide the quantitative evidence to inform labeling. The modeling and simulation results will be the primary driver for assignment of risk and the basis for developing prevention and management strategies. Limited clinical DDI data (Study 408-C-1806) with strong and moderate CYP3A inhibitors were available to inform the modeling analysis; however, there is an apparent inconsistency in the clinical DDI results and modeling (see section 2. Results, Q2).

3.2 Decision consequence

The Reviewer considered the decision consequence high. If the model is incorrect regarding the magnitude of the DDI effect (i.e., overprediction), (1) the avoidance of moderate CYP3A modulators will limit therapeutic options for the patient population, or (2) dosage modification of omaveloxolone may result in underdosage and treatment failure in a severe diseased population with no treatment alternatives.

3.3 Model risk

The level of model risk is high because the PBPK modeling analysis has high influence and high decision consequence.

4. Conclusions

The PBPK analysis was inadequate to predict the effect of CYP3A inhibitors and inducers on the exposure of omaveloxolone because of the following reasons:

- uncertainties on the percent contribution of CYP3A4 to omaveloxolone clearance,
- lack of in vitro metabolic profile information for metabolites to support assumption on intestinal first pass metabolism,
- apparent overestimation of CYP3A4 auto-induction by omaveloxolone,
- limitation in the current model structure of omaveloxolone related to its absorption,
- high model risk.

References

[1] Hanke N, Türk D, Selzer D, et al. Mechanistic, Enantioselective, Physiologically Based Pharmacokinetic Model of Verapamil and Norverapamil, Built and Evaluated for Drug-Drug Interaction Studies. Pharmaceutics. 2020 Jun 16;12(6):556.

[2] Backman JT, Olkkola KT, Aranko K et al. Dose of midazolam should be reduced during diltiazem and verapamil treatments. Br J Clin Pharmacol. 1994 Mar;37(3):221-5.

This is a representation of an electronic record that was signed electronically. Following this are manifestations of any and all electronic signatures for this electronic record.

/s/

ADARSH S GANDHI
02/23/2023 09:19:22 AM

MICHAEL A BEWERNITZ
02/23/2023 01:27:49 PM

MANUELA GRIMSTEIN
02/23/2023 01:39:17 PM

YUCHING N YANG
02/23/2023 03:21:56 PM

BILAL S ABUASAL
02/23/2023 03:43:56 PM

MEHUL U MEHTA
02/23/2023 07:01:18 PM

U.S. FOOD & DRUG ADMINISTRATION

Date: August 15, 2022

From: Donna A. Volpe Ph.D., Keith Burkhart M.D., Kenrick Semple Ph.D.
Division of Applied Regulatory Science, Office of Clinical Pharmacology (DARS/OCP)

Through: Rebecca Racz Pharm.D., Consult Lead, DARS/OCP
David Strauss M.D., Ph.D., Division Director, DARS/OCP

To: Adarsh Gandhi and Bilal AbuAsal
Division of Neuropsychiatric Pharmacology (DNP), OCP

Subject: Omaveloxolone Nrf2 Mechanism of Action

EXECUTIVE SUMMARY

Friedreich's Ataxia is a neurodegenerative disorder involving the central and peripheral nervous systems, musculoskeletal system, the myocardium and endocrine pancreas. Alterations to the frataxin (*FXN*) gene result in alterations in iron and mitochondrial homeostasis, and sensitivity to oxidative stress. Nrf2 activation is being considered as a therapeutic target for Friedreich's Ataxia to protect against oxidative stress. Omaveloxolone is a Nrf2 activator and in clinical trials for treatment of Friedreich's Ataxia. Treated patients experienced elevations in their serum transaminase levels with no increase in total bilirubin or other evidence of liver toxicity. It is suggested that these alterations in serum liver enzymes and bilirubin are due to Nrf2-mediated increases in glutathione synthesis enzymes and mitochondrial bioenergetics, and induction of related proteins. Two other Nrf2 activators, bardoxolone methyl and oltipraz, caused increased transaminase levels without an associated increase in total bilirubin which would indicate hepatotoxicity. Rodent studies have found various Nrf2 activators to be hepatoprotective in liver injury due to drugs or chemicals. Aminotransferase enzyme activity has been shown to correlate with Nrf2 activity in mice. Based on *in vitro*, animal and clinical studies, it appears that the increased levels of aminotransferases following omaveloxolone administration is a pharmacodynamic effect related to Nrf2 activation rather than liver toxicity.

BACKGROUND

Omaveloxolone is being studied as a potential treatment for Friedreich's Ataxia. The sponsor's proposed mechanism of action for the drug is activation of Nrf2, which leads to upregulation of downstream liver enzymes (ALT, AST, GGT), ferritin and a decrease in creatine kinase. The sponsor dose selection rationale is partly based on the changes in these biomarkers. However, the Clinical Pharmacology reviewers feel that there is no evidence of increase in liver enzymes due to activation of Nrf2, and the sponsor's observations are contradictory with the literature studies.

U.S. Food & Drug Administration
10903 New Hampshire Avenue
Silver Spring, MD 20903
www.fda.gov

Questions to be Addressed by DARS:

1. *We would like DARS to specifically verify and comment on the accuracy of the sponsor's proposed mechanism of action (activation of Nrf2) for omaveloxolone which they used to support their dose selection rationale. Can DARS comment on the validity of sponsor's claims?*
2. *Do increases (and not decreases) in ALT, AST, GGT enzyme levels and ferritin have any clinical evidence with Nrf2 activation?*
3. *Can DARS share their experience where a clinically relevant (safe and effective) dose was selected based on increases in ALT, AST, GGT enzyme levels?*

EVALUATION

Friedreich's Ataxia

The neurodegenerative disorder Friedreich's Ataxia involves the central and peripheral nervous systems, musculoskeletal system, the myocardium and endocrine pancreas. An expansion in the non-coding first intron of the frataxin (*FXN*) gene is found in the majority of cases of Friedreich's Ataxia while the remaining cases (1-3%) are associated with a compound heterozygous expansion with a point mutation or deletion [Cook & Giunti, 2017]. As a result of the frataxin deficiency, there are alterations in iron sulfur cluster biogenesis, mitochondrial iron homeostasis, and sensitivity to oxidative stress [Cook & Giunti, 2017; La Rosa *et al*. 2020].

Evidence suggests that the defects in the *FXN* gene increase vulnerability to oxidative stress and reactive oxygen species production [La Rosa *et al*. 2020]. This is aggravated by a faulty regulation of the expression and signaling pathway modulation of the nuclear factor erythroid 2-related factor 2 (Nrf2) [La Rosa *et al*. 2020; Ghanekar *et al*. 2019]. In cultured fibroblasts from Friedreich's Ataxia patients, there was a faulty induction of antioxidant enzymes due to hypersensitive response to oxidative insults as the result of a compromise in the Nrf2 signaling pathway [Paupe *et al*. 2009]. In fibroblasts obtained from skin biopsies of Friedreich's Ataxia patients, glutathione (GSH) content was significantly decreased in comparison to control cells and subsequently increased by the Nrf2 activators sulforaphane, dimethyl fumarate and omaveloxolone [Petrillo *et al*. 2019]. Therefore, activators of Nrf2 are being considered as therapeutic agents for Friedreich's Ataxia [Petrillo *et al*. 2019; La Rosa *et al*. 2020].

Nrf2

NRF2 is recognized as a master regulator of a series of antioxidant response element (ARE)-containing cytoprotective genes whose expression is induced in response to cell stress [He *et al*. 2020; Cuadrado *et al*. 2019]. A network of cooperating enzymes encoded by these genes are implicated in both endobiotic and xenobiotic biotransformation reactions, antioxidant metabolism, intermediate metabolism of carbohydrates and lipids, iron catabolism, protein degradation, and inflammation regulator [Cuadrado *et al*. 2019]. Nrf2 influences many attributes of intermediary metabolism and mitochondrial function, either through direct regulation of key metabolic genes or indirectly by crosstalk with other transcription factors changing gene expression [Hayes & Dinkova-Kostova 2014]. These include antioxidant genes such as γ-glutamyltransferase (GGT)

and those involved in heme and iron metabolism (*e.g.*, ferritin) [Dinkova-Kostova 2014; Kerins & Ooi 2018; Zhang *et al*. 2006].

NRF2 is expressed in all cell types, and it typically has low basal activity in unstressed cells as the result of Kelch-like ECH-associated protein 1 (Keap1)-mediated proteasomal degradation [He *et al*. 2020]. The KEAP1-NRF2 pathway is the primary protective response to both oxidative and electrophilic stresses. KEAP1 forms part of an E3 ubiquitin ligase, under homeostatic conditions, which closely regulates the activity of NRF2 via ubiquitination and proteasome-dependent degradation [Baird & Yamamoto 2020]. Keap1 allows Nrf2 to escape ubiquitination in response to stress and translocate to the nucleus to promote its antioxidant transcription program [Baird & Yamamoto 2020].

Omaveloxolone

Omaveloxolone (N-(2-cyano-3,12-dioxo-28-noroleana-1,9(11)-dien-17-yl)-2,2-difluoropropan-amide, RTA 408) is a synthetic oleanane triterpenoid compound and Nrf2 activator (Figure 1). In human primary fibroblasts from Friedreich's Ataxia patients, omaveloxolone reversed an elevated level of endogenous lipid peroxidation and mitochondrial reactive oxygen species (ROS), thus protecting the cells against oxidative stress [Abeti *et al*. 2018]. In two murine models of Friedreich's Ataxia, where cerebellar granule neurons (CGNs) presented Complex I deficiency, substrate availability and Complex I activity were restored by omaveloxolone [Abeti *et al*. 2018].

Figure 1. Chemical Structure of Omaveloxolone

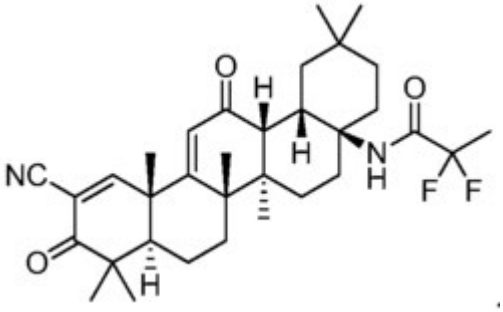

Oral administration of omaveloxolone to monkeys resulted in a significant and dose-dependent induction of Nrf2 target genes (*e.g.*, NQO1, SRXN1, TXNRD1) in liver and lung tissue [Reisman *et al*. 2019]. There was a significant and concentration-dependent induction by omaveloxolone and dose- and concentration-dependent induction of mRNA expression of Nrf2 target genes in peripheral blood mononuclear cells from monkeys [Reisman *et al*. 2019].

Data from the sponsor's report of a phase II clinical study of omaveloxolone found that five Friedreich's Ataxia patients (3 in the 160 mg group and 2 in the 300 mg group) exceeded the threshold criterion of alanine transaminase (ALT) or aspartate transaminase (AST) greater than 5× the upper limit of normal (ULN) [Reata Pharmaceuticals]. The increases occurred on or before week 4 for the five patients and were below the threshold limit by week 8. Figure 2 shows the changes in liver enzymes at weeks 4 and 12 according to dose. There was high interpatient variability in the changes for the liver enzymes, which are shown in greater detail in Figure 3 for

the 160 mg dose. Of note, total bilirubin levels did not increase in these patients; therefore, Hy's Law criteria was not met by any patient in the study [Reata Pharmaceuticals].

Figure 2. Changes in Liver Enzymes at Week 4 and 12

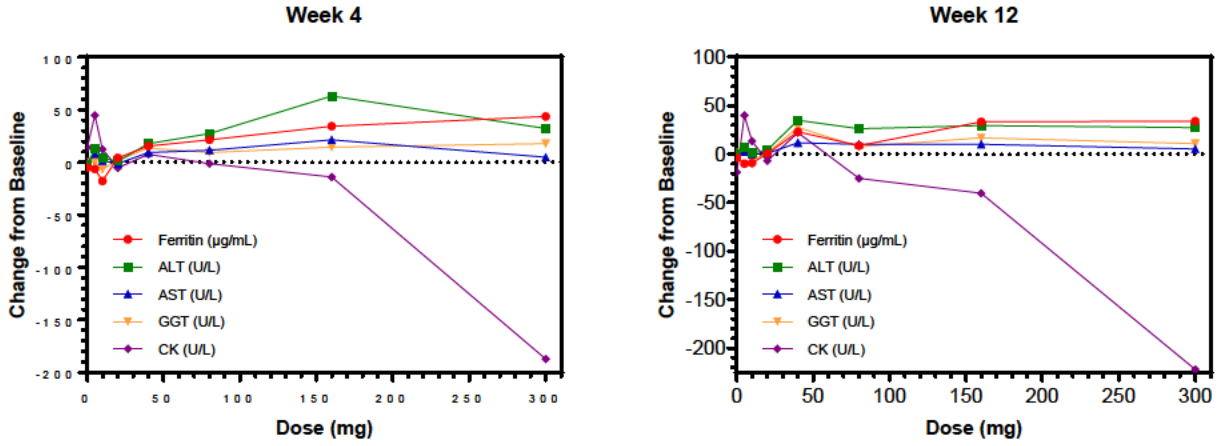

Figure 3. Changes in Liver Enzymes for 160 mg Omaveloxolone

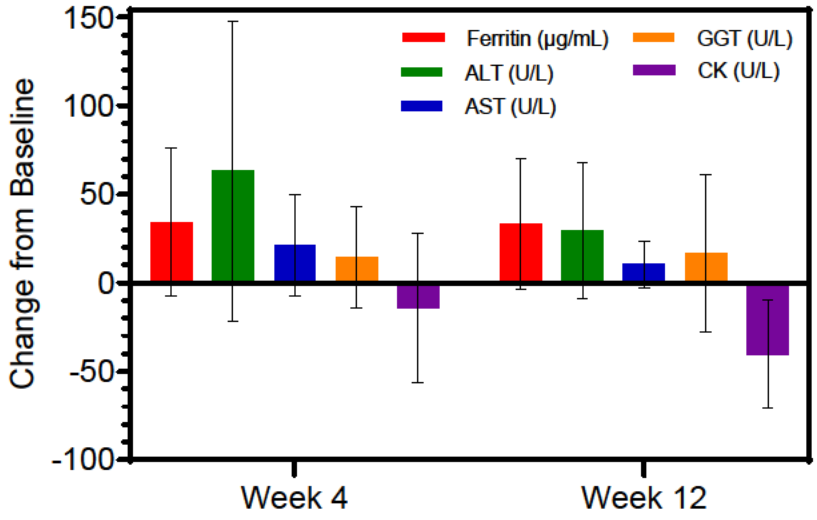

The MOXie trial evaluated the clinical effects of omaveloxolone in Friedreich's Ataxia patients over 12 weeks at dose levels of 2.5-300 mg/day [Lynch *et al*. 2018]. A small number of patients displayed increased ALT (12%) or AST (12%) levels which were not related with other indicators of liver injury such as increased direct bilirubin, decreased albumin, or changes in total protein [Lynch *et al*. 2018]. In another report on the MOXie trial, the increased serum ALT and AST levels in treated patients were maximal within the first 12 weeks of treatment and declining to baseline values within 4 weeks following the end of drug administration [Lynch *et al*. 2021]. Of the treated patients, 15 (29%) had maximum ALT elevations ≥3× ULN of which 80% had normal ALT levels within 4 weeks after drug termination [Lynch *et al*. 2021]. The increases in ALT and AST were not related to increased total bilirubin. None of the patients met the criteria for Hy's law and had no other symptoms indicative of liver injury. In fact, the treated patients had a small, but statistically significant, reduction in total bilirubin in relation to baseline and compared to placebo

patients [Lynch *et al*. 2021]. None of the patients who received omaveloxolone met potential Hy's law criteria, had clinical symptoms, or had other testing to suggest hepatic injury. The authors proposed that the alterations in serum liver enzymes and bilirubin noted in the omaveloxolone-treated patients are not related with liver injury but rather due to Nrf2-mediated increases in glutathione synthesis enzymes and mitochondrial bioenergetics [Lynch *et al*. 2021].

In the MOTOR trial in patients with mitochondrial myopathy, omaveloxolone was administered at doses of 5 to 160 mg in comparison to placebo [Madsen *et al*. 2020]. There were increases in plasma ferritin and GGT, along with significant elevations in ALT and AST following 4 weeks of treatment at 80 and 160 mg omaveloxolone compared to baseline [Madsen *et al*. 2020]. These changes in transaminases were not connected to any indications for liver toxicity nor were there observed increases in bilirubin. It was proposed that the elevations of ferritin, ALT, AST and GGT in the treated patients were the result of strong Nrf2 activation [Madsen *et al*. 2020].

Bardoxolone Methyl

Bardoxolone methyl (RTA 402; CDDO-Me) is another synthetic triterpenoid and antioxidant inflammation modulator that potently induces Nrf2 [Hong *et al*. 2012]. It interacts with KEAP1 promoting the translocation of Nrf2 to the nucleus and binding to ARE, leading to induction of antioxidant and cytoprotective enzymes and related proteins [Lewis *et al*. 2021]. In a phase 1 trial in patients with advanced cancers, the dose limiting toxicity with bardoxolone methyl was grade 3 reversible liver transaminase elevations [Hong *et al*. 2012]. In a phase 2 study in patients with type 2 diabetes mellitus and stage 3-4 chronic kidney disease with bardoxolone methyl, increased ALT, AST and GGT were among the most common adverse events [Nangaku *et al*. 2020]. However, these were not associated with elevated total bilirubin and Hy's law criteria was not met in these patients. In another phase 2 trial in patient with chronic kidney disease and types 2 diabetes, bardoxolone methyl treatment resulted in mild increases in ALT and AST [Pergola *et al*. 2011].

In a phase 3 trial patients with type 2 diabetes mellitus and stage 4 chronic kidney disease, bardoxolone methyl reversibly increased serum ALT, AST and GGT which was greatest after 4 weeks of treatment and decreased aver 48 weeks of treatment [Lewis *et al*. 2021]. There was no increase in total bilirubin concentrations and no cases of increased transaminases met Hy's Law criteria. Total bilirubin decreased relative to baseline and placebo, and <3% of treated patients showed hepatobiliary adverse events [Lewis *et al*. 2021]. The researchers also conducted *in vitro* experiments in cell lines derived from tissues that express aminotransferase proteins and/or are targets of bardoxolone methyl (liver, skeletal muscle, kidney, intestine, macrophages). There was a significant and concentration-dependent rise in aminotransferase gene expression in the cell lines exposed to bardoxolone methyl [Lewis *et al*. 2021]. The authors suggest that the elevation of ALT and AST levels observed in the clinical trial was due to the induction of aminotransferases via Nrf2 activation, rather than drug-induced hepatotoxicity.

In a trial with Alport syndrome adolescent and adult patients, bardoxolone methyl caused a transient increase in aminotransferase levels in pediatric patients (<3×ULN) that returned to

baseline 4 weeks after drug administration [Warady *et al*. 2021]. These increases were not accompanied by an elevation in total bilirubin.

Bardoxolone methyl is currently being studied for Alport Syndrome, a rare kidney disease, in an application from Reata Pharmaceuticals, Inc. A December 2021 Cardiorenal Advisory Committee (AC) meeting where the sponsor's briefing document reviewed the aminotransferase enzyme elevations noting them to be on-target actions (attached). The document provides *in vitro* and *in vivo* research that supports the on-target activity. In addition, CDER's Division of Hepatology and Nutrition was asked to evaluate the aminotransferase enzyme elevations and whether there was a concern for DILI (attached). Those reviewers, who reviewed information discussed earlier in this section, concluded that the elevation, as an on-target effect of Nrf2 activation, is plausible. They did not otherwise see evidence for this being a liver injury signal. There was evidence for a dosing effect where higher doses produced larger transaminase increases. This same pattern seems to be evident for omaveloxolone.

Dimethyl Fumarate

Dimethyl fumarate is another Nrf2 activator, that is approved for treatment of multiple sclerosis. In the phase 3 trails, patients with relapsing-remitting multiple sclerosis were treated with dimethyl fumarate [Fox *et al*. 2012; Gold *et al*. 2012]. There were increased incidences of liver transaminase elevations in 6% of the patients, mostly between months 1 and 6 [Gold *et al*. 2012]. However, there were no patients with liver transaminase levels ≥3× ULN associated with bilirubin >2× ULN and no reports of hepatic failure [Fox *et al*. 2012; Gold *et al*. 2012]. In a long-term study in Japanese patients with relapsing-remitting multiple sclerosis, common adverse events with dimethyl fumarate included increased ALT and AST [Ochi *et al*. 2018]. The incidence in treated patients was 6-11% for ALT and 2-8% for AST as compared to 2-3% in the placebo group [Ochi *et al*. 2018].

Dimethyl fumarate administration produces transaminase elevations, but there have also been reports of hepatotoxicity with it that may result from a different mechanism than Nrf2 activation. The FDA published a summary of 14 post-marketing cases from a FAERS evaluation of primarily hepatocellular liver injury with no cases of liver failure [Muñoz *et al*. 2017]. Dimethyl fumarate because of its anti-inflammatory actions is being studied to treat DILI from many substances including acetaminophen [Marguer-Ripolles *et al*. 2021]. It is our observation that omaveloxolone shares structural features with some steroids which are anti-inflammatory drugs that are rarely associated with reports of hepatoxicity. [Shahshahani *et al*. 2011]. However, glucocorticoids may antagonize Nrf2 activation [Chen *et al*. 2020; Alam *et al*. 2017].

Oltipraz

Oltipraz (4-methyl-5-(2-pyrazinyl)-1,2-dithiol-3-thione) is a dithiolethione that modulates gene expression through Nrf2 among other nuclear factors [Merrell *et al*. 2008]. In a mouse model of acetaminophen-induced acute liver injury, oltipraz was able to significantly decrease resultant ALT and AST levels and diminish other markers of hepatotoxicity [Ma *et al*. 2018]. In rats with dimethylnitrosamine-induced liver fibrogenesis, oltipraz was able to inhibit the increases in plasma

ALT, AST, GGT and bilirubin and decrease liver fibrosis [Kang *et al*. 2002]. In a clinical trial with oltipraz for non-alcoholic fatty liver disease, there were no significant increases in ALT, AST and GGT in treated patients [Kim *et al*. 2017].

Nrf2 Activation and Liver Enzymes/Ferritin

Several studies have shown that Nrf2 activation attenuates acute liver injury. One group compared serum ALT, LDH, hepatic hemorrhage, and necrosis levels between Nrf2-null and Nrf2-enhanced mice in cadmium-induced acute liver injury mice model and reported that Nrf2-enhanced mice were associated with lower ALT and LDH levels and with fewer morphological alterations [Wu *et al*. 2012]. The mRNA levels of cytoprotective genes, including sulfiredoxin-1, glutamate-cysteine ligase, and glutathione peroxidase-2 were expressed only in Nrf2-enhanced mice, suggesting that Nrf2 activation prevents oxidative stress and acute liver injury through modulation of antioxidant defense-associated genes [Wu *et al*. 2012]. The protective effects of Nrf2 were tested in LPS and D-GalN-induced liver injury mouse models by treatment with mangiferin, which could upregulate the gene expression of Nrf2 in a dose-dependent manner [Pan *et al*. 2016]. Mangiferin treatment suppressed serum levels of ALT, AST, IL-1β, TNF-α, and ROS levels, adding evidence that activation of Nrf2 pathway protects against acute liver injury [Pan *et al*. 2016].

Bardoxolone methyl is an antioxidant inflammation modulator that potently induces Nrf2. Treatment with bardoxolone methyl in hepatocytes, myocytes, renal cells, and macrophages increased in a concentration- and time-dependent manner transaminase mRNA and protein levels [Miller *et al*. 2011]. HuH-7 human hepatoma cells and AML12 mouse hepatocytes exposed to bardoxolone methyl displayed both time- and concentration-dependent increases in glutathione (GSH) levels which are the result of transaminase enzymatic reactions [Miller *et al*. 2011].

Studies conducted in rodent models have demonstrated the hepatoprotective effects of Nrf2 activators. In a mouse model of nonalcoholic steatohepatitis, omaveloxolone decreased liver injury with marked improvements in hepatic histology, lipid accumulation, and collagen deposition [Reisman *et al*. 2020]. In mice treated with acetaminophen, dimethyl fumarate raised Nrf-2 levels and reduced liver injury demonstrated by reduced levels of serum aminotransferases, alkaline phosphatase, GGT and bilirubin [Abdelrahman *et al*. 2019]. In Wistar rats treated with thioacetamide, dimethyl fumarate reversed the increases in hepatotoxicity markers (AST, ALT, GGT, total bilirubin) and histopathological outcomes [Dwivedi *et al*. 2020]. In a rat model of ischemia-reperfusion injury, dimethyl fumarate was able to significantly reduce the increased levels of AST and ALT compared to the untreated group [Ibrahim *et al*. 2020; Taksu *et al*. 2017].

Rosiglitazone, a Nrf2 and heme oxygenase 1 (HO-1) inducer, reversed the increased levels of ALT and AST in mice treated with carbon tetrachloride [Ma *et al*. 2022]. Similarly, pretreatment with isoliquiritigenin significantly prevented the triptolide-induced hepatotoxicity in mice as evidenced by reduced activities of AST, ALT, alkaline phosphatase and lactate dehydrogenase [Cao *et al*. 2016]. Furthermore, isoliquiritigenin lessened the histopathological changes induced by triptolide indicating that isoliquiritigenin pretreatment produced an increase in the Nrf2 protein expression [Cao *et al*. 2016]. Sulforaphane was protective against valproic acid-induced liver toxicity in rats

as determined by liver function biomarkers (*i.e*., ALT, AST, ALP, albumin) [Nazmy *et al*. 2017]. Andrographolide and biochanin A were protective against lipopolysaccharide/D-galactosamine-induced acute liver injury in mice [Liu *et al*. 2016; Pan *et al*. 2017]. Both compounds reduced ALT and AST levels in treated mice and andrographolide increased expression of Nrf2 and HO-1 [Liu *et al*. 2016; Pan *et al*. 2017]. Sulforaphane was also protective in rats with hepatic ischemia-reperfusion injury via activation of the Nrf-2/HO-1 signal pathway [Chen *et al*. 2021; Zhao *et al*. 2010].

Biochanin A, morin, curcumin, andrographolide, oxymatrine, and madecassoside were also found to play a protective role via activation of Nrf2 in LPS and D-GalN-induced acute liver injury in mice [Liu *et al*. 2016; Pan *et al*. 2017; Tian *et al*. 2017; Wang *et al*. 2018; Xie *et al*. 2017]. Further, the antioxidant pathway of Nrf2 was effective in carbon tetrachloride-induced and acetaminophen-induced mouse acute liver injury models [Cao et al. 2017; Huang et al. 2016; Peng et al. 2018; Shen *et al*. 2018]. Corilagin reduced mortality, AST and ALT levels, and histopathological liver changes induced by acetaminophen in Nrf2-deficienct mice [Lv *et al*. 2019]. Luteolin was protective against aflatoxin B_1-induced hepatotoxicity, alleviating growth retardation and serum biochemical alterations (ALT, AST, ALP, and GGT) under AFB1 exposure [Rajput *et al*. 2021].

Nrf2 modulates both heavy chain (Fth1) and light chain (Ftl) ferritin transcription after depletion of glutathione in rat livers [Cairo *et al*. 1995]. The antioxidant response elements (AREs) were identified within the promoter regions of murine Ftl and Fth1 genes [Tsuji *et al*. 2000; Wasserman & Fahl 1997] However, it was unknown which transcription factors could bind to the AREs or whether that binding affected transcription. The heavy chain of ferritin, Fth1, was first identified as an Nrf2 target gene when basal Fth1 mRNA levels in Nrf2-deficient mice were lower than in Nrf2-wild-type mice [Kwak *et al*. 2001]. Further, the relationship between Nrf2 activation and Ftl was uncovered when Ftl transcripts were twofold higher in $Nrf2^{+/+}$ compared with Nrf2-deficient mouse intestines [Thimmulappa *et al*. 2022].

Chemopreventive xenobiotics dithiolethiones oltipraz and 1,2-dithiole-3-thione activate Nrf2 [Kwak *et al*. 2002] and induce ferritin [Primiano *et al*. 1996]. Both Ftl and Fth1 could be induced approximately twofold by 70 μM of various dithiolethiones only in the presence of Nrf2 in primary mouse embryo fibroblasts [Pietsch *et al*. 2003]. Pietsch *et al*. demonstrated with gel shift assays that Nrf2 directly binds to Fth1 ARE after exposure to dithiolethiones oltipraz and 1,2-dithiole-3-thione [Pietsch *et al*. 2003]. Therefore, Nrf2 is responsible for basal transcription of ferritin, and xenobiotic-activated Nrf2 can further induce ferritin beyond normal expression levels.

Aminotransferase enzyme activity has been shown to correlate with Nrf2 activity in mice. Lower serum concentrations of ALT and AST have been observed in mice lacking Nrf2 than in wild-type and genetically-activated Nrf2 (Keap1-knockdown) animals [Osburn *et al*. 2008; Zhang *et al*. 2010]. In a comparison of wild-type and Nrf2 knockout mice, ischemia-reperfusion injury resulted in significantly higher levels of ALT and AST in the knockout mice [Kudoh *et al*. 2013]. Preactivation of Nrf2 in the wild-type mice resulted in a decrease in AST and ALT following ischemia-reperfusion injury, which was not observed in the knockout mice. Therefore, the depletion of Nrf2 resulted in mice more susceptible to hepatic ischemia-reperfusion injury, suggesting a role for Nrf2 in reducing liver damage in this model [Kudoh *et al*. 2013]. Nrf2

activation protected livers from the hepatotoxicant 3,5-diethoxycarbonyl-1,4-dihydrocollidine (DDC), a heme synthesis inhibitor. Following 2 weeks exposure to DDC, ALT and bilirubin where elevated in wild-type and Nrf2 knockout mice [Taguchi *et al*. 2019]. It was determined that Nrf2 activation protected livers against DDC-induced hepatotoxicity in the mice models [Taguchi *et al*. 2019].

It has been proposed that the mechanism by which omaveloxolone elevates aminotransferases is related to its pharmacologic actions [Ghanekar *et al*. 2019]. Nrf2 activation has been shown to alter *in vitro* GGT expression, and other enzymes in GSH homeostasis, through the antioxidant response element [Ravuri *et al*. 2013; Zhang *et al*. 2006]. In rats treated with a Nrf2 activator, GGT and other liver genes were induced in a dose-dependent manner [Goess *et al*. 2021].

SUMMARY AND CONCLUSIONS

1. *We would like DARS to specifically verify and comment on the accuracy of the sponsor's proposed mechanism of action (activation of Nrf2) for omaveloxolone which they used to support their dose selection rationale. Can DARS comment on the validity of sponsor's claims?*
   Based on *in vitro*, animal and clinical studies, it appears that the increased levels of aminotransferases in omaveloxolone is a pharmacodynamic effect related to Nrf2 activation rather than liver toxicity. *In vitro* experiments in cell lines derived from tissues that express aminotransferase there was a significant and concentration-dependent rise in aminotransferase gene expression and proteins in the cell lines exposure to the Nrf2 activator bardoxolone methyl.

2. *Do increases (and not decreases) in ALT, AST, GGT enzyme levels and ferritin have any clinical evidence with Nrf2 activation?*
   Nrf2 activation has been shown to induce GGT and ferritin protein expression. Omaveloxolone, bardoxolone methyl and oltipraz, caused increased transaminase levels without an associated increase in total bilirubin which would indicate hepatotoxicity. There is *in vitro* and animal data showing that Nrf2 activation results in increased expression of these enzymes. Additionally, numerous studies have shown that Nrf2 activators are hepatoprotective in rodent models of drug- or chemical-induced liver injury through their effects on antioxidant stress responses.

3. *Can DARS share their experience where a clinically relevant (safe and effective) dose was selected based on increases in ALT, AST, GGT enzyme levels?*
   DARS does not have such experience in setting doses based upon liver enzymes levels for a new drug. This question may be best answered by review divisions who are consulted regarding hepatoxicity signals for new drugs. Such divisions may have experience with other drugs where liver enzyme increases were determined to be a biomarker of drug effect and not a hepatoxicity signal.

REFERENCES AND SUPPORTING DOCUMENTS

References

Abdelrahman RS, Abdel-Rahman N. Dimethyl fumarate ameliorates acetaminophen-induced hepatic injury in mice dependent of Nrf-2/HO-1 pathway. Life Sci. 2019; 217:251-260.

Abeti R, Baccaro A, Esteras N, Giunti P. Novel Nrf2-inducer prevents mitochondrial defects and oxidative stress in Friedreich's Ataxia models. Front Cell Neurosci. 2018; 12:188.

Alam MM, Okazaki K, Nguyen LTT, Ota N, Kitamura H, Murakami S, Shima H, Igarashi K, Sekine H, Motohashi H. Glucocorticoid receptor signaling represses the antioxidant response by inhibiting histone acetylation mediated by the transcriptional activator NRF2. J Biol Chem. 2017; 292(18):7519-7530.

Baird L, Yamamoto M. The molecular mechanisms regulating the KEAP1-NRF2 pathway. Mol Cell Biol. 2020; 40(13):e00099-20.

Cairo GL, Tacchini G, Pogliaghi E, Tomasi AA, Bernelli-Zazzera A. Induction of ferritin synthesis by oxidative stress. Transcriptional and post-transcriptional regulation by expansion of the "free" iron pool. J Biol Chem. 1995; 270(2):700-703.

Cao L, Yan M, Ma YX, Zhang BK, Fang PF, Xiang DX, Li ZH, Gong H, Deng Y, Li HD. Isoliquiritigenin protects against triptolide-induced hepatotoxicity in mice through Nrf2 activation. Pharmazie. 2016; 71(7):394-397.

Cao M, Wang H, Guo L, Yang S, Liu C, Khor TO, Yu S, Kong AN. Dibenzoylmethane protects against CCl_4-induced acute liver injury by activating Nrf2 via JNK, AMPK, and calcium signaling. AAPS J. 2017; 19(6):1703-1714.

Chen HC, Yip T, Lee JK, Juliani J, Sernia C, Hill AF, Lavidis NA, Spiers JG. Restraint stress alters expression of glucocorticoid bioavailability mediators, suppresses Nrf2, and promotes oxidative stress in liver tissue. Antioxidants. 2020; 9(9):853.

Chen L, Zhang WL, Xie DQ, Jia W. Sulforaphane alleviates hepatic ischemia-reperfusion injury through promoting the activation of Nrf-2/HO-1 signaling. Transpl Immunol. 2021; 68:101439.

Cook A, Giunti P. Friedreich's ataxia: clinical features, pathogenesis and management. Br Med Bull. 2017; 124(1):19-30.

Cuadrado A, Rojo AI, Wells G, Hayes JD, Cousin SP, Rumsey WL, Attucks OC, Franklin S, Levonen AL, Kensler TW, Dinkova-Kostova AT. Therapeutic targeting of the NRF2 and KEAP1 partnership in chronic diseases. Nat Rev Drug Discov. 2019; 18(4):295-317.

Dwivedi DK, Jena G, Kumar V. Dimethyl fumarate protects thioacetamide-induced liver damage in rats: Studies on Nrf2, NLRP3, and NF-κB. J Biochem Mol Toxicol. 2020; 34(6):e22476.

Fox RJ, Miller DH, Phillips JT, Hutchinson M, Havrdova E, Kita M, Yang M, Raghupathi K, Novas M, Sweetser MT, Viglietta V, Dawson KT; CONFIRM Study Investigators. Placebo-controlled phase 3 study of oral BG-12 or glatiramer in multiple sclerosis. N Engl J Med. 2012; 367(12):1087-1097.

Ghanekar SD, Miller WW, Meyer CJ, Fenelon KJ, Lacdao A, Zesiewicz TA. Orphan drugs in development for the treatment of Friedreich's Ataxia: Focus on omaveloxolone. Degener Neurol Neuromuscul Dis. 2019; 9:103-107.

Goess C, Terrillon S, Mayo M, Bousquet P, Wallace C, Hart M, Mathieu S, Twomey R, Donnelly-Roberts D, Namovic M, Jung P, Hu M, Richardson P, Esbenshade T, Cuff CA. NRF2 activator

A-1396076 ameliorates inflammation in autoimmune disease models by inhibiting antigen dependent T cell activation. J Transl. Autoimmun. 2021; 4:100079.

Gold R, Kappos L, Arnold DL, Bar-Or A, Giovannoni G, Selmaj K, Tornatore C, Sweetser MT, Yang M, Sheikh SI, Dawson KT; DEFINE Study Investigators. Placebo-controlled phase 3 study of oral BG-12 for relapsing multiple sclerosis. N Engl J Med. 2012; 367(12):1098-1107.

Hayes JD, Dinkova-Kostova AT. The Nrf2 regulatory network provides an interface between redox and intermediary metabolism. Trend Biochem Sci. 2014; 39(4):199-218.

He F, Antonucci L, Karin M. NRF2 as a regulator of cell metabolism and inflammation in cancer. Carcinogenesis. 2020; 41(4):405-416.

Hong DS, Kurzrock R, Supko JG, He X, Naing A, Wheler J, Lawrence D, Eder JP, Meyer CJ, Ferguson DA, Mier J, Konopleva M, Konoplev S, Andreeff M, Kufe D, Lazarus H, Shapiro GI, Dezube BJ. A phase I first-in-human trial of bardoxolone methyl in patients with advanced solid tumors and lymphomas. Clin Cancer Res. 2012; 18(12):3396-3406.

Huang YJ, Chen P, Lee CY, Yang SY, Lin MT, Lee HS, Wu YM. Protection against acetaminophen-induced acute liver failure by omentum adipose tissue derived stem cells through the mediation of Nrf2 and cytochrome P450 expression. J Biomed Sci. 2016; 23:5.

Ibrahim SG, El-Emam SZ, Mohamed EA, Abd Ellah MF. Dimethyl fumarate and curcumin attenuate hepatic ischemia/reperfusion injury via Nrf2/HO-1 activation and anti-inflammatory properties. Int Immunopharmacol. 2020; 80:106131.

Kang KW, Choi SH, Ha JR, Kim CW, Kim SG. Inhibition of dimethylnitrosamine-induced liver fibrosis by [5-(2-pyrazinyl)-4-methyl-1,2-dithiol-3-thione] (oltipraz) in rats: Suppression of transforming growth factor-β1 and tumor necrosis factor-α expression. Chem Biol Interact. 2002; 139(1):61-77.

Kerins MJ, Ooi A. The roles of NRF2 in modulating cellular iron homeostasis. Antioxid Redox Signal. 2018; 29(17):1756-1773.

Kim W, Kim BG, Lee JS, Lee CK, Yeon JE, Chang MS, Kim JH, Kim H, Yi S, Lee J, Cho JY, Kim SG, Lee JH, Kim YJ. Randomised clinical trial: the efficacy and safety of oltipraz, a liver X receptor alpha-inhibitory dithiolethione in patients with non-alcoholic fatty liver disease. Aliment Pharmacol Ther. 2017; 45(8):1073-1083.

Kudoh K, Uchinami H, Yamamoto Y. Activation of NRF2-A novel strategy to protect the liver from ischemia-reperfusion injury. Eur Surg Res. 2013; 50(2 suppl. 4):130.

Kwak MK, Itoh K, Yamamoto M, Kensler TW. Enhanced expression of the transcription factor Nrf2 by cancer chemopreventive agents: role of antioxidant response element-like sequences in the nrf2 promoter. Mol Cell Biol. 2002; 22(9):2883-2892.

Kwak MK, Itoh K, Yamamoto M, Sutter TR, Kensler TW. Role of transcription factor Nrf2 in the induction of hepatic phase 2 and antioxidative enzymes in vivo by the cancer chemoprotective agent, 3H-1, 2-dimethiole-3-thione. Mol Med. 2001; 7(2):135-145.

La Rosa P, Bertini ES, Piemonte F. The NRF2 signaling network defines clinical biomarkers and therapeutic opportunity in Friedreich's Ataxia. Int J Mol Sci. 2020; 21(3):916.

Lewis JH, Jadoul M, Block GA, Chin MP, Ferguson DA, Goldsberry A, Meyer CJ, O'Grady M, Pergola PE, Reisman SA, Wigley WC, Chertow GM. Effects of bardoxolone methyl on hepatic enzymes in patients with type 2 diabetes mellitus and stage 4 CKD. Clin Transl Sci. 2021; 14(1):299-309.

Liu X, Wang T, Liu X, Cai L, Qi J, Zhang P, Li Y. Biochanin A protects lipopolysaccharide/D-galactosamine-induced acute liver injury in mice by activating the Nrf2 pathway and

inhibiting NLRP3 inflammasome activation. Int Immunopharmacol. 2016; 38:324-331.
Lv H, Hong L, Tian Y, Yin C, Zhu C, Feng H. Corilagin alleviates acetaminophen-induced hepatotoxicity via enhancing the AMPK/GSK3β-Nrf2 signaling pathway. Cell Commun Signal. 2019; 17(1):2.
Lynch DR, Farmer J, Hauser L, Blair IA, Wang QQ, Mesaros C, Snyder N, Boesch S, Chin M, Delatycki MB, Giunti P, Goldsberry A, Hoyle C, McBride MG, Nachbauer W, O'Grady M, Perlman S, Subramony SH, Wilmot GR, Zesiewicz T, Meyer C. Safety, pharmacodynamics, and potential benefit of omaveloxolone in Friedreich ataxia. Ann Clin Transl Neurol. 2018; 6(1):15-26.
Lynch DR, Chin MP, Delatycki MB, Subramony SH, Corti M, Hoyle JC, Boesch S, Nachbauer W, Mariotti C, Mathews KD, Giunti P, Wilmot G, Zesiewicz T, Perlman S, Goldsberry A, O'Grady M, Meyer CJ. Safety and efficacy of omaveloxolone in Friedreich Ataxia (MOXIe Study). Ann Neurol. 2021; 89(2):212-225.
Ma L, Ma Y, Ma BX, Ma M. Rosiglitazone ameliorates acute hepatic injury via activating the Nrf2 signaling pathway and inhibiting activation of the NLRP3 inflammasome. Exp Ther Med. 2022; 23(4):300.
Ma X, Chang Y, Zhang Y, Muhammad I, Shi C, Li R, Li C, Li Z, Lin Y, Han Q, Liu F. Effects of C2-ceramide and oltipraz on hepatocyte nuclear factor-1 and glutathione S-transferase A1 in acetaminophen-mediated acute mice liver injury. Front Pharmacol. 2018; 9:1009.
Madsen KL, Buch AE, Cohen BH, Falk MJ, Goldsberry A, Goldstein A, Karaa A, Koenig MK, Muraresku CC, Meyer C, O'Grady M, Scaglia F, Shieh PB, Vockley J, Zolkipli-Cunningham Z, Haller RG, Vissing J. Safety and efficacy of omaveloxolone in patients with mitochondrial myopathy: MOTOR trial. Neurology. 2020; 94(7):e687-e698.
Merrell MD, Jackson JP, Augustine LM, Fisher CD, Slitt AL, Maher JM, Huang W, Moore DD, Zhang Y, Klaassen CD, Cherrington NJ. The Nrf2 activator oltipraz also activates the constitutive androstane receptor. Drug Metab Dispos. 2008; 36(8):1716-1721.
Meseguer-Ripolles J, Lucendo-Villarin B, Tucker C, Ferreira-Gonzalez S, Homer N, Wang Y, Starkey Lewis PJ, M Toledo E, Mellado-Gomez E, Simpson J, Flint O, Jaiswal H, Beer NL, Karlsen AE, Forbes SJ, Dear JW, Hughes J, Hay DC. Dimethyl fumarate reduces hepatocyte senescence following paracetamol exposure. iScience. 2021; 24(6):102552.
Miller GA, Bumeister R, Laidlaw J, Kambuj P, Probst B, Ferguson DA, Wigley WC. Bardoxolone methyl transcriptionally regulates transaminase levels and increases glutathione levels. J Am Soc Nephrol. 2011; 22:770A.
Muñoz MA, Kulick CG, Kortepeter CM, Levin RL, Avigan MI. Liver injury associated with dimethyl fumarate in multiple sclerosis patients. Mult Scler. 2017; 23(14):1947-1949.
Nazmy EA, El-Khouly OA, Atef H, Said E. Sulforaphane protects against sodium valproate-induced acute liver injury. Can J Physiol Pharmacol. 2017; 95(4):420-426.
Nangaku M, Kanda H, Takama H, Ichikawa T, Hase H, Akizawa T. Randomized clinical trial on the effect of bardoxolone methyl on GFR in diabetic kidney disease patients (TSUBAKI Study). Kidney Int Rep. 2020; 5(6):879-890.
Ochi H, Niino M, Onizuka Y, Hiramatsu K, Hase M, Yun J, Matta A, Torii S. 72-week safety and tolerability of dimethyl fumarate in Japanese patients with relapsing-remitting multiple sclerosis: Analysis of the randomised, double blind, placebo-controlled, phase III APEX study and its open-label extension. Adv Ther. 2018; 35(10):1598-1611.
Osburn WO, Yates MS, Dolan PD, Chen S, Liby KT, Spron MB, Taguchi K, Yamamoto M,

Kensler TW. Genetic or pharmacologic amplification of Nrf2 signaling inhibits acute inflammatory liver injury in mice. Toxicol Sci. 2008; 104(1):218-227.

Pan CW, Pan ZZ, Hu JJ, Chen WL, Zhou GY, Lin W, Jin LX, Xu CL. Mangiferin alleviates lipopolysaccharide and D-galactosamine-induced acute liver injury by activating the Nrf2 pathway and inhibiting NLRP3 inflammasome activation. Eur J Pharmacol. 2016; 770:85-91.

Pan CW, Yang SX, Pan ZZ, Zheng B, Wang JZ, Lu GR, Xue ZX, Xu CL. Andrographolide ameliorates d-galactosamine/lipopolysaccharide-induced acute liver injury by activating Nrf2 signaling pathway. Oncotarget. 2017; 8(25):41202-41210.

Paupe V, Dassa EP, Goncalves S, Auchère F, Lönn M, Holmgren A, Rustin P. Impaired nuclear Nrf2 translocation undermines the oxidative stress response in Friedreich Ataxia. PLoS ONE. 2009; 4(1):e4253.

Peng X, Dai C, Liu Q, Li J, Qiu J. Curcumin attenuates on carbon tetrachloride-induced acute liver injury in mice via modulation of the Nrf2/HO-1 and TGF-beta1/Smad3 pathway. Molecules. 2018; 23(1):215.

Pergola PE, Raskin P, Toto RD, Meyer CJ, Huff JW, Grossman EB, Krauth M, Ruiz S, Audhya P, Christ-Schmidt H, Wittes J, Warnock DG. Bardoxolone methyl and kidney function in CKD with type 2 diabetes. N Engl J Med. 2011; 365(4):327-336.

Petrillo S, D'Amico J, La Rosa P, Bertini ES, Piemonte F. Targeting NRF2 for the treatment of Friedreich's Ataxia: A comparison among drugs. Int J Mol Sci. 2019; 20:article 5211.

Pietsch EC, Chan JY, Torti FM, Torti SV. Nrf2 mediates the induction of ferritin H in response to xenobiotics and cancer chemopreventive dithiolethiones. J Biol Chem. 2003; 278(4): 2361-2369.

Primiano T, Kensler TW, Kuppusamy P, Zweier JL, Sutter TR. Induction of hepatic heme oxygenase-1 and ferritin in rats by cancer chemopreventive dithiolethiones. Carcinogenesis. 1996; 17(11): 2291-2296.

Rajput SA, Shaukat A, Wu K, Rajput IR, Baloch DM, Akhtar RW, Raza MA, Najda A, Rafał P, Albrakati A, El-Kott AF, Abdel-Daim MM. Luteolin alleviates aflatoxinB_1-induced apoptosis and oxidative stress in the liver of mice through activation of Nrf2 signaling pathway. Antioxidants (Basel). 2021; 10(8):1268.

Ravuri C, Svineng G, Huseby NE. Differential regulation of γ-glutamyltransferase and glutamate cysteine ligase expression after mitochondrial uncoupling: γ-glutamyltransferase is regulated in an Nrf2- and NFκB-independent manner. Free Radic Res. 2013; 47(5):394-403.

Reata Pharmaceuticals, Inc. Clinical Study Report. RTA 408 (OMAVELOXOLONE) 408-C-1402 PART 1. A phase 2 study of the safety, efficacy, and pharmacodynamics of RTA 408 in the treatment of Friedreich's Ataxia.

Reisman SA, Gahir SS, Lee CI, Proksch JW, Sakamoto M, Ward KW. Pharmacokinetics and pharmacodynamics of the novel Nrf2 activator omaveloxolone in primates. Drug Des Devel Ther. 2019; 13:1259-1270.

Reisman SA, Ferguson DA, Lee CYI, Proksch JW. Omaveloxolone and TX63682 are hepatoprotective in the STAM mouse model of nonalcoholic steatohepatitis. J Biochem Mol Toxicol. 2020; 34(9):article e22526.

Shahshahani MM, Azizahari S, Soori T, Manavi S, Balighi K, Daneshpazhooh M, Davatchi CS, Esmaili N. Hepatotoxicity and liver enzyme alteration in patients with immunobullous diseases receiving immunosuppressive therapy. J Dermatol. 2011; 38:1153-1157.

Shen Z, Wang Y, Su Z, Kou R, Xie K, Song F. Activation of p62-keap1-Nrf2 antioxidant pathway

in the early stage of acetaminophen-induced acute liver injury in mice. Chem Biol Interact. 2018. 282:22-28.

Taguchi K, Masui S, Itoh T, Miyajima A, Yamamoto M. Nrf2 activation ameliorates hepatotoxicity induced by a heme synthesis inhibitor. Toxicol Sci. 2019; 167(1):227-238.

Takasu C, Vaziri ND, Li S, Robles L, Vo K, Takasu M, Pham C, Farzaneh SH, Shimada M, Stamos MJ, Ichii H. Treatment with dimethyl fumarate ameliorates liver ischemia/reperfusion injury. World J Gastroenterol. 2017; 23(25):4508-4516.

Thimmulappa RK, Mai KH, Srisuma S, Kensler TW, Yamamoto M, Biswal S. Identification of Nrf2-regulated genes induced by the chemopreventive agent sulforaphane by oligonucleotide microarray. Cancer Res. 2002; 62(18):5196-203.

Tian Y, Li Z, Shen B, Zhang Q, Feng H. Protective effects of morin on lipopolysaccharide/d-galactosamine-induced acute liver injury by inhibiting TLR4/NF-κB and activating Nrf2/HO-1 signaling pathways. Int Immunopharmacol. 2017; 45: 148-155.

Tsuji Y, Ayaki H, Whitman SP, Morrow CS, Torti SV, Torti FM. Coordinate transcriptional and translational regulation of ferritin in response to oxidative stress. Mol Cell Biol. 2000; 20(16):5818-5827.

Wang W, Wu L, Li Q, Zhang Z, Xu L, Lin C, Gao L, Zhao K, Liang F, Zhang Q, Zhou M, Jiang W. Madecassoside prevents acute liver failure in LPS/D-GalN-induced mice by inhibiting p38/NF-κB and activating Nrf2/HO-1 signaling. Biomed Pharmacother. 2018; 103: 1137-1145.

Warady B, Chadha V, Chin M, Gbadagesin RA, Gibson K, Gipson D, Goldsberry A, Lieberman K, Meyer C, Meyers K, Nozu K, O'Grady M, Rheault M, Kashtan C. Safety of bardoxolone methyl in pediatric patients with Alport syndrome in cardinal phase 3 trial. Nephrol Dialysis Transplant. 2021; 36(Suppl 1):i17.

Wasserman WW, Fahl WE. Functional antioxidant responsive elements. Proc Natl Acad Sci USA. 1997; 94(10):5361-5366.

Wu KC, Liu JJ, Klaassen CD. Nrf2 activation prevents cadmium-induced acute liver injury. 2012; Toxicol Appl Pharmacol. 263(1):14-20.

Xie YL, Chu JG, Jian XM, Dong JZ, Wang LP, Li GX, Yang NB. Curcumin attenuates lipopolysaccharide/d-galactosamine-induced acute liver injury by activating Nrf2 nuclear translocation and inhibiting NF-κB activation. Biomed Pharmacother. 2017; 91:70-77.

Zhang H, Liu H, Dickinson DA, Liu RM, Postlethwait EM, Laperche Y, Forman HJ. γ-Glutamyl transpeptidase is induced by 4-hydroxynonenal via EpRE/Nrf2 signaling in rat epithelial type II cells. Free Radical Biol Med. 2006; 40(8):1281-1292.

Zhang S, Napierala M, Napierala JS. Therapeutic prospects for Friedreich's Ataxia. Trends Pharmacol Sci. 2019; 40(4):229-233.

Zhang YK, Yeager RL, Tanaka Y, Klaassen CD. Enhanced expression of Nrf2 in mice attenuates the fatty liver produced by a methionine- and choline-deficient diet. Toxicol Appl Pharmacol. 2010; 245(3):326-334.

Zhao HD, Zhang F, Shen G, Li YB, Li YH, Jing HR, Ma LF, Yao JH, Tian XF. Sulforaphane protects liver injury induced by intestinal ischemia reperfusion through Nrf2-ARE pathway. World J Gastroenterol. 2010; 16(24):3002-3010.

Supporting Documents

- Advisory Committee Briefing Materials: Bardoxolone Methyl (RTA 402) for Treatment of Alport Syndrome. December 8, 2021.
- CDER's Division of Hepatology and Nutrition consult on bardoxolone methyl and aminotransferase enzyme elevations.

This is a representation of an electronic record that was signed electronically. Following this are manifestations of any and all electronic signatures for this electronic record.

/s/

TRACEY B LEE
08/22/2022 08:36:46 AM

REBECCA L RACZ
08/22/2022 04:06:08 PM

JAMES L WEAVER
08/22/2022 04:14:54 PM